Triplet-triplet annihilation photon up-conversion: accessing triplet excited states with minimum energy loss

Article

Accepted Version

Triplet-Triplet Annihilation Photon Up-conversion: Accessing Triplet Excited States with Minimum Energy Loss

Mushraf Hussain,[a,] Syed S. Razi,[b] Tao Tao, [a, c, d] and František Hartl [e]**

[a] NUIST-Reading Academy, Nanjing University of Information Science and Technology, Nanjing 210044, P. R. China.

E-mail: mushraf_chemist@yahoo.com

[b] Department of Chemistry, Gaya College, Magadh University, Bodhgaya, Bihar-823001, India.

[c] Jiangsu Collaborative Innovation Center of Atmospheric Environment and Equipment Technologies, Jiangsu Key Laboratory of Atmospheric Environmental Monitoring and Pollution Control, School of Environmental Science and Engineering, Nanjing University of Information Science and Technology, Nanjing 210044, P. R. China.

[d] School of Chemistry and Materials Science, Institute of Advanced Materials and Flexible Electronics, Nanjing University of Information Science and Technology (NUIST), Nanjing 210044, P. R. China.

[e] Department of Chemistry, University of Reading, Whiteknights, Reading RG6 6DX, United Kingdom.

ABSTRACT: Triplet-triplet annihilation photon up-conversion (TTA-PUC) has gained immense attention among the scientific community in the last decade due to its application in the fields of energy, biology, and photocatalytic organic synthesis. One of the main aims to improve the efficiency of these low-to-high photon-energy conversion is to reduce energy losses during the intersystem crossing (ISC). Since 2015, many strategies have been reported to address this challenge and a significant update has been noticed in this field. This review is aimed to critically analyze these updates and provide an outlook for the future. A detailed mechanism of ISC in thermally activated delayed-fluorescence (TADF) molecules that possess a small singlet−triplet energy gap, is discussed with a focus on its deeper understanding and the impact of molecular design. In this context, a range of selected organic and inorganic TADF molecules are thoroughly evaluated. Osmium(II) complexes that exhibit a spin-forbidden metal-to-ligand charge-transfer (^{3}MLCT) transition in their Vis-NIR-IR absorption spectra and can be excited directly into their triplet state, thereby bypassing the energy loss during ISC, are also debated in sufficient detail for their advantages as well as shortcomings in being used in TTA-PUC. This work aims at reviewing the latest progress in this field, understanding the fundamental ISC mechanism of these photosensitizers, and critically addressing the challenges that are faced in this field. This review is anticipated to serve as a helpful script for identifying future directions and designing molecular sensitizers for TTA-PUC, which can sensitize the triplet state with minimum energy loss during ISC and can be helpful for increasing the anti-Stokes shift in TTA-PUC.

Key Words: Intersystem Crossing, Triplet-Triplet Annihilation Upconversion, Thermally Activated Delayed Fluorescence, Osmium Complexes, Zirconium Complexes

CONTENT

1. INTRODUCTION

Recently a tremendous interest has been noticed in the field of triplet−triplet annihilation photon up-conversion (TTA-PUC) due to potential applications of this process in diverse areas such as bio-sensing,[1,2] bio-imaging,[3,4] photodynamic therapy (PDT),[5,6] photocatalysis,[7,8] and optoelectronic devices[9,10] etc. The PUC is a counterintuitive process of absorption of low-energy photons whilst emission of high-energy photons is observed relative to the excitation source (an anti-Stokes shift). In other words, upon the absorption of longer-wavelength light, an emission of a shorter-wavelength light is observed.[11–14] A number of traditional up-conversion methodologies such as the use of rare-earth metals, inorganic crystals, and two-photon absorbing materials have been known to the scientific community for a long time.[15–20] However, triplet−triplet annihilation photon up-conversion (TTA-PUC) has recently received immense interest due to the use of a low-power excitation source (< 2 mW cm^{-2}), strong absorption of UV-Vis-NIR light, high PUC quantum yield (up to 45%) and non-coherent excitation source such as terrestrially available sunlight (1.5 AM).[21–23]

4.1 Scope of the Review. This review is mainly focused on different strategies that have been used to minimize the singlet−triplet energy gap during ISC of a molecular photosensitizer to be used in TTA-PUC. A review article related to this topic was published in 2017 but at that time only a few examples of molecules used to probe the strategy were reported.[22] A major part of that review article was dedicated to materials (nanocrystals) and only three examples of thermally activated delayed fluorescence (TADF)-based photosensitizer for TTA-PUC were discussed. For osmium-based complexes, two published examples were included in that review. Since that time, many new reports have been published on TTA-PUC with different types of TADF sensitizers, along with new osmium(II)-based complexes that need to be critically analyzed in the context of

molecular chemistry. Moreover, the scope of our review is not only to focus on these photosensitizers for TTA-PUC application but also to look into their ISC mechanisms that can be a useful script available to the scientists not only for energy applications, but also for bioimaging, photocatalysis and LED applications, etc.

2. TRIPLET-TRIPLET ANNIHILATION PHOTON UPCONVERSION

TTA-PUC, generally a bimolecular system, consists of a triplet photosensitizer and a triplet acceptor/annihilator. In this system, a triplet photosensitizer absorbs low-energy (= long-wavelength) photon to reach a singlet excited state (S_1) and then accesses the triplet excited state (T_1) via spin inversion; this process is called the intersystem crossing (ISC).[8,24,25] The sensitizer in the triplet state transfers its energy to a triplet-energy acceptor/annihilator by triplet−triplet energy migration (TEnM). The detailed mechanism of a general TTA up-conversion system containing a triplet photosensitizer and triplet acceptor is shown in Figure 1a. This process of TEnM process from a triplet sensitizer to the triplet acceptor can be direct or can be mediated by charge transfer as shown in Figure 2.[26–29] Due to the diffusion, collision, and TTA of two triplet beneficiary molecules, a singlet state (S_1) is formed, followed by a radiative relaxation (emitting high-energy (short-wavelength) photons) to the ground state, and anti-Stokes shift is observed.[303132]

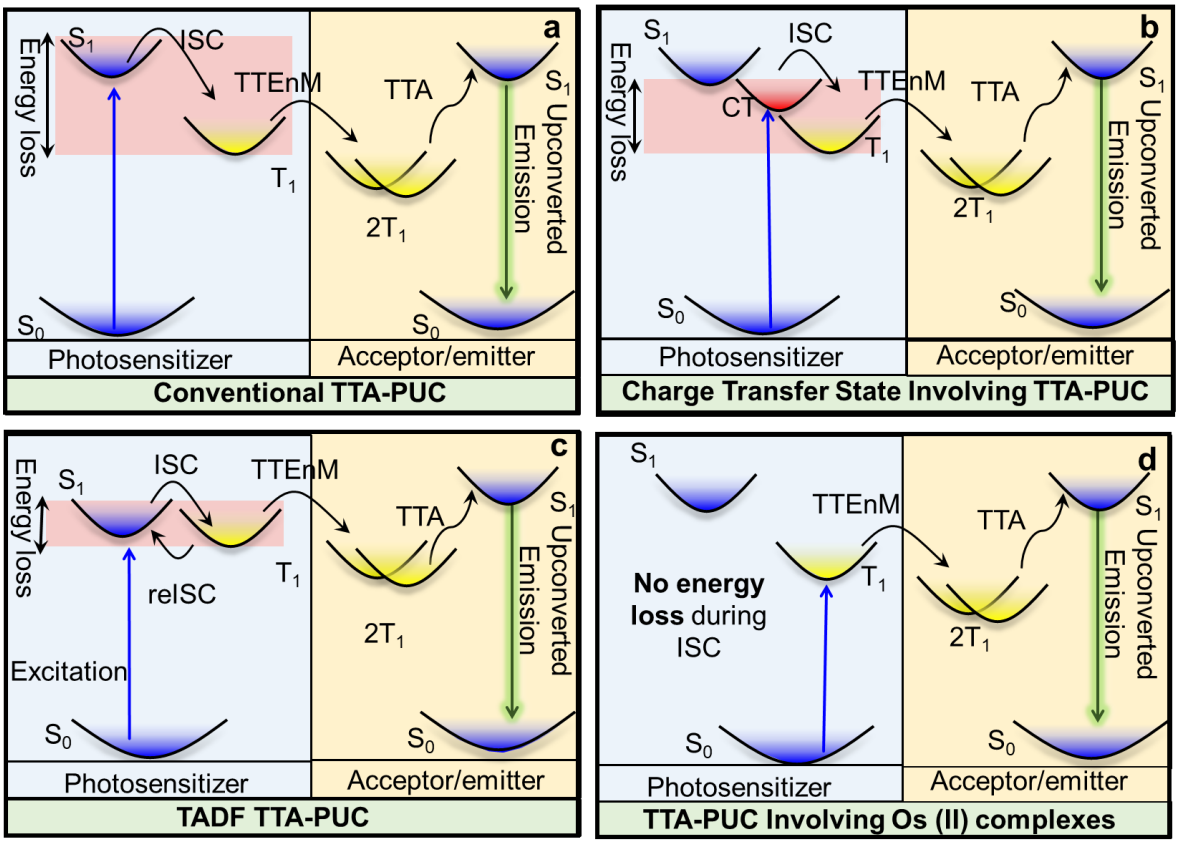

Figure 1. Schematic representation of a conventional TTA-PUC system (a), and strategies used to prevent energy loss during ISC of photosensitizers in TTA-PUC systems involving a charge-transfer excited state (b), a TADF-based photosensitizer (c), and an Os(II) complex-based photosensitizer (d). S_0, S_1 and T_1 represent the ground state, lowest singlet excited state and lowest triplet excited state, respectively. Blue lines and green lines are representing absorption of the photosensitizer and emission of the acceptor, respectively.

In order to ensure efficient TEnM and TTA, the molecules should be in close vicinity (10 Å) because these electron-exchange mechanisms are of the Dexter-type by nature.[33] As shown in Equation (1), the rate constant for the Dexter energy migration, k_{EnM}, depends upon the distance r separating the energy donor from the acceptor molecule, as well as on the sum of the energy donor

and acceptor radii (R), and J, the integral for spectral overlap between the electron donor and acceptor in Equation 1.

$$k_{\mathrm{EnM}} \propto Jexp\left[\frac{-2r}{R}\right] \qquad (1)$$

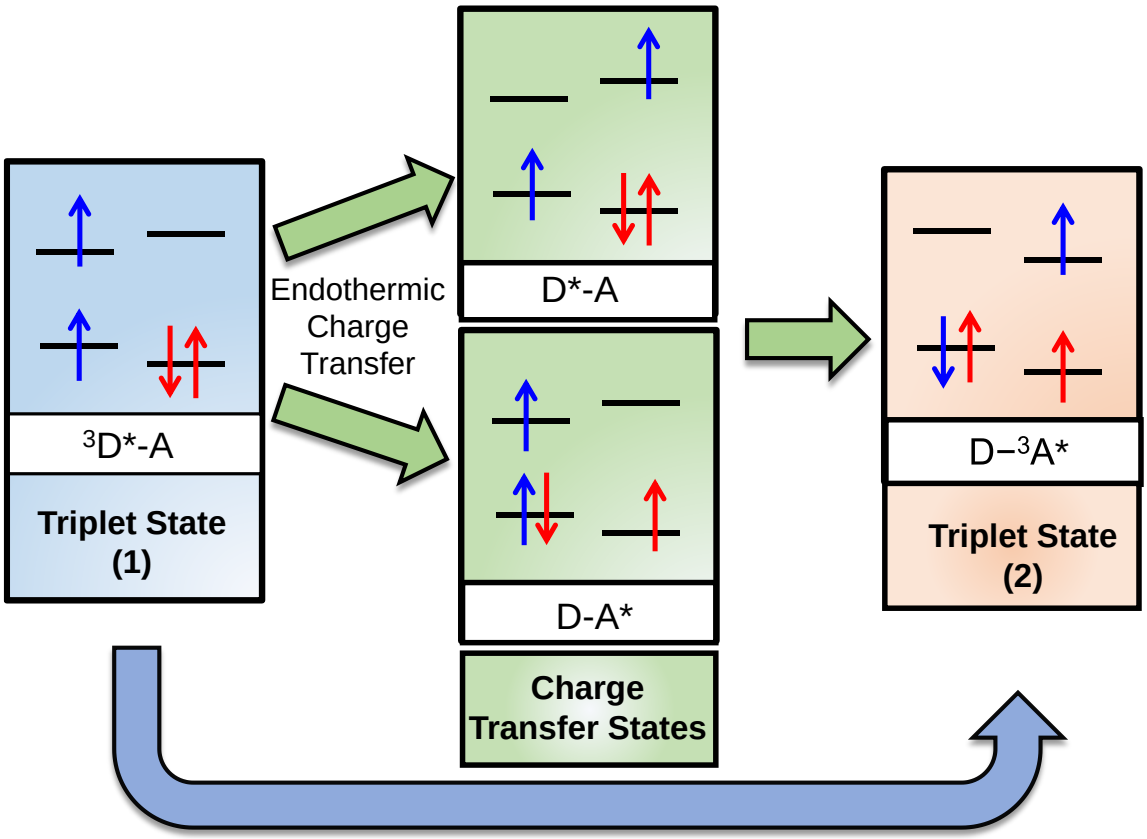

Figure 2. Schematic representation of direct and CT mediated TEnM. D and A stand for a donor and acceptor compound and D* and A* for a photoexcited donor and acceptor, respectively. The green arrows represent CT meditated TEnM and the blue arrow direct TEnM from a donor to acceptor molecule.

Due to the dominant TTA process in the high excitation energy region, the relation between emitter triplet and excitation energy becomes quasilinear, as compared to the quadratic relation observed in the low excitation energy region for TTA-PUC. The cross point obtained by fitting lines of

these low and high excitation-energy regions is denoted as the I_{th} value (upconversion threshold) and its relation with α (the molar absorption coefficient at the excitation point of the photosensitizer), Φ_{EM} (the sensitizer-to-annihilator TEnM efficiency), D_{AT} (the diffusion constant for annihilator triplet), τ_T (the triplet excited-state lifetime of annihilator), and a_r (the annihilation distance in-between triplets of annihilator, that is ~ 1 nm) is presented in Equation 2.

$$I_{th} = [\alpha \emptyset_{EM} 8\pi D_{AT} a_r]^{-1}[\tau_T]^{-2} \quad (2)$$

This equation elaborates that a high molar absorption coefficient and a longer triplet lifetime of photosensitizer, as well as significant efficiency for TEnM between triplet sensitizer and triplet acceptor, and remarkable triplet diffusion are all essential to get a lower I_{th} value.[34,35]

The photon up-conversion quantum yield, that is, the ratio between the absorbed incident photons to the emitted photons, of an up-conversion system can be represented by Equation 3.

$$\emptyset_{UC} = \frac{1}{2} f \emptyset_{ISC} \emptyset_{EnM} \emptyset_{TTA} \emptyset_{FL} \quad (3)$$

where Φ_{ISC} is singlet-to-triplet intersystem crossing quantum yield for a sensitizer, Φ_{EnM} is the sensitizer-to-triplet acceptor energy migration efficiency, Φ_{TTA} is the triplet-triplet annihilation efficiency for a triplet annihilator, Φ_{FL} is the fluorescence quantum yield for a triplet annihilator and f is statistical probability factor of annihilator to generate singlet state through triplet-triplet annihilation.[31,36]

2.1 Role of ISC in TTA photon upconversion

Intersystem crossing (ISC) from a singlet to triplet excited state is a phenomenon of significant importance in the fundamentals of photochemistry and photophysics.[37–41] A deeper insight into the difference between the corresponding singlet and triplet excited states could be apprehended by the principle of quantum chemistry. For a single electron, the spin quantum number (S) is 1/2 and its projection parallel to the magnetic field can be denoted by $m = \pm$ ½. According to the Pauli

exclusion principle, the spin of two electrons in an orbital is always inverted (cannot be identical) because the value of four quantum numbers cannot be similar. The state multiplicity can be determined by using the simple formula $2S+1$ (where S = spin of system given by the cumulative sum of individual electrons spin). For neutral molecules, the spin of an electron pair is inverted ($S = 0$) and the overall multiplicity is a singlet. However, for a two-electron system with identical spins, the overall multiplicity is a triplet. For a triplet state, there are three allowed components of the spin state (−1, 0, and +1), as shown in Figure 3.

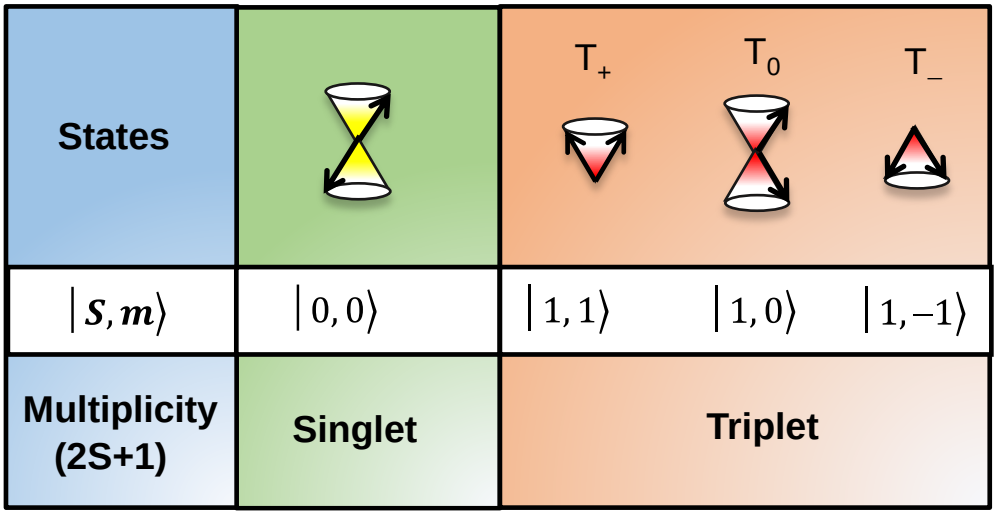

Figure 3. Vector-diagram presentation of singlet and triplet states. The term '*S'* represents the spin of an electron and '*m'* its projection. T_+, T_0 and T_- are the components of the triplet state.

The ISC rate constant is represented by Equation 4, where S_x and T_y are representing singlet and triplet states, respectively, H is the Hamiltonian operator for spin-orbit coupling (SOC), and ΔE is the energy difference between singlet and triplet states.

$$K \propto \frac{\langle T_y | H | S_x \rangle^2}{\left(\Delta E_{S_x - T_y}\right)^2} \qquad (4)$$

From Equation 4 it is apparent that large values of SOC and a small energy gap between singlet-triplet states are crucial factors determining an efficient ISC. However, the singlet-triplet energy gap is generally large for most organic and inorganic molecules and its origin can be traced to the exchange energy J ($2J = \Delta E_{S_x - T_y}$). Since crossing from a singlet state to a triplet state is a spin forbidden process, triplet-state lifetimes are generally longer compared to those of singlet states.[38,42] The long-lived triplet state ensures efficient energy- and electron-migration processes, making triplet photosensitizing useful for various applications.[43–45] Most of the conventional triplet photosensitizers depend upon the SOC effect of heavy atoms on ISC. Complexes of heavy transition metals, including platinum, are not only costly to synthesize but also feature shortening of triplet lifetimes and increased dark toxicity (cell viability in the absence of irradiation). These drawbacks make alternative strategies for efficient singlet-to-triplet ISC highly desired.[38,46,47]

2.2 Strategies to avoid energy loss during ISC and their application in TTA-PUC

Recently many new techniques have been introduced to attain ISC such as by appending a stable radical to a chromophore[48–50] or twisting a π-conjugated framework[51–53]. Replacement of carbonyl oxygen in an organic compound with sulfur in a thiocarbonyl group (thionated photosensitizers) and orthogonally connected electron donor-acceptor molecules can also induce ultrafast singlet-to-triplet ISC.[54–57] For most of these techniques, energy is lost during ISC from a singlet to triplet state due to the singlet−triplet energy difference. This review is aimed to discuss some strategies to minimizing excitation-energy loss when accessing the triplet state of a photosensitizer by either decreasing the singlet−triplet energy gap or by populating directly the triplet state, and the application of such molecules for TTA-PUC.

As mentioned above, the TTA-PUC quantum yield depends upon the ISC quantum yield (Equation 2). Equation 4 reveals that ISC depends upon the energy difference between the singlet

and triplet states. Hence, decreasing the energy gap between the singlet and triplet states may lead to high triplet quantum yield by overcoming the energy loss during ISC.[58,59] The following section is dedicated to the discussion on different strategies used to obtain efficient ISC by avoiding energy loss during ISC.

3. Charge-transfer state to minimize energy loss during ISC for TTA-PUC

Photo-activated charge separation (CS) between electron donor and acceptor molecules is an important phenomenon in the fields of photovoltaic solar cells, natural/artificial photosynthesis, photocatalytic reactions, etc.[60–66] However, the discussion in this review is confined to the role of CS and charge-transfer (CT) states in ISC. To start the description, we may consider a [D-A] molecule consisting of electron donor (D) and acceptor (A) units. Usually, electronic excitation promotes the molecule from its ground state to an excited state called the locally excited state (^{1}LE). In the LE state either the donor [D*−A] or acceptor [D−A*] become excited, inducing electron transfer from D to A to reach a CT state and form a zwitterion [$D^{+\bullet}-A^{-\bullet}$], as shown in Figure 4. This charge-transfer state is a singlet and short-lived, as the reverse process, $^1CT \rightarrow S_0$, is a spin-allowed transition.[67–70] Apart from the D−A energy difference and the SOC value, polarity and viscosity of the surrounding medium are two other vital factors influencing this process.[71–74]

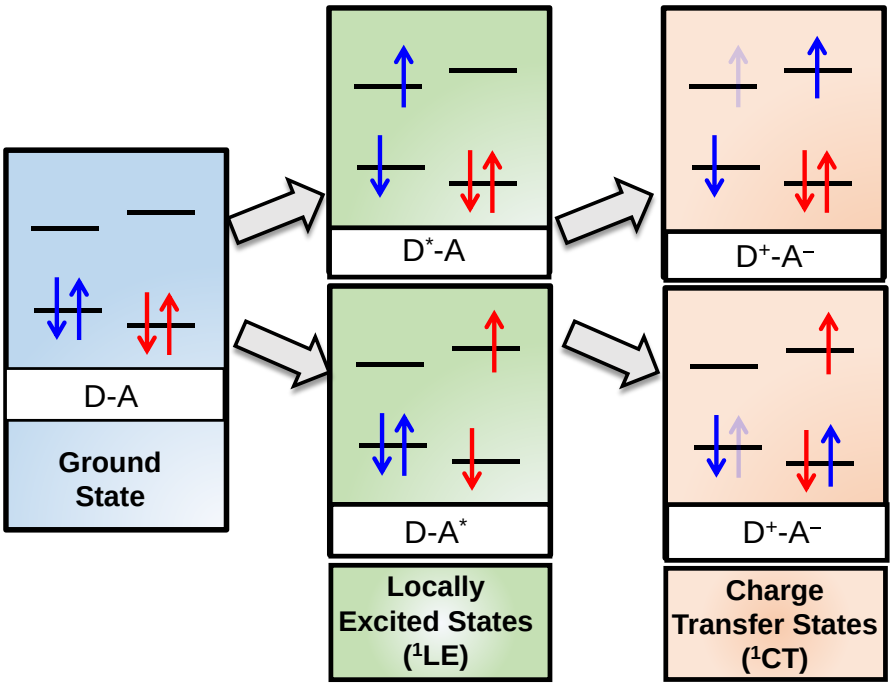

Figure 4. Schematic representation of an electron donor (D) and acceptor (A) molecule (D-A) in the ground state, locally excited singlet state (^{1}LE) and charge-transfer singlet state (^{1}CT) having a zwitterionic character, $D^{+\bullet}-A^{-\bullet}$. D* and A* represent photoexcited donor and acceptor units, respectively. In the charge-transfer state energy levels, the semi-transparent arrows denote the position where the electron has been transferred from.

The first reports of charge-transfer mediated ISC to populate a triplet state can be traced back to the work published by El-Sayed[75] and later by Okada et al.[76] The schematic representation of the formation of charge transfer mediated SOCT-ISC and RP-ISC is provided in Figure 5. Typically, when electron donor and electron acceptor moieties are connected with a spacer bridge, the ^{1}CT state acts as a precursor to trigger radical-pair intersystem crossing (RP-ISC) due to hyperfine coupling (HFC). The latter usually occurs when there is a spacer molecule between the D and A moieties and a very weak D−A electronic interaction that eventually decreases the *J* value (where *J* is a spatial overlapping wavefunction for two electrons, corresponding to the singlet−triplet

energy difference) for the radical pair [$D^{+\bullet}-A^{-\bullet}$], and ^{3}CT is populated due to HFC. If the ^{3}CT state is lying higher than the ^{3}LE state, the latter can be populated by charge recombination (CR). However, if ^{3}CT has a lower energy than the ^{3}LE state, a long-lived ^{3}CT state can be observed. Moreover, in compact, orthogonally connected D−A systems, in which the molecular orbital angular momentum changes during CR, causing variation in the electron-spin angular momentum, the CR-induced ISC, also called spin-orbital charge-transfer (SOCT) ISC, becomes evident.[77–80] Recently, a tremendous interest has been witnessed in exploring the CS-involved ISC to yield triplet states in D−A systems comprising a boron dipyrromethene (Bodipy; 4,4-difluoro-4-bora-3a,4a-diaza-s-indacene),[66,81–85] naphthalenediimide,[86–89] perylene,[90,91] perylenebisimide,[78,92–95] etc.

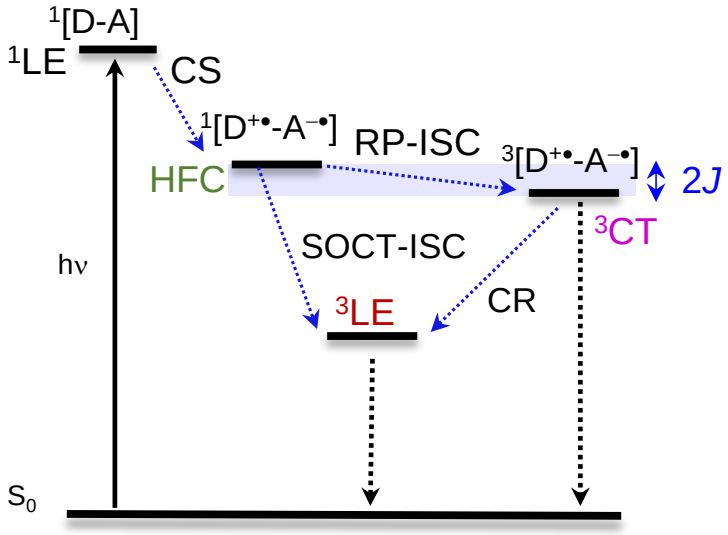

Figure 5. Schematic representation of CT-mediated ISC. HFC stands for a hyperfine coupling interaction. ^{1}[$D^{+\bullet}-A^{-\bullet}$] and ^{3}[$D^{+\bullet}-A^{-\bullet}$] represent charge-transfer singlet (^{1}CT) and triplet (^{3}CT) excited states, respectively. ^{3}LE and *J* denote the locally excited triplet state and the exchange energy of electrons, respectively. Where D and A represents an electron donor and electron acceptor unit in the molecule.

It is important to mention that in compact D−A-based molecules, the electronic coupling between D and A can be tuned by controlling their geometry. One of the interesting aspects of this tuning is to attain a new band in the electronic absorption and emission spectra at long wavelengths, i.e., a new (broad) absorption/emission band that is absent in the absorption/emission spectra of the separate D and A moieties.[96–99] Its origin in the D−A system lies in an appropriate electronic coupling between the D and A moieties, resulting in an accessible charge-transfer absorption ($S_0 \rightarrow {}^1CT$).[100–103] The energy and intensity of the CT absorption is strongly dependent upon the viscosity and polarity of the solvent media used for the measurement.[104]

3.1 Significance of $S_0 \rightarrow {}^1CT$ photo-excitation for efficient TTA-PUC

The CT electronic absorption is important for two reasons. First, the CT absorption band is red-shifted compared to the LE singlet state (S_1) and hence it is possible to excite the molecule at longer wavelengths and attain a sufficiently prolonged anti-Stokes shift in a TTA up-conversion (Figure 1b). Secondly, although $S_0 \rightarrow {}^1CT$ absorption is observed at a longer wavelength (a lower energy), the triplet energy state remains uncompromised. Hence, there is a reduced energy loss in ISC upon the population of the ${}^1CT$ state ($S_0 \rightarrow {}^1CT \rightarrow T_1$) as there is a smaller energy gap between ${}^1CT$ and the triplet state compared to the locally excited singlet ($S_0 \rightarrow S_1$ (LE) $\rightarrow T_1$) separated from the triplet state by a large energy gap, as illustrated in Figure 2b. The use of CT state for photoexcitation of a chromophore is helpful for limiting the energy losses during ISC by electronic excitation into the ${}^1CT$ state, which can further improve the up-conversion quantum yield. To use this strategy for TTA-PUC, Zhao et al. synthesized a Bodipy−perylene D−A dyad (Figure 6).

Table 1. Photophysical and TTA-PUC Properties of CT excitable and TADF Photosensitizers.

Sensitizer	Emitter	Solvent/ Medium	λ_{exc}[a]/nm	τ_T[b]/μs	$\Delta E_{S/T}$[c]/eV	Φ_{UC}[d]/%	ΔE_{UC}[e]	Ref.[f]
BDP-Pery	**perylene**	toluene	589	196	0.64	5.7	0.65	[105]
4Cz-TPN-Ph	**DPA**	thin film	532	NS	0.11	0.28	0.56	[106]
4-Cz-IPN	**q-Ph**	benzene	445	80	0.083	3.9	0.73	[107]
4-Cz-IPN	**t-Ph**	benzene	445	80	0.083	2.8	0.83	[107]
4-Cz-IPN	**PPO**	OA-THF	445	80	0.083	-[g]	0.52	[108]
4-Cz-IPN	**pyrene**	OA-THF	445	80	0.083	0.66	0.44	[108]
4-Cz-IPN	**BPh-TIPS**	C-HEX	447	80	0.083	4.0	1.17	[109]
4-Cz-IPN	**R-/S-TP**	toluene	445	80	0.083	7.9	0.40	[110]
BTZ-DMAC	**DPA**	toluene	545	-[g]	0.11	1.9	0.52	[111]
DCF-MPYM	**DPA**	THF	635	22.1	0.03	11.2	0.94	[112]
DCF-MPYM	**Py**	THF	635	22.1	0.03	7.0	0.80	[112]
DCF-MPYM-Me	**DPA**	THF	635	40	0.02	13.6	0.94	[113]

[a] Excitation wavelength used for TTA-PUC. [b] Triplet lifetime. [c] Singlet-triplet energy gap. [d] Up-conversion quantum yield. [e] Anti-Stokes shift. [f] Literature reference. [g] Not reported. For literature references lacking the anti-Stokes shift values, the latter were calculated from the TTA-PUC spectra supplied in the research papers.

Free Bodipy absorbs at 500 nm and perylene between 400−450 nm (showing a vibronic structure). For the Bodipy-perylene dyad (**BDP-Pery**) a new, moderately broad absorption band is

observed at a lower energy (at 535−635 nm). The CT origin of the absorption has been confirmed by time dependent density functional theory (TD-DFT) calculations. This CT absorption band appears as a result of increased electronic coupling between the two moieties in the dyad featuring a coplanar conformation that is permitted in the absence of the methyl groups in the 1,3,5,7-positions at the Bodipy moiety. This dyad is used for TTA up-conversion with perylene as the triplet acceptor.[105] The CT absorption band permits excitation at a longer wavelength (589 nm) and the up-conversion quantum yield of 5.7% was determined in this case (Figure 1b). The detailed photophysical parameters are listed in Table 1. An increased anti-Stokes shift of 0.65 eV was observed by the excitation into the CT state, compared to the anti-Stokes shift of merely 0.37 eV for the LE excitation.[105]

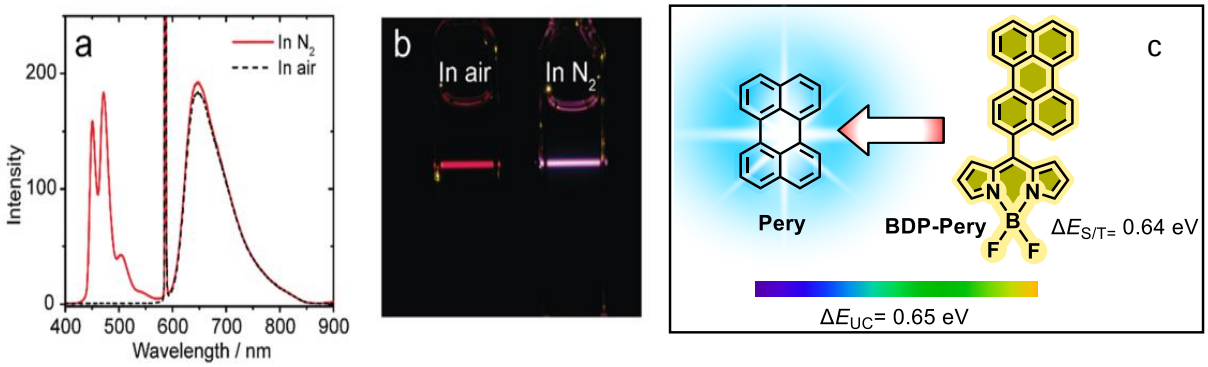

Figure 6. TTA-PUC of **BDP-Pery** (sensitizer) and **Pery** (acceptor/emitter) upon the excitation at 589 nm in N_2- and air-saturated solutions. (a) UV-visible photoluminescence up-conversion spectra of **BDP-Pery** (sensitizer) and **Pery** (acceptor/emitter) in toluene. (b) A photographic representation of the TTA-PUC solutions containing the sensitizer and acceptor showing UC emission in N_2 saturated solution along with reference in air saturated environment (c) Molecular structures of the sensitizer and acceptor. Reproduced by the permission of the *American Chemical Society* (Figures 6a and 6b).[105]

4. TADF TO MINIMIZE ENERGY LOSS DURING ISC FOR TTA-PUC

Thermally activated delayed fluorescence (TADF) has recently gained prodigious attention due to its intensive use in the organic light emitting diodes (OLEDs).[114–119]TADF molecules are usually made up of at least one electron donor and one electron acceptor moiety. The energy difference between the singlet and triplet states is very small, which is favorable for facile reverse ISC (reISC). The reISC is due to a transition from a triplet to a singlet state of the system. As a result, a radiative decay is observed from the singlet state after reISC with a time delay, being termed as delayed fluorescence (DF). The DF spectral profile is same as normal fluorescence; however, due to the involvement of a triplet state, the fluorescence decay lifetime is longer and emission intensity is oxygen senstive.[120,121] To exhibit an efficient TADF, the molecules should not only feature a minimum singlet/triplet energy gap (< 150 meV) but also experience a low non-radiative decay.[43,122,123]

Another important aspect that influences the TADF efficiency is the exchange energy of electrons, J, which can be defined as the singlet−triplet energy gap ($2J = \Delta E_{S/T}$).[124,125] The diminished value of electron exchange energy consequently favors an efficient TADF. The evaluation of J value for a TADF system can be represented by Equation 5.

$$J = \iint \emptyset_{\mathrm{H}}(r_1)\varphi_L(r_2)\left[\frac{e^2}{r_1 - r_2}\right]\emptyset_{\mathrm{H}}(r_2)\varphi_L(r_1)dr_1dr_2 \qquad (5)$$

In Equation 5, e represents electronic charge, $\emptyset_{\mathrm{H}}$ and φ_{L} stand for HOMO and LUMO wave functions, respectively, and r_1, r_2 denote positions of coordinates. It can be apprehended that decreasing the overlap of HOMO−LUMO electronic densities in the donor and acceptor moieties in a D−A molecule can be useful for an efficient TADF manifestation. From the perspective of a

molecular structure designed to improve the separation of the HOMO and LUMO electronic densities, the connecting bonds between the D and A moieties should be twisted to obtain a spatially perpendicular geometry.

SOC also plays a substantial role in reISC. In early research on the TADF mechanism it was believed that low-lying singlet and triplet energy levels were involved in the singlet-to-triplet ISC and triplet-to-singlet reISC. However, recent studies have revealed that this mechanism is relatively complicated. Usually, upon photoexcitation of a TADF molecule, ^{1}LE or ^{1}CT states are populated, followed by ISC to ^{3}CT and/or ^{3}LE states.[126] In most of the molecules, a ^{1}CT singlet state is predominantly generated upon photoexcitation due to a D→A electron transfer. ^{1}CT→^{3}CT ISC is a forbidden process because singlet−triplet coupling with an identically occupied spatial orbital is zero.[127] Population of ^{3}LE directly from a ^{1}LE is also forbidden due to the same reason. The El-Sayed rule for ISC rates states that SOC and efficient reISC (and hence TADF) from a ^{1}CT state is possible if donor and/or acceptor ^{3}LE is in resonance with ^{1}CT.[128–134] The significant role of a closely lying ^{3}LE state in the overall TADF process was reported by many scientists; however, the high reISC rate constants (TADF k_{reISC} >10^6 s^{-1}) obtained experimentally cannot be justified by SOC between ^{1}CT and ^{3}LE or by the hyperfine coupling (HFC) between ^{1}CT and ^{3}CT states. It was proposed that both triplet states (^{3}CT and ^{3}LE) are crucial to achieve the reISC process by using quantum dynamics technique. This has led to the discovery that when optimizing TADF molecules, there are at least two energy gaps to be considered. To achieve an equilibrium between the ^{3}LE and ^{3}CT states and enable adiabatic crossover between the ^{1}CT and ^{3}CT states, there is possibility of a spin inversion between the ^{3}CT and ^{1}CT states while ^{3}LE-TADF is vibronically coupled to these states. [134–137] The mixing of the ^{3}CT and ^{3}LE states is illustrated in Figure 7. Part 7(a) corresponds to a scenario where the ^{3}CT and ^{3}LE states do not interact at all, resulting in a

very low reISC rate. In Part 7(b) the ^{3}CT and ^{3}LE states are mixing at the crossing point due to vibrational coupling, which enhances the reISC process to ^{1}CT.[134–137]

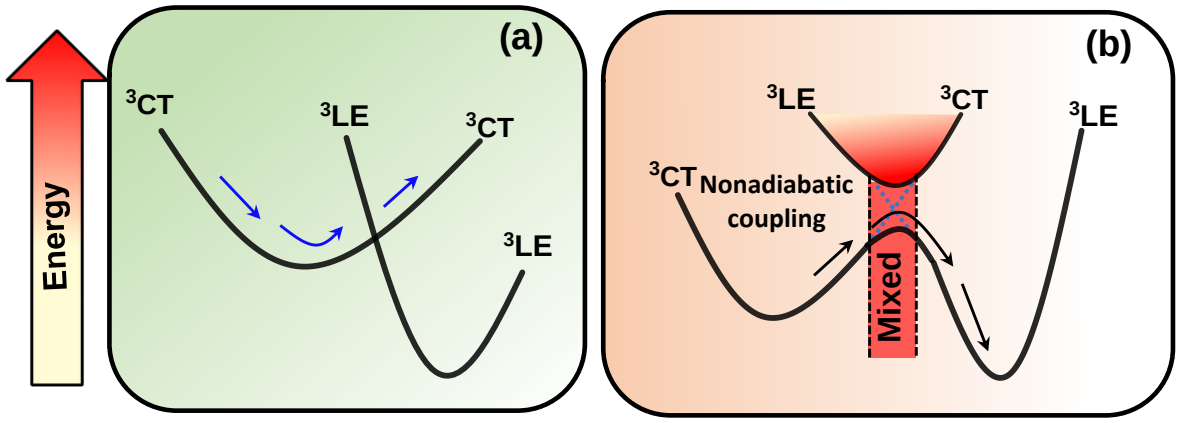

Figure 7. A typical TADF model demonstrating (a) non-adiabatic coupling in the absence of a ^{3}LE and ^{3}CT interaction, and (b) non-adiabatic vibronic coupling at the coincidence point of the ^{3}LE and ^{3}CT states.

4.1 Desired characteristics of TADF sensitizers for efficient TTA-PUC

A great deal of interest in using TADF molecules as light-harvesting contenders for TTA-PUC has been noticed in the last decade. The uprising use of TADF photosensitizers in converting low-energy photons to high-energy photons can be explained with the special characteristics of these molecules. First, TADF molecules typically show ISC without involving a heavy atom. The first and second generation of triplet photo-excitable sensitizers were capable of undergoing singlet-to-triplet ISC due to the SOC effect of heavy atoms, that is, metals such as platinum, iridium, palladium, ruthenium, or non-metals, for instance bromine and iodine.[138–145] These heavy atoms bring with them many disadvantages, including high costs of precious metals. Hence, triplet photo-excitable sensitizers without a heavy atom, such as TADF sensitizers, are superior compared to the first and second generation of sensitizers because of the small singlet-triplet energy gap, $\Delta E_{S/T}$,

in the TADF molecules facilitating ISC. Secondly, due to small $\Delta E_{S/T}$, the energy loss during ISC is diminished. In most triplet photo-excitable sensitizers $\Delta E_{S/T}$ is large. Some of the excitation energy therefore becomes dissipated during the singlet-to-triplet ISC. In ^{1}CT-excitable photosensitizers the singlet−triplet energy gap is decreased (as discussed earlier) compared to traditional triplet photo-excitable sensitizers, which reduces energy losses during ISC. However, in TADF molecules this singlet-triplet energy gap is further reduced, enhancing energy saving during the ISC (Figure 1). Currently most of the major studies on TADF photo-excitable sensitizers focus on achieving high delayed-fluorescence quantum efficiency, which is desired for practical applications such as in LEDs. For these applications an efficient reISC is therefore crucial to enable a delayed radiative decay from singlet state. However, contrary to LED applications, the desired properties of TADF photo-excitable sensitizers for TTA-PUC are slightly different. A suitable TADF sensitizer for TTA-PUC and LED applications should manifest a high ISC quantum yield and a small singlet-triplet energy gap to avoid energy loss during ISC. However, the requirement inverse to LED application is that the reISC from a triplet to singlet state should be inefficient for TTA-PUC application. Due to inefficient reISC in the triplet sensitizer, TEnM from a sensitizer to acceptor can be promoted. Reversely, a TADF photo-excitable sensitizer with an efficient reISC may manifest poor TEnM from sensitizers to acceptor in a TTA-PUC system due to an active triplet-to-singlet ISC channel. A high up-conversion luminescence quantum yield may accordingly emerge from TTA-PUC exhibiting poor reISC and efficient TEnM.

4.2 Carbazolyl dicyanobenezene-based TADF sensitizers for TTA-PUC

Baldo and co-workers used a red TADF (600 nm)-manifesting molecule for the first time in a TTA up-conversion system.[106] Specifically, **4CzTPN-Ph** (Figure 8), previously reported for its application in OLEDs, was used as a triplet sensitizer with DPA as a triplet acceptor.[122] This

photosensitizer exhibits a photoluminescence quantum yield of 26%. Its synthesis was carried out under an inert an atmosphere assisted by sonication to reach a high product yield (76%). TTA-PUC up-conversion for **4CzTPN-Ph** was evidenced in a solid-state system where a 20−50 nm-thick layer of a triplet annihilator and sensitizer was fabricated on a quartz surface by a vacuum thermal evaporation methodology. A linear relationship was observed between the UC luminescence intensity and laser power. The delayed emission lifetime was reported to be 1.72 μs for the neat film. The TEnM efficiency for the TADF sensitizer and the acceptor was reported to reach 9.1%. Although the reported TTA-PUC efficiency (0.28%) was not very high and the anti-Stokes shift was 0.56 eV, these results have opened the door to utilizing a new type of photosensitizer in TTA-PUC. Later many attempts were made to improve the up-conversion quantum yield and the anti-Stokes shift in TTA-PUC systems by using TADF photosensitizers as light-harvesting molecules. These photosensitizers, despite of red-shifted absorption, maintain an uncompromised, high triplet-energy state, making it possible to use triplet acceptors with a higher-energy state (shorter wavelength), resulting in an increased anti-Stokes shift for a TTA-PUC system.

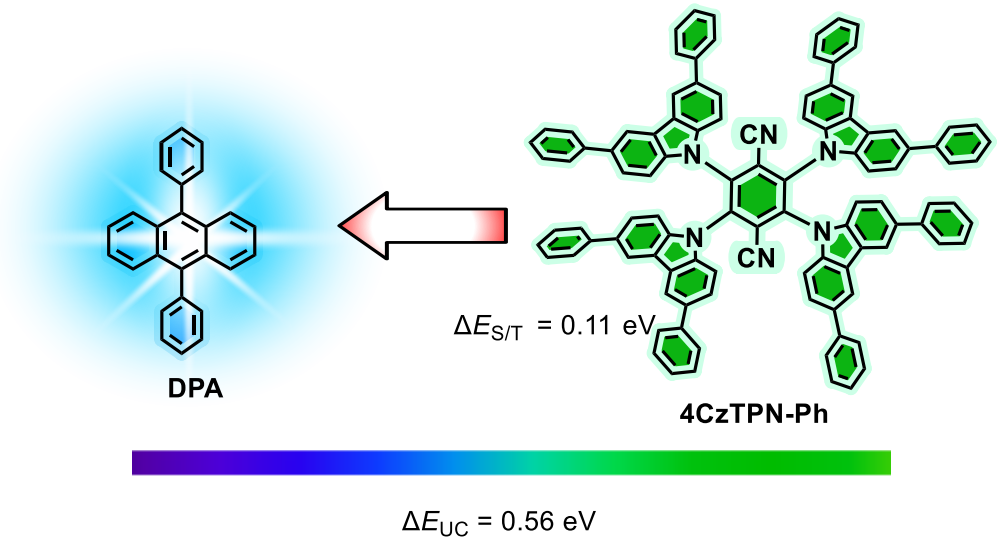

Figure 8. A TTA-PUC system consisting of **4CzTPN-Ph** as the TADF sensitizer and **DPA** as the acceptor, along with the value of the anti-Stokes shift and the singlet−triplet energy gap in the TADF photosensitizer.

Carbazolyl dicyanobenezene (**4-Cz-IPN**; Figure 9) is a widely studied TADF sensitizer, first reported by Adachi et al. for organic LED applications.[122] This molecule shows strong absorption of UV-visible light in the range of 280-490 nm. The contribution of a charge-transfer character to the electronic excitation in the visible region (for the S_1 state) was revealed by TD-DFT calculations showing the HOMO and LUMO localized on the electron donor (carbazolyl) and acceptor (dicyanobenzene) moieties, respectively. This is a green-light emitting molecule (λ_{em} = 507 nm) with a very high luminescence quantum yield reaching up to 94% and a delayed-fluorescence lifetime of 5.1 μs for the longer component. The steric hindrance created between dicyanobenezene and carbazolyl groups in **4-Ca-IPN** is responsible for 60^o dihedral angle between them. Hence, the HOMO and LUMO are clearly separated, leading to a small singlet−triplet energy gap of 0.083 meV. These properties make **4-Cz-IPN** a suitable contender for manifesting TADF that is indeed experimentally observed.[122] The synthesis of this compound is relatively easy and straightforward.

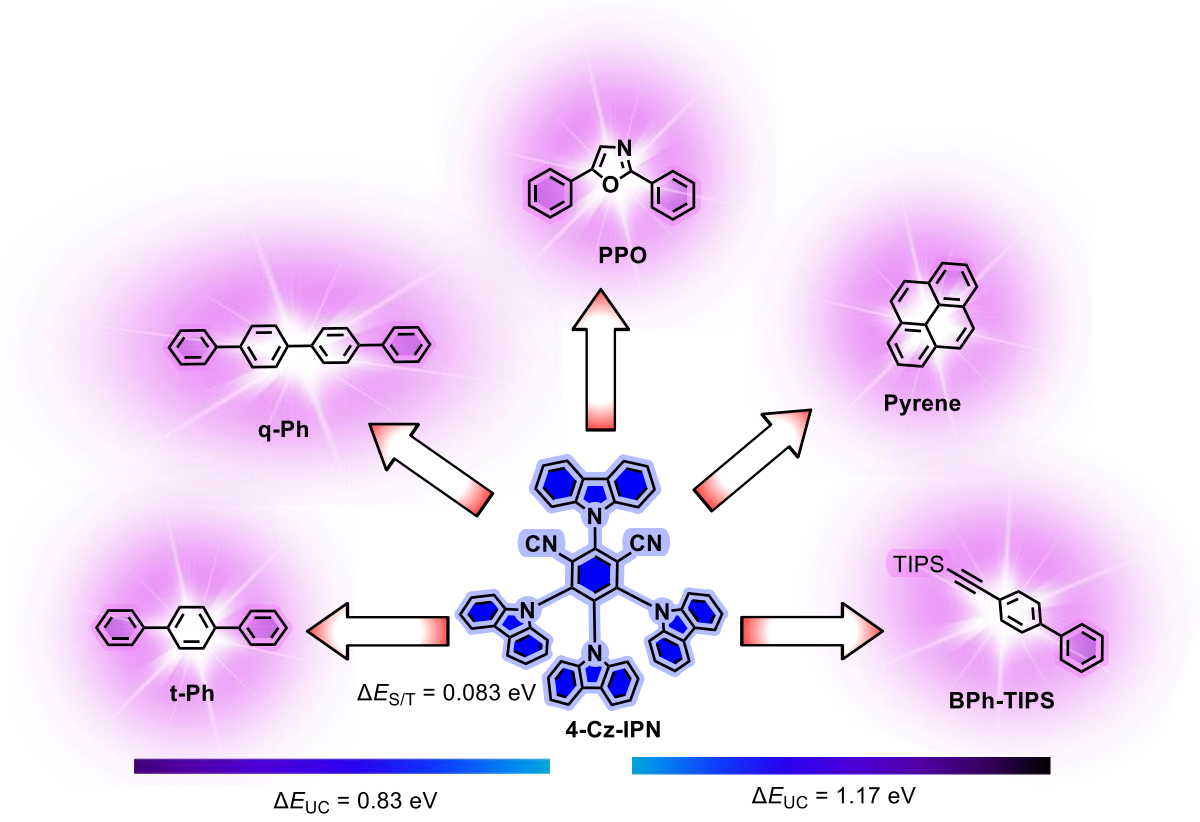

Figure 9. A TTA-PUC system consisting of a TADF sensitizer (**4-Cz-IPN**) combined with **t-Ph**, **q-Ph**, **PPO**, **pyrene**, and **BPh-TIPS** triplet acceptors. Two highest anti-Stokes shift values obtained with **t-Ph** and **BPh-TIPS** and the singlet−triplet energy gap in the TADF photosensitizer are also added.

4-Cz-IPN has been an intensively studied TADF photosensitizer for TTA up-conversion. The discussion of the nature of the triplet state in **4-Cz-IPN** will benefit from a brief overview of electron paramagnetic resonance (EPR) spectroscopy as a useful technique to unravel this TADF property. The nature of the triplet state in TADF sensitizers can be ^{3}LE, ^{3}CT, or co-existence of both. EPR spectroscopy is a useful technique to distinguish these paramagnetic states due to its remarkable selectivity towards the populated triplet sublevels leading to electron-spin polarization (ESP) of the lowest triplet sublevels. As a matter of fact, usually very dissimilar ESP patterns as

well as different rates for the populated sublevels of the triplet state are observed for the two different ISC mechanisms.[146] EPR is therefore very useful to differentiate between the ISC mechanisms, i.e., the ^{3}LE or ^{3}CT states.[78–80] In EPR spectra, as a result of ESP transitions, a polarization-enhanced emission 'E' or absorption 'A' signals are observed. Consequently, different spin-polarization patterns are observed for different molecules in their EPR spectra. For **4-Cz-IPN**, the spin polarization mechanism is represented in Figure 10. The EPR spectral pattern for **4-Cz-IPN** was observed to be AEE/EAA. With the aid of spectral simulations, none of separate SOC- or HFC-based mechanisms could reproduce the experimental EPR spectra. However, when the HFC and SOC mechanisms were considered together, the spectral match was perfect. Hence based on these results it was suggested that the direct involvement of HFC between ^{1}CT and the higher triplet states T_n is a precursor to populate a ^{3}CT state that upon internal conversion to a closely-lying lower triplet state, ultimately populates the ^{3}LE state (Figure 10). A small energy gap between ^{1}CT and ^{3}CT states, which is smaller than the Zeeman energy (0.21−0.40 cm^{-1}), also favors this claim.[147]

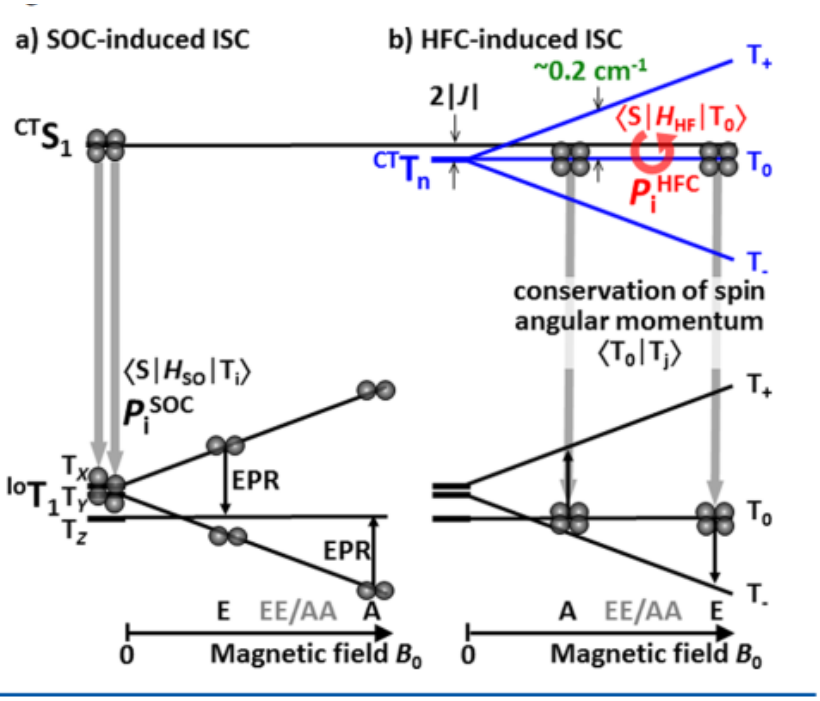

Figure 10. A spin-polarized mechanistic representation of the triplet excited state of **4-Cz-IPN** induced by ISC from the singlet excited state (S_1) in the presence of an external magnetic field along the *z*-axis. Reproduced by permission of the *American Chemical Society*.[147]

In 2016, Kimizuka and co-workers utilized TADF-manifesting **4-Cz-IPN** as a photosensitizer combined with *p*-quarterphenyl (**q-Ph**) and *p*-terphenyl (**t-Ph**; Figure 9) triplet acceptors, in an attempt to further increase the anti-Stokes shift of TTA up-conversion.[107] Upon photoexcitation of the sensitizer at 445 nm, up-converted UV emission of **q-Ph** and **t-Ph** was observed, with anti-Stokes shifts of 0.73 eV and 0.83 eV, respectively. The up-conversion quantum yield was estimated slightly below 2.8% for **t-Ph** and increased to 3.9% when **q-Ph** was used as the triplet acceptor. The up-converted emission observed in the near-UV region (below 420 nm) is supremely beneficial for photocatalytic splitting of water molecules to produce H_2 as a green fuel for energy devices. Such applications can effectively amplify the efficiency of solar energy utilization at wavelengths that are usually hard to harvest due to small bandgaps of solar devices.[22,148]

Photostability of the TTA-PUC system based on the **4-Cz-IPN** photosensitizer and **t-Ph**, **q-Ph** as triplet acceptors was studid in 2019 by Kim and co-workers.[108] Two new acceptors, viz. 2,5-diphenyloxazole (**PPO**; Figure 9) and pyrene were also tested. Oleic acid was used as a medium for the TTA-PUC due to its ability to act as a singlet-oxygen receptor in aerated solutions, thereby providing a facility to observe TTA-PUC under aerated conditions. Their work demonstrated that no decrease in up-converted emission was observed upon excitation of **4-Cz-IPN** with a 445-nm laser light up to 30 min, when pyrene was used as the triplet acceptor. Contrary to pyrene, the other acceptors (**t-Ph**, **q-Ph**, **PPO**) paired with **4-Cz-IPN** in the TTA-PUC were less efficient and a decrease in TTA-PUC luminescence was evidenced. This undesired result was ascribed to photodegradation of **4-Cz-IPN** and a modified proportion of reISC and TEnM. Although the **4-Cz-IPN** /**pyrene** pair demonstrated photostability for up to 1 h, with an up-conversion quantum yield reaching 0.66% in air, the anti-Stokes shift for this visible-to-near UV up-conversion was merely 0.44 eV.

Although a sharp drop in the solar absorption spectrum occurs below 310 nm, the photons with energies in this hazardous UV-B/C range are highly important in many applications, such as the treatment of industrial waste waters[149] and photocatalytic water splitting,[150,151] not accessible with low-energy photons in the visible spectral range from commercial ready-to-use LEDs.[152] Hence in an effort to harvest energy from the visible spectral region and up-convert it into the near-UV/UV region, a team of German scientists reported[109] an organic TTA-PUC system consisting of the **4-Cz-IPN** photosensitizer paired with a novel triplet acceptor *p*-biphenyl-triisopropylsilylethynyl (**BPh-TIPS**) (Figure 9) to provide an alternative annihilator with emission beyond 310 nm. They succeeded to achieve a blue to UV-A TTA-PUC with a remarkably large anti-Stokes shift of 1.17

eV by photoexciting **4-Cz-IPN** at 447 nm. The up-conversion quantum yield for this system was reported to reach 4.0%.

Chiral compounds are capable of displaying circularly polarized luminescence (CPL)[153–156] that has various potential applications, for example in the field of biology for cancer diagnosis,[157] in synthetic chemistry for photo-driven chemical synthesis,[158,159] and in physics for the optical displays.[160–163] However, this property is rarely reported in real-time applications due to the poor luminescence dissymmetry factor (g_{lum}). Duan and his co-workers used chiral *R*(S)-4,12-biphenyl[2,2]paracyclophane (**R-/S-TP**; Figure 11) as an annihilator paired with the **4-Cz-IPN** photosensitizer to obtain a high TTA-PUC quantum yield of 7.9% by excitation with 445-nm laser light.[110] They designed and used this TTA-PUC system to improve the value of the g_{lum} of the triplet emitter, which serves as a pivotal index for the quantification of the CPL performance. It can be expressed as $g_{lum} = 2 \times (IL - IR)/(IL + IR)$, where IL and IR represent left-handed and right-handed CPL intensities of a chiral luminescent molecule. Its value ranges between +2 and −2, corresponding to left- or right-handed CPL. The authors claimed to have amplified the g_{lum} value of **R-/S-TP** by TTA-PUC significantly, from 3.1×10^{-3} to 9.2×10^{-3}. Moreover, this CPL-active TTA-PUC was also realized in a smart material called (disordered) nematic liquid crystals (NLC) and the g_{lum} value was further boosted up to 0.19, which was associated with special optical properties of NLC such as circular dichroism and optical rotation (Figure 11). This high g_{lum} value of was further utilized in enantioselective photo-triggered polymerization of diacetylene.[110]

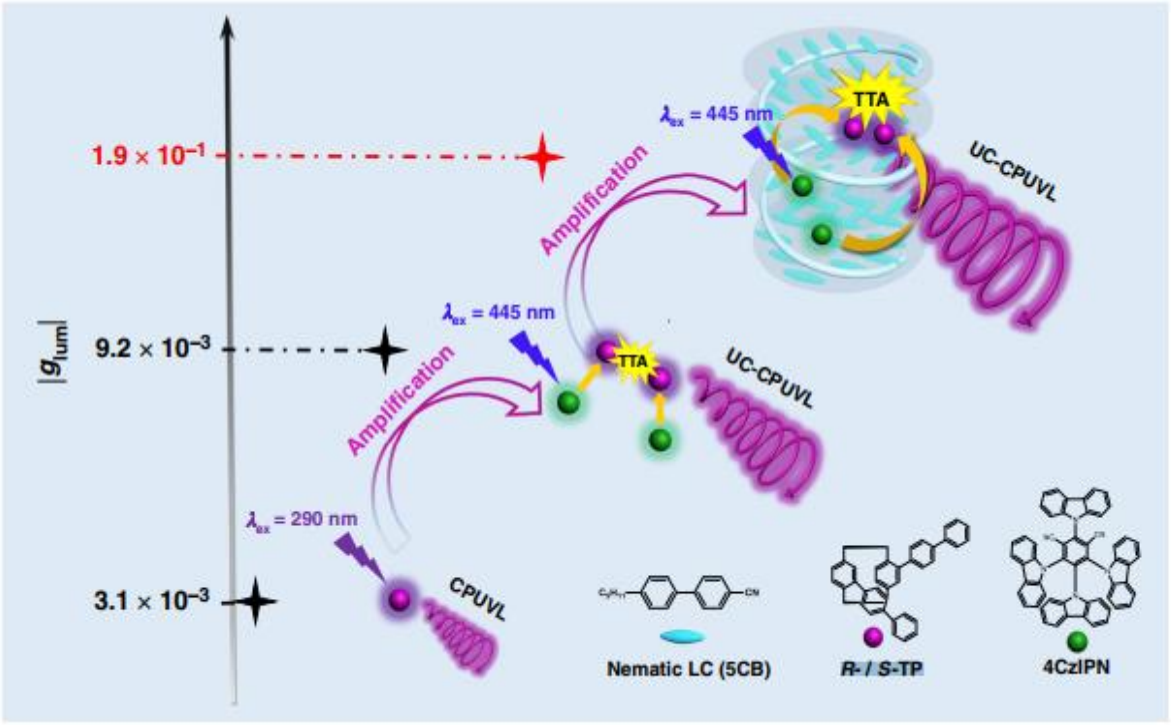

Figure 11. A circularly polarized luminescence (CPL)-active TTA-PUC system consisting of the TADF sensitizer (**4-CZ-IPN**) and the triplet acceptor (**R-/S-TP**), which results in a boosted in g_{lum} value realized in a nematic liquid crystalline phase (**5CB**). UC-CPUVL stands for up-converted circularly polarized ultraviolet luminescence. Reproduced by permission of the *Nature Publishing Group*.[110]

Ma and co-workers reported a series of TADF-based carbazolyl dicyanobenezene derivatives (**4CzPN**, **4CzPN-1DBP**, **4CzPN-2DBP, 4CzPN-8DBP,** Figure 12) along with **4-Cz-IPN** as a reference photosensitizers for visible to near-UV photon up-conversion with 2,7-di-*t*-butyl-pyrene (**DBP**) as a triplet annihilator.[164] They found that efficient reISC in the TADF molecules (**4-CzPN** and **4-Cz-IPN**) causes inefficient TEnM to the annihilator (**DBP**) and, consequently, a low up-conversion quantum yield. To address this issue, **DBP** was appended to the photosensitizer with a linker (Figure 12) to suppress reISC and to achieve efficient TEnM to the annihilator. As a result,

reduced singlet−triplet equilibrium facilitated the triplet exciton to shift and become localized on the appended triplet annihilator. The results in polyurethane films demonstrated a very weak TTA-PUC with **4-CzPN** and **4-Cz-IPN**; however, **4CzPN-1DBP** exhibited 80× higher up-converted emission intensity.

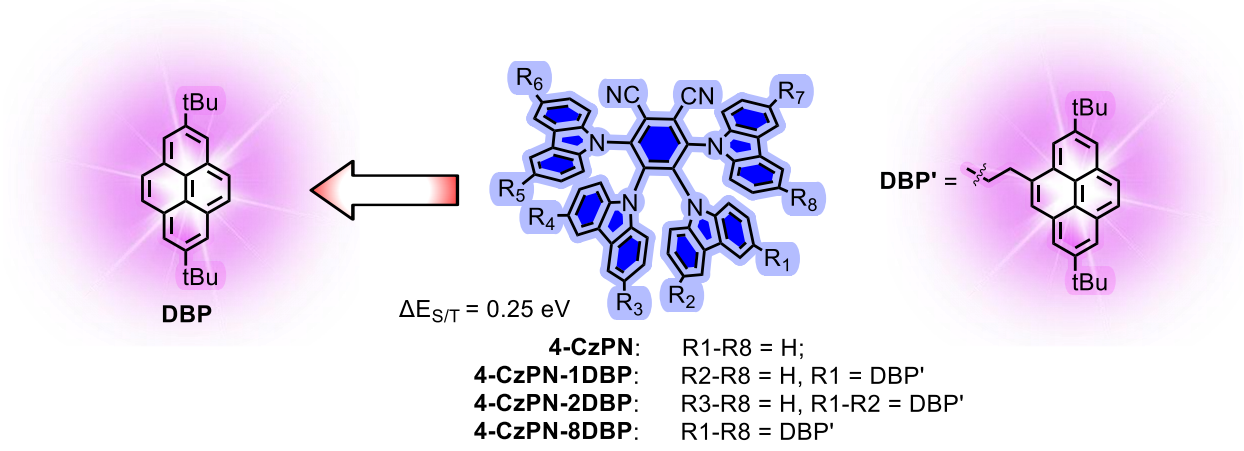

Figure 12. TTA-PUC system consisting of TADF sensitizers, **4CzPN**, **4CzPN-1DBP**, **4CzPN-2DBP** and **4CzPN-8DBP**, paired with the appended **DBP** triplet acceptors.

In 2018 Ma, Castellano and their co-workers reported energy migration dynamics of **4CzPN-1DBP**.[165] They found that the triplet exciton of **4CzPN** was transmitted to the **DBP** moiety, followed by a transfer to free **DBP** by TEnM in an organic solvent. Ultrafast transient absorption (TA) spectroscopy revealed triplet decay rate constants reaching $9.9 \times 10^2\ s^{-1}$ and $7.4 \times 10^2\ s^{-1}$ for tethered and monochromophoric molecules, respectively. An efficient and irreversible intramolecular TEnM from **4CZPN** to **DTBP** was observed due to the slower triplet decay of **DTBP** in the tethered molecule, which was responsible for the higher yield of TTA-PUC

4-Cz-IPN is the most widely used TADF photo-excitable sensitizer for the application in TTA-PUC and high up-conversion quantum yields and remarkably large anti-Stokes shifts have been demonstrated. However, this molecule and its reported derivatives absorb in the green region of

the visible light. A careful design of **4-Cz-IPN** derivatives with appended chromophores that shift the visible absorption of the molecules to the red/near-IR region while keeping the triplet energy levels uncompromised, can be can appealing choice for their future use in biological and energy applications.

4.3 Benzothiadiazole- and naphthalenediimide-based TADF photosensitizer for TTA-PUC

The D-A-D triad obtained by the condensation of donor benzothiadiazole (BTD) and two acceptor 9,9-dimethyl-9,10-dihydroacridine (DMAC) moieties (**BTD-DMAC**, Figure 13) exhibits an intramolecular CT behavior.[122,166,167] This photo-excitable sensitizer was initially reported to be used for a red LED, with the external quantum efficiency reaching up to 8.8% and the triplet quantum yield of 51.2%. It can be easily synthesized by a C−N coupling reaction between dibromobenzothiadiazole and DMAC under an inert atmosphere, using Pd(II) acetate as a catalyst to obtain a high reaction yield (76%).[168]

Yang and co-workers utilized red TADF-emitting **BTD-DMAC** as a photosensitizer in TTA-PUC.[111] DPA was used as a triplet annihilator paired with this sensitizer and a very long anti-Stokes shift (97 nm) was determined for this system. The luminescence of this UC system covers almost all the blue (up-converted emission) and red (TADF emission) visible region, with up-conversion quantum yield reaching 1.9% (Table 1). For this system, photon up-conversion was also evidenced even in aerated toluene at increased concentration of the sensitizer and acceptor (1:20), which was attributed to the non-quenched triplet state of the sensitizer in the aerated environment. A moderately large anti-Stokes shift (0.52 eV) was observed for this system.

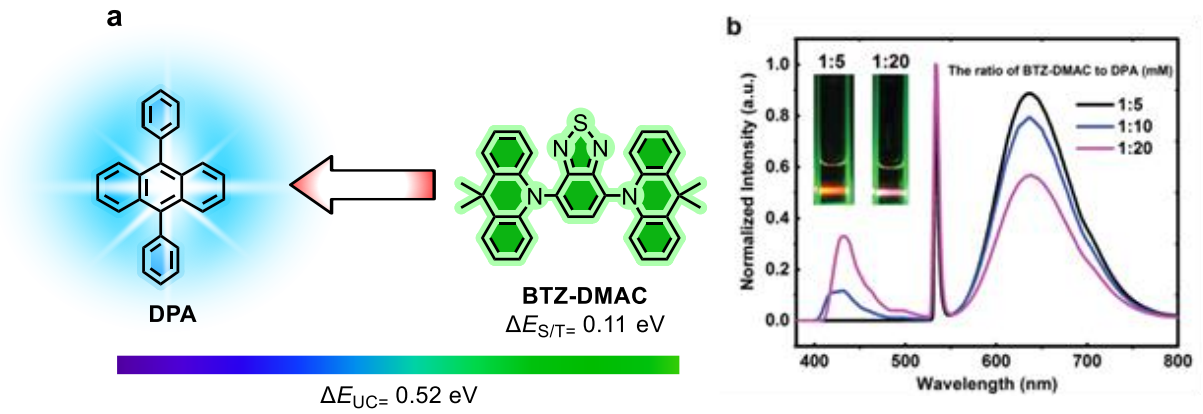

Figure 13. (a) TTA-PUC system consisting of a TADF sensitizers **BTZ-DMAC** paired with **DPA** as the triplet acceptor, with the corresponding values of the singlet−triplet energy gap in the photosensitizer and the anti-Stokes shift. (b) TTA-PUC emission spectra of the **BTZ-DMAC** and **DPA** mixture at three different concentration ratios and photographs in inset showing TTA-PUC. Reproduced by the permission of the *Royal Society of Chemistry*.[111]

Naphthalenediimide (**NDI**) is a well-known chromophore and has intensively been studied in the fields of photochemistry, photobiology and photophysics.[169–172] Hussain et al. have recently reported a series of **NDI**-carbazole-based compact electron donor-acceptor systems demonstrating SOCT-ISC and TADF. For these molecules, population of a triplet state upon photoexcitation of **NDI-Cz-Ph** and **NDI-Ph-Cz** (Figure 14**)** via a charge-transfer state was evidenced with fs-ns TA spectroscopy. A moderate $^1O_2$ production (~26% quantum yield) further supported the population of the triplet state.[88] The photophysical properties of these molecules were also studied with the time resolved electron paramagnetic resonance (TR-EPR) spectroscopy to clarify the nature of the populated triplet states. TR-EPR is a useful tool to investigate spin polarization of a triplet state.[78–80,173,174] With the aid of this technique it was confirmed that for **NDI-Cz-Ph** ^{1}CT→^{3}LE followed by a long lived ^{3}CT state was observed, with a lifetime of 45 µs (Table 2). For **NDI-Ph-Cz**, ^{1}CT→^{3}LE ISC occurs and the lifetime of 51.9 µs was determined for the triplet state. The small

singlet−triplet energy gap in these triads is responsible for reISC and hence TADF. These TADF molecules were used as sensitizers for TTA up-conversion with **DPA** as a triplet acceptor and a high up-conversion quantum yield of 8.2% with the anti-Stokes shift of 0.55 eV were observed at very low concentrations of the photosensitizer (10^{-5} M) and acceptor (4×10^{-5} M).

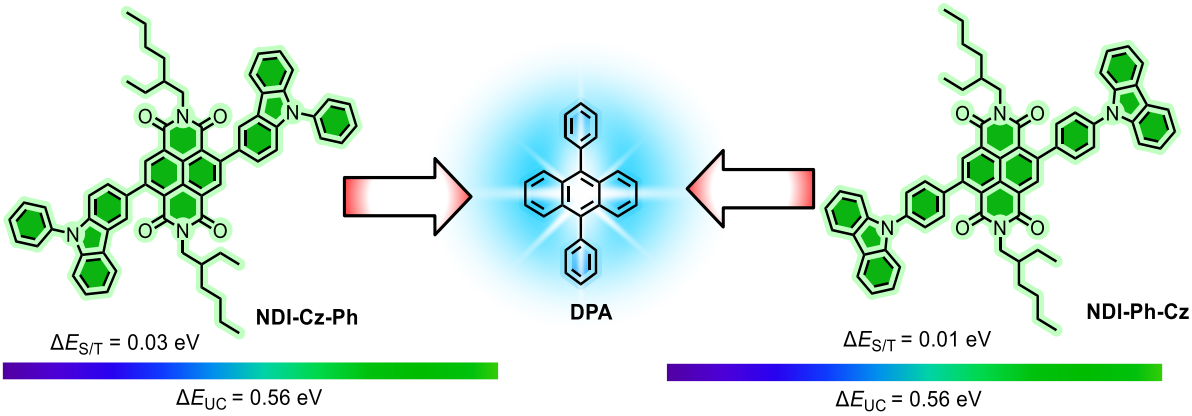

Figure 14. TTA-PUC systems consisting of TADF sensitizers **NDI-Cz-Ph** and **NDI-Ph-Cz** paired with **DPA** as the triplet acceptor. The corresponding values for the singlet−triplet energy gaps in the photosensitizers and the anti-Stokes shift of the DPA emission are also given.

4.4 Fluorescein-based TADF photosensitizer for TTA-PUC

Peng and co-workers reported a fluorescein derivative (**DCF-MPYM**) (Figure 15) for the detection of serum albumin in bovine samples. The **DCF-MPYM** compound was synthesized by the Knoevenagel condensation; however, an intermediate step involving the Duff reaction was also required to yield the final product.[175] Shortly afterwards they reported this compound again for TADF properties that were studied in a sufficient detail by steady-state and nanosecond time-resolved transient absorption and emission spectroscopies. The TADF property of this compound was manipulated for high-resolution bioimaging in living cells and excellent results were obtained by getting flawless imaging of cellular organelles.[176] In 2019 they once again used the same

multipurpose compound for applications in photon up-conversion, aimed to enhance the up-conversion quantum yield and enlarge the anti-Stokes shift for the TTA-PUC system. **DCF-MPYM** was used as the photo-excitable sensitizer that featured strong absorption of visible light reaching down to the red region. Making this sensitizer capable of electronic excitation with 635-nm laser light rendered it suitable for TTA up-conversion with perylene and **DPA** paired as triplet acceptors and a large anti-Stokes shift of 0.94 eV was determined for the **DPA** acceptor. **DCF-MPYM** with a sufficiently longer triplet lifetime (22.1 μs) was claimed to ensure an efficient TEnM and, hence, a high up-conversion quantum yield (11.2%). In a combination with perylene as the triplet acceptor, this sensitizer exhibited a lower efficiency of up-conversion luminescence (7.0%).[112] Recently a new study on **DCF-MPYM** and its methylated derivative **DCF-MPYM-Me** (ee Figure 15**)** suggested, based on the reISC rate constants of 0.047 s^{-1} and 7.723 s^{-1} for **DCF-MPYM** and **DCF-MPYM-Me**, respectively, that direct $T_1 \rightarrow S_1$ reISC is impossible in these systems. An alternative pathway was proposed based on deep-going computational studies.[113]

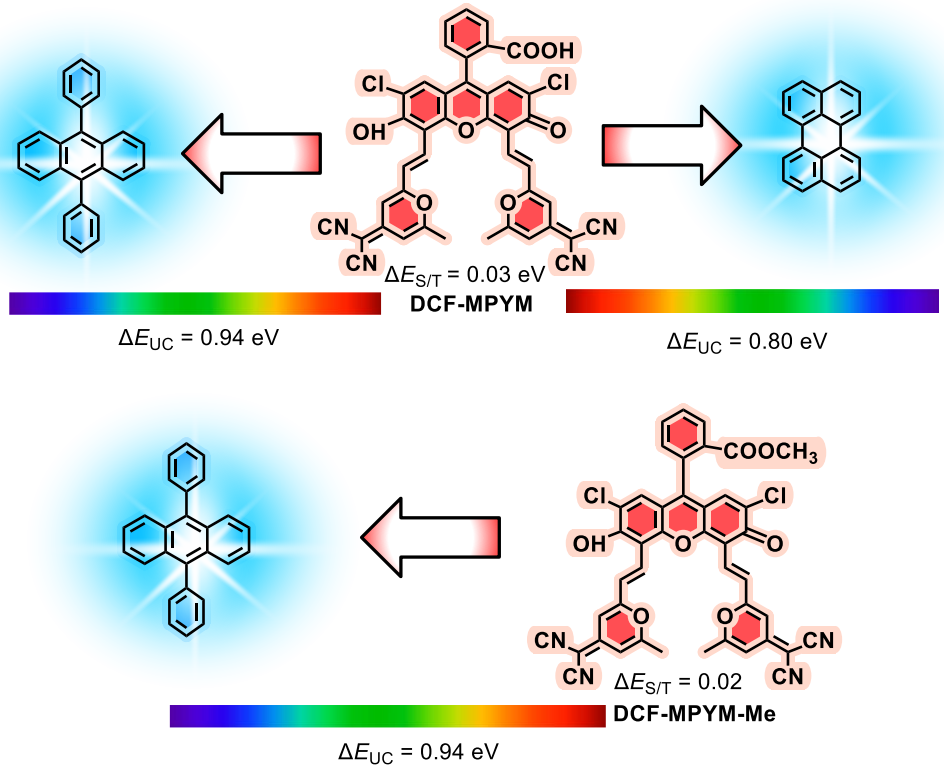

Figure 15. TTA-PUC systems consisting of **DCF-MPYM** and **DCF-MPYM-Me** TADF sensitizers paired with **DPA** and perylene as triplet acceptors. The values of singlet−triplet energy gaps in the photosensitizers and the corresponding anti-Stokes shifts are also given.

The newly proposed pathway involves thermally activated reverse internal conversion. According to this study, the $T_1 \rightarrow T_2$ transition (internal conversion) is facilitated by the conical intersection between the two states and $T_2 \rightarrow S_1$ reISC passes through the minimum energy crossing point. The newly designed **DCF−MPYM−Me** molecule was also used as a triplet photosensitizer for TTA up-conversion with **DPA** paired as the triplet acceptor. A remarkably high up-conversion quantum yield was observed (13.6%) in this case, which is slightly higher compared with the non-methylated carboxyl group-containing derivative. The authors have claimed that the increased up-conversion quantum yield of the methylated derivative is attributed to the longer triplet lifetime (40 μs) of **DCF−MPYM-ME**. The methyl group in the ester substituent occupies a larger space,

Table 2. Photophysical and TTA-PUC Properties of Organic and Inorganic TADF Photosensitizers.

Sensitizer	Emitter	Solvent/ Medium	λ_{exc}[a]/ nm	τ_T[b] /μs	$\Delta E_{S/T}$[c] /eV	Φ_{UC}[d] /%	ΔE_{UC}[e]	Ref.[f]
NDI-Cz-Ph	**DPA**	TOL	532	45.1	0.03	8.2	0.56	[88]
NDI-Ph-Cz	**DPA**	TOL	532	51.9	0.01	7.9	0.56	[88]
4-Cz-IPN	**Me-Naph**	BENZ	457	80	0.08	2.5	0.99	[177]
4-Cz-IPN	**t-Ph**	BENZ	457	80	0.08	3.4	0.83	[177]
4-Cz-IPN	**Me-Naph +t-Ph**	BENZ	457	80	0.08	7.6	0.83	[177]
Bn-Cz	**1,4-DT-Naph**	TOL	517	NS	0.003	7.6	0.91	[178]
Bn-Cz	**1,5-DT-Naph**	TOL	517	NS	0.003	6.4	0.98	[178]
tBu-Bn-Cz	**1,4-DT-Naph**	TOL	532	NS	0.003	6.0	NS	[178]
tBu-Bn-Cz	**1,5-DT-Naph**	TOL	532	NS	0.003	5.0	1.05	[178]
$Zr(MPPP)_2$	**Cz-DPA**	THF	514.5	350	0.20	37.4[g]	0.59	[179]
$Zr(MPPP)_2$	**F-DPA**	THF	514.5	350	0.20	37.8[g]	0.59	[179]
$Zr(MPPP)_2$	**CN-Cz-DPA**	THF	514.5	350	0.20	74.7[g]	0.50	[179]

[a] Excitation wavelength used for TTA-PUC. [b] Triplet lifetime. [c] Singlet−triplet energy gap. [d] Up-conversion quantum yield. [e] Anti-Stokes shift. [f] Literature reference. [g] Up-conversion quantum efficiency.

reducing the non-radiative transition and thereby extending the lifetime as compared with **DCF−MPYM** (22.1 μs). Although **DCF-MPYM** has demonstrated a very promising increase of the up-conversion quantum yield, the delayed fluorescence efficiency for this molecule is very

high (84%).[176] This implies that reISC is dominant in this TADF sensitizer and the triplet exciton is predominantly converted to the singlet exciton. Efforts should be made to minimize reISC in such molecules to achieve higher ISC quantum yields and hence elevated TTA-PUC efficiency.

4.5 TADF photosensitizer with an intermediate acceptor in TTA-PUC

A limited TTA-PUC efficiency is observed in some systems due to inefficient TEnM and unwanted backward energy migration from the triplet energy acceptor to the triplet energy donor.[180,181] In order to address this problem, the Kimizuka group reported in 2018 a new strategy of using three different interacting compounds (a photosensitizer, an intermediate acceptor and a second acceptor/emitter) in TTA-PUC system, contrary to the traditional TTA-PUC system that utilizes two interacting compounds (a photosensitizer and an acceptor/emitter).[182] A triplet sensitizer and a triplet acceptor/annihilator (here called intermediate acceptor) are similar to the conventional TTA up-conversion system; however, a third chromophore is introduced as an emitter that receives singlet energy from the intermediate acceptor via Förester resonance energy transfer (FRET). This mechanism is illustrated in Figure 16.

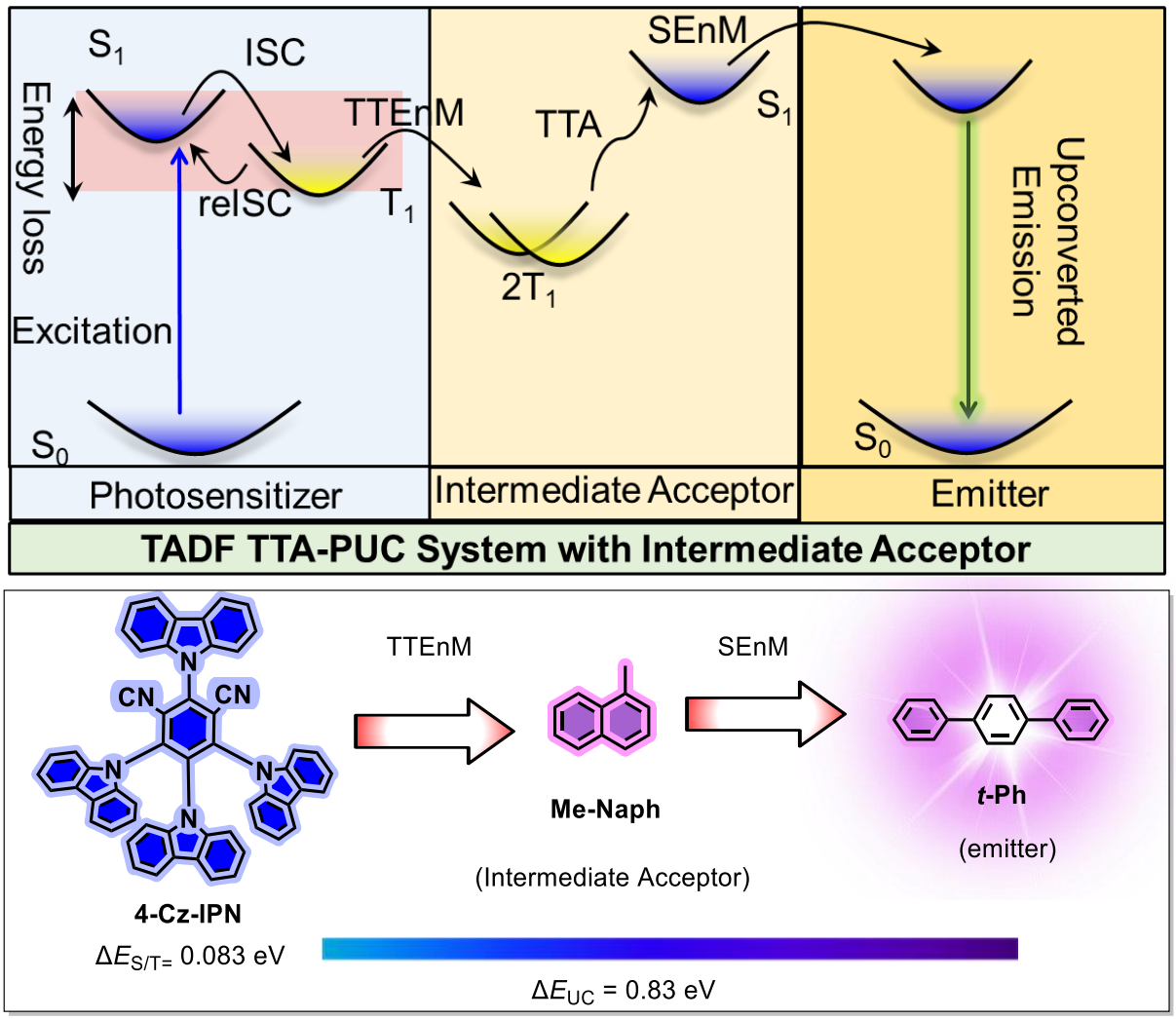

Figure 16. A schematic diagram of the TTA-PUC systems consisting of an intermediate acceptor, a TADF sensitizers, **4-Cz-IPN,** paired with an intermediate acceptor (**Me-Naph)** and emitter **TPh**.

In a system as shown in Figure 16, the absolute quantum yield of the TTA photon up-conversion process can be described by modification in the conventional expression of Equation 3.

$$\emptyset_{\mathrm{UC}} = \frac{1}{2} f \emptyset_{\mathrm{ISC}} \emptyset_{\mathrm{EnM}} \emptyset_{\mathrm{EnMI}} \emptyset_{\mathrm{TTA}} \emptyset_{\mathrm{FL}} \qquad (6)$$

where Φ_T is the triplet quantum yield for sensitizer, Φ_{EnM} is the sensitizer to intermediate triplet acceptor energy migration efficiency, Φ_{EnMI} is intermediate acceptor to triplet emitter energy migration efficiency, Φ_{TTA} is the triplet-triplet annihilation efficiency for triplet annihilator, Φ_{FL} is the fluorescence quantum yield for a triplet annihilator. In a recent article Yurash et al. used the standard TADF sensitizer **4-Cz-IPN** to adopt this strategy of pairing three chromophores in a photon up-conversion system (Figure 16).[177] The TTA up-conversion quantum yield for the **4-Cz-IPN** and 1-methylnaphthalene (**Me-Naph**) binary system was determined to reach 3.4% and the anti-Stokes shift value was 0.99 eV. However, the up-conversion quantum yield of the corresponding ternary system, comprising **4CzIPN**, **Me-Naph**, and ***t*-Ph**, was found to be more than two times higher (7.6%) compared to the binary system, which was tentatively attributed to the increased efficiency of TEnM from the sensitizer to the end-acceptor (mediated by **Me-Naph**).

4.6 Multiple resonance TADF photosensitizer in TTA-PUC

Multiple-resonance TADF (MR-TADF) sensitizers are polycyclic organic compounds with electron-rich nitrogen atoms located in ortho positions to an electron-deficient boron atom, inducing the MR effect. The MR effect efficiently minimizes the vibrational relaxation (VR; $S_1^* \rightarrow S_1$) during ISC by reducing the antibonding/bonding characteristics of frontier molecular orbitals and sharp emission spectra are observed.[183–186] The MR effect makes these sensitizers different from normal TADF emitters. MR-TADF sensitizers only demonstrate the signature property of a small singlet-triplet energy gap, and reISC, but also manifest a small VR in a TTA-PUC sensitizer as compared to a conventional TADF photosensitizer (Figure 17). In 2021, MR-TADF molecules were used as sensitizers to observe an efficient green to UV TTA-PUC. By the 517-nm optical excitation of the MR-TADF sensitizer, **Bn-Cz**, paired with **1,4-DT-Naph** as the acceptor/emitter (Figure 17c) an anti-Stokes shift of 0.91 eV was measured.

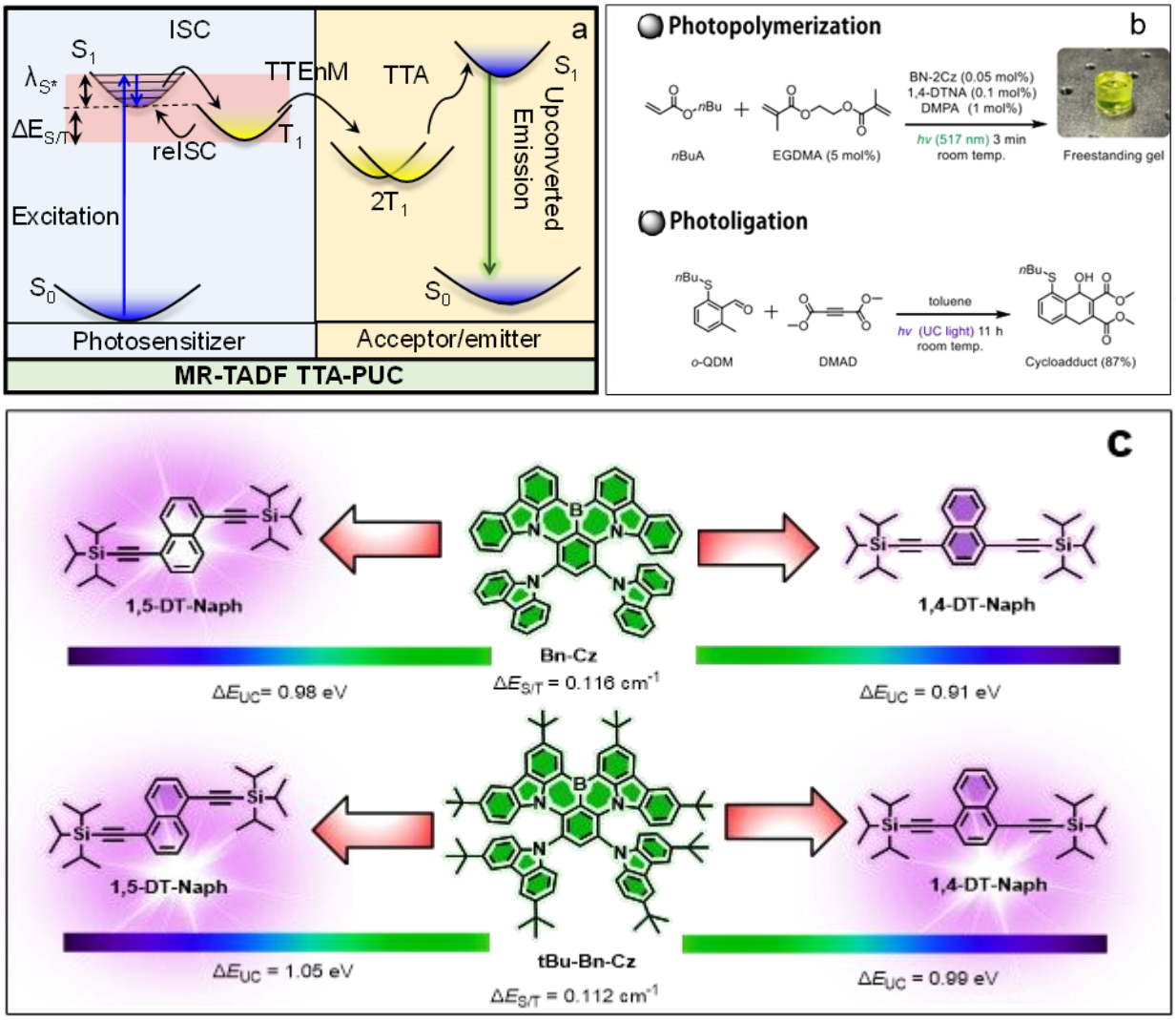

Figure 17. (a) Schematic representation of the role of MR-TADF photosensitizers in TTA-PUC. (b) Application of MR-TADF photosensitizer in photopolymerization and photo-ligation. (c) TTA-PUC systems consisting of MR-TADF sensitizers **Bn-Cz** and **tBu-Bn-Cz** paired with **1,4-DT-Naph** and **1,5-DT-Naph** as triplet acceptors. Values of singlet−triplet energy gaps in the photosensitizers and the anti-Stokes shift are also given. Reproduced by the permission of the *Chinese Chemical Society*.[178]

The anti-Stokes shift increased to 0.98 eV when **1,5-DT-Naph** was used as an acceptor/emitter paired with **Bn-Cz**. A *t*-butyl-substituted derivative, **tBu-Bn-Cz**, was also used as a triplet sensitizer paired with **1,5-DT-Naph**, which could be excited at a lower-energy side of the green spectral region (532 nm) to increase the anti-Stokes shift to 1.05 eV. The up-conversion quantum yield was found to reach 7.6% and 6.0% for **BN-Cz** and **tBu-Bn-Cz**, respectively, with **1,4-DT-Naph** paired as the triplet acceptor. As shown in Figure 17b, the importance of the TTA-PUC pair (**BN-Cz** and **1,4-DT-Naph**) was also demonstrated by using this system in photopolymerizion to induce quick gelation (within 3 min) in a photoligation reaction to obtain a cycloadduct with a remarkably high product yield.[178]

4.7 Zirconium(IV)-based TADF photosensitizer in TTA-PUC

Many transition metal complexes exhibit phosphorescence due to radiative decay from the triplet metal-to-ligand charge-transfer (^{3}MLCT) state to the ground state. However, thermally activated delayed fluorescence that is usually observed in organic compounds, is less likely to be observed in transition metal complexes. While some complexes of late transition metals such as copper,[187–189] zinc,[190] gold[191] and silver[192–194] have been reported for delayed fluorescence with or without prompt fluorescence, complexes of early transition metals such as zirconium are rarely studied to unravel such properties. Zirconium, the member of the Group-4 triad, is categorized as the fourth most abundant transition metal on the Earth, hence capable of forming cost-effective molecules. There are only very few studies on zirconium(IV)-based metal complexes in the field of photophysics because of the main challenge that arises due to its unique electronic configuration which requires comparatively different strategies to design a molecule for required photophysical properties as compared to those that are generally used for designing molecular complexes of late transition metals.[195–198] Transition metals with a deficiency of electrons in their *d* orbitals (e.g., the

d^0 electronic configuration of Zr(IV)) may undergo charge transfer from symmetry-adapted occupied ligand orbitals (LMCT) as opposed to metal-to-ligand charge transfer (MLCT) commonly observed in complexes of late-transition-metals with acceptor ligands. To achieve LMCT in d^0 metal complexes, the ligands are chosen carefully to be electron-rich in nature, acting as electron donors stabilizing the electron deficient transition metal centres in these complexes.[199–201]

Recently the Castellano group have utilized a moisture- and air-stable zirconium(IV) complex, **Zr(MPPP)$_2$**, where **MPPP** stands for 2,6-bis(5-methyl-3-phenyl-1*H*-pyrrol-2-yl)pyridine)[202] as a triplet photosensitizer for TTA up-conversion paired with **DPA** and a new series of carbazole appended **DPA** derivatives (**Cz-DPA**, **F-Cz-DPA**, **CN-Cz-DPA**; Figure 18) as triplet acceptors. **Zr(MPPP)$_2$** absorbs strongly visible light (λ_{max} = 525 nm; ε = 21570 $M^{-1}cm^{-1}$), which corresponds to optical population of an excited state having a mixed ^{1}LMCT and intraligand (^{1}IL) character, and manifests TADF with an exceptionally long triplet excited-state lifetime of 350 µs.[202] Upon the excitation of **Zr(MPPP)$_2$** at 514.5 nm, blue up-converted emission (also visible to unaided eye) was observed with the whole series of **DPA**, **Cz-DPA**, **F-Cz-DPA** and **CN-Cz-DPA** triplet acceptors. An exceptionally high up-conversion yield (< 31%) was determined throughout the series, with the maximum yield of 43% with the traditional **DPA** triplet acceptor. It is noteworthy that with increasing power, a linear slope with UC luminescence was observed for all the acceptors. This transition metal sensitizer-based PUC system also demonstrated maximum PUC efficiency with solar irradiance (26.7 mW cm^{-2}), proposing its potential real-time applications in solar energy-based systems.[179]

A closer look at the Table 1 and 2 indicates that as compared to ^{1}CT excitable sensitizers TADF sensitizers generally manifest small singlet-triplet energy gap and MR-TADF sensitizers have even

smaller singlet-triplet energy gap. It is also apparent that smaller singlet-triplet energy gap of sensitizers along with longer triplet excited state lifetimes can facilitate higher quantum efficiencies and quantum yields of TTA upconversion.

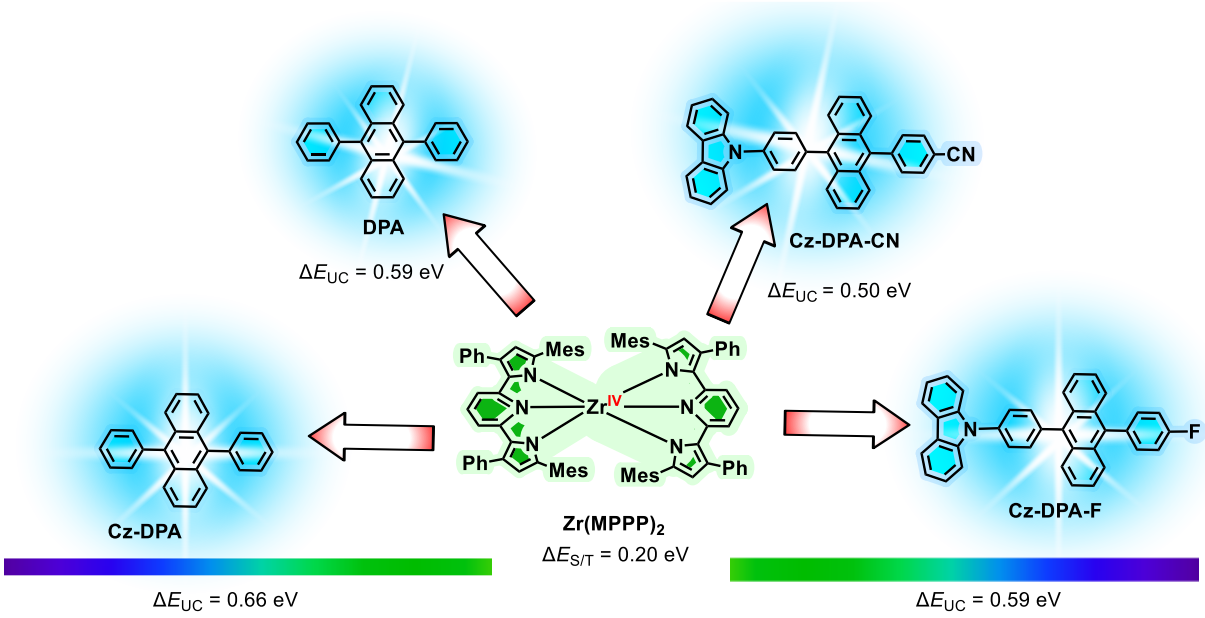

Figure 18. TTA-PUC systems consisting of Zr(IV)-bound sensitizers Zr(MPPP)$_2$ **tBu-Bn-Cz** paired with **DPA, Cz-DPA, Cz-DPA-CN** and **Cz-DPA-F** triplet acceptors. Values of the singlet−triplet energy gap in the photosensitizers and the anti-Stokes shift are also given.

5. DIRECT EXCITATION INTO TRIPLET STATE FOR TTA-PUC MEDIATED BY OSMIUM COMPLEXES

In all the strategies described in the preceding section, energy loss during the intersystem crossing from a singlet to a triplet state was reduced by decreasing the singlet−triplet energy gap. However, the direct excitation of a molecule into the triplet state can bypass ISC and hence overcome the total energy loss during ISC (Figure 1).[180,203–205] A great number of Os(II) pseudoctahedral

complexes with diimine or similar redox-active ligands have been studied for the photophysical and electron transfer properties.[206–215] The main reason why these osmium(II) complexes are highly interesting is the distinguished possibility to get optically excited directly into the lowest-energy T_1 state. These complexes show triplet character (normally spin-forbidden for 3*d* transition metal centers) in their Vis-near-IR absorption spectrum,[216–218] which provides an opportunity to save the energy lost during ISC. The molar absorption coefficient for $S_0 \rightarrow T_1$ (^{3}MLCT) transitions in Os(II) complexes is sufficiently large ($\varepsilon > 1000\ M^{-1}cm^{-1}$) due to the strong spin-orbital coupling of the heavy Os atom (with the large spin-orbit coupling constant of 3381 cm^{-1}) and this feature is normally not apparent in isoelectronic platinum, iridium and ruthenium-based complexes.[219–225]

Kimizuka and co-workers have intensively studied Os(II) complexes for TTA-PUC. In 2016, they exploited for the first time an Os complex for direct population of a triplet state to observe NIR-to-visible PUC. They reported a novel lipophilic osmium(II) chlorido complex (**OsCl-Tpy/Bpy**; Figure 19) with branched (amino)alkyl and *t*-butyl groups on the 2,2:6′,2″-terpyridine (**Tpy**) and 2,2′-bipyridine (**Bpy**) ligands, respectively, to increase its solubility in organic solvents.[203] This complex show strong $S_0 \rightarrow T_1$ MLCT absorption at 888 nm tailing below 950 nm. By using rubrene (**Rub**) as a triplet acceptor, photoexcitation at 938 nm led to NIR-to-visible up-converted emission observed at 570 nm.

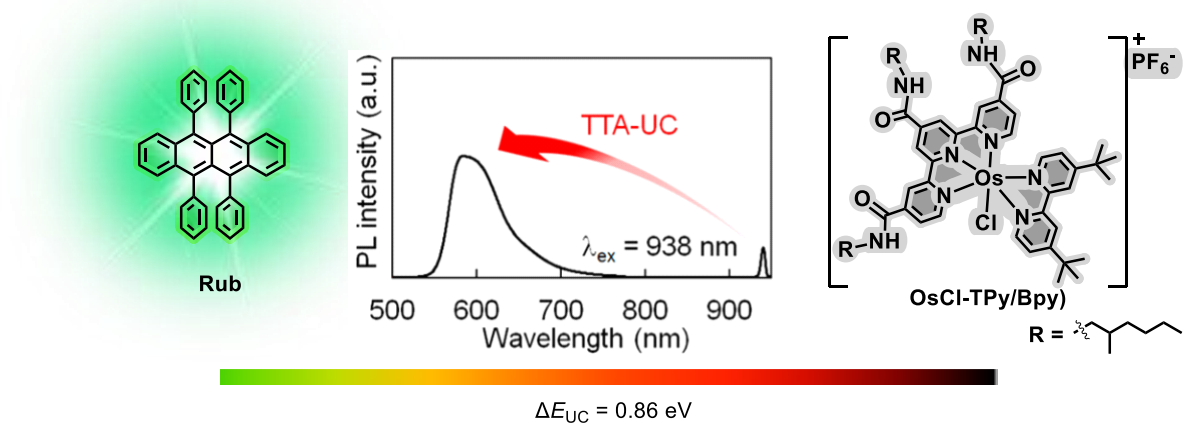

Figure 19. A TTA-PUC system consisting of an Os(II)-based sensitizers, **OsCl-Tpy/Bpy,** that is directly excited into a ^{3}MLCT state, and the **Rub** triplet acceptor. The value of the anti-Stokes shift determined for this system is also given. Photoluminescence spectra was reproduced by the permission of the *American Chemical Society*.[203]

Due to the direct excitation into the T_1 (^{3}MLCT) state, the energy loss during the ISC was completely bypassed and a large anti-Stokes shift of 0.86 eV was observed. However, due to the heavy-atom effect of Os, the triplet lifetime of **OsCl-Tpy/Bpy** is very short (12 ns; Table 3) and hence inefficient TEnM during TTA-PUC is manifested. Consequently, a very weak up-conversion quantum yield (0.001%) was observed in solution, which is a drawback of these photosensitizers. However, Kimizuka and co-workers prepared nanoparticles (NP) of this sensitizer with the rubrene emitter by precipitation in water and synthesized an NP-based polyvinyl-alcohol (NP-PVA) film. The up-conversion quantum yield of this solid TTA-PUC system improved significantly to 0.34%.[226] This results was attributed to efficient TEnM. After this pioneering report of an osmium(II) complex designed for the TTA-PUC application, not only the Kimizuka group but also many other research groups have paid their attention to osmium(II)-based complexes and modified their structures to tune the photophysical properties to be beneficial for the TTA-PUC applications.

Blue light (< 500 nm) is a very convenient tool for biological systems due to its use in various photochemical reactions and targeted release of drug upon photoexcitation.[14,227] Due to this importance, the Kimizuka group synthesized an osmium complex (**Os-(BrPh-Tpy)** (Figure 20) with bromophenyl substituents at the **Tpy** ligands in order to decrease their LUMO energy and shift the ^{3}MLCT absorption to the NIR spectral region (750 nm).[181] The NIR light is very useful for biological system due to its ability to penetrate deeply into the living tissues. In combination

with a blue light emitter in a TTA-PUC system this be an exceptionally useful tool. **TTBPy** (Figure 20) was used as the triplet emitter paired with **Os-(BrPh-Tpy)**. Upon excitation with 724-nm light, NIR-to-visible up-conversion was witnessed with a moderate quantum yield of 2.7%. The anti-Stokes shift for this system reached 0.97 eV. Experiments were also performed to observe up-conversion of this system in a solid mixture, but no PUC emission was noticed. When the sensitizer and triplet acceptor, after grinding, were fused in a capsule in a PVA solid-matrix film, quenching by triplet dioxygen was sufficiently blocked and PUC was observed.[228] However, the PUC quantum yield was lower due to an acceptor-to-donor back energy migration.

Table 3. Photophysical and TTA-PUC Properties of Selected Osmium(II) Complexes

Sensitizer	Emitter	Solvent/ Medium	λ_{exc}[a]/nm	τ_T[b]/ns	Φ_{UC}[c]/%	ΔE_{UC}[d]	Ref.[e]
OsCl-Tpy/Bpy	**Rub**	$CHCl_3$	938	12	0.001	0.86	[203]
Os-(BrPh-Tpy)	**TTBPy**	DMF	724	207 [g]	2.7	0.97	[181]
Os(bPey-Tpy)	**TTBPy**	DMF	724	23 [g, h]	5.9	0.86	[229]
Os-BDP	**PBI**	DCM	635	1729	1.2	0.55	[230]
Os-Ph	**PBI**	DCM	635	23	0.2	0.55	[230]
Os-Bpy	**DPA**	DCM	663	107	0.4	1.14	[231]
Os-Bpy	**Py**	DCM	663	107	1.1	0.92	[231]
Os-Bpy	**BPEA**	DCM	663	107	3.0	0.71	[231]
Os-Phen	**DPA**	DCM	663	373	5.9	1.14	[231]
Os-Phen	**Py**	DCM	663	373	2.3	0.92	[231]

Os-Phen	**BPEA**	DCM	663	373	12.5	0.71	[231]
Os-Phen-Ph	**DPA**	DCM	663	386	1.2	1.14	[231]
Os-Phen-Ph	**Py**	DCM	663	386	2.5	0.92	[231]
Os-Phen-Ph	**BPEA**	DCM	663	386	10.3	0.71	[231]
Os-DPA	**Mt-DPA**	DCM	663	1.2	5.3	1.12	[232]
Os-Ph-DPA	**Mt-DPA**	DCM	663	1.1	9.7	1.12	[232]

[a] Excitation wavelength used for TTA-PUC. [b] Triplet lifetime. [c] Up-conversion quantum yield. [d] Anti-Stokes shift. [e] Literature reference. [f] Not reported. [g] Phosphorescence lifetime. [h] In μs.

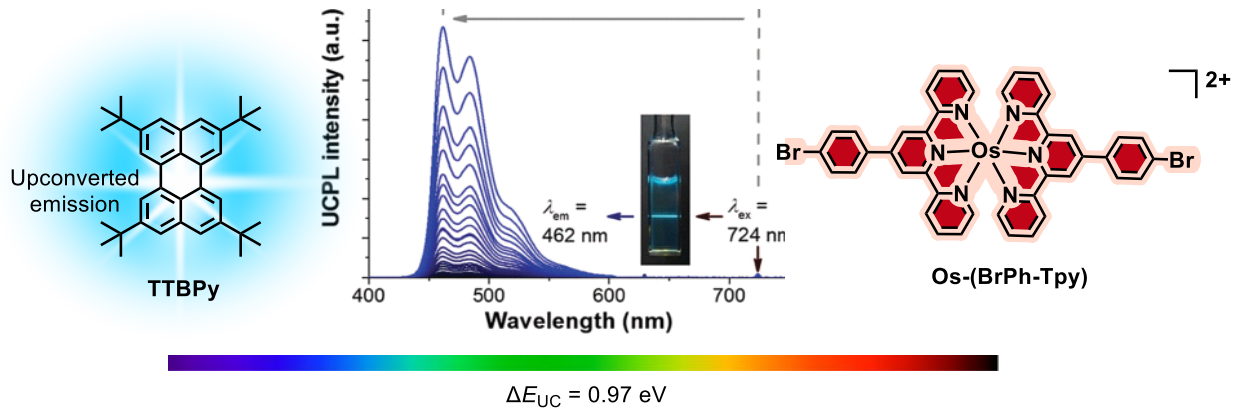

Figure 20. A TTA-PUC system consisting of an Os(II)-based sensitizer **Os-(BrPh-Tpy)** that is directly excited into a low-lying ^{3}MLCT state, and the **TTBPy** triplet acceptor. The value of the anti-Stokes shift determined for this system is also given. Reproduced by the permission of the *Royal Chemical Society* (photoluminescence up-conversion spectra).[181]

In 2019 photophysical properties of three osmium(II) complexes, **Os-Bpy**, **Os-Phen**, and **Os-Phen-Ph** (Figure 21), were reported.[231] The ^{3}MLCT lifetimes of these complexes span the range of 107-386 ns. These molecules were used as sensitizers in TTA-PUC in pairs with **DPA**, **Py** and **DPEA** triplet acceptors. The maximum up-conversion quantum yield of 5.9% and the largest anti-Stokes shift of 1.14 eV were determined for the **Os-Phen** and **DPA** system. Although these osmium(II) complexes proved to be very useful due to their capability of being directly excited into the T_1 state, most of these sensitizer have, however, very short triplet lifetimes. A short triplet lifetime is usually considered a drawback of a triplet photosensitizer because it cannot secure sufficient duration for the energy- and electron-migration processes which are the key for photophysical applications of triplet sensitizers including TTA-PUC.

Looking at the photophysical parameters of osmium complexes in Table 3, it can be concluded that an increased lifetime of the ISC involved processes could be helpful to get higher quantum yield of upconversion.

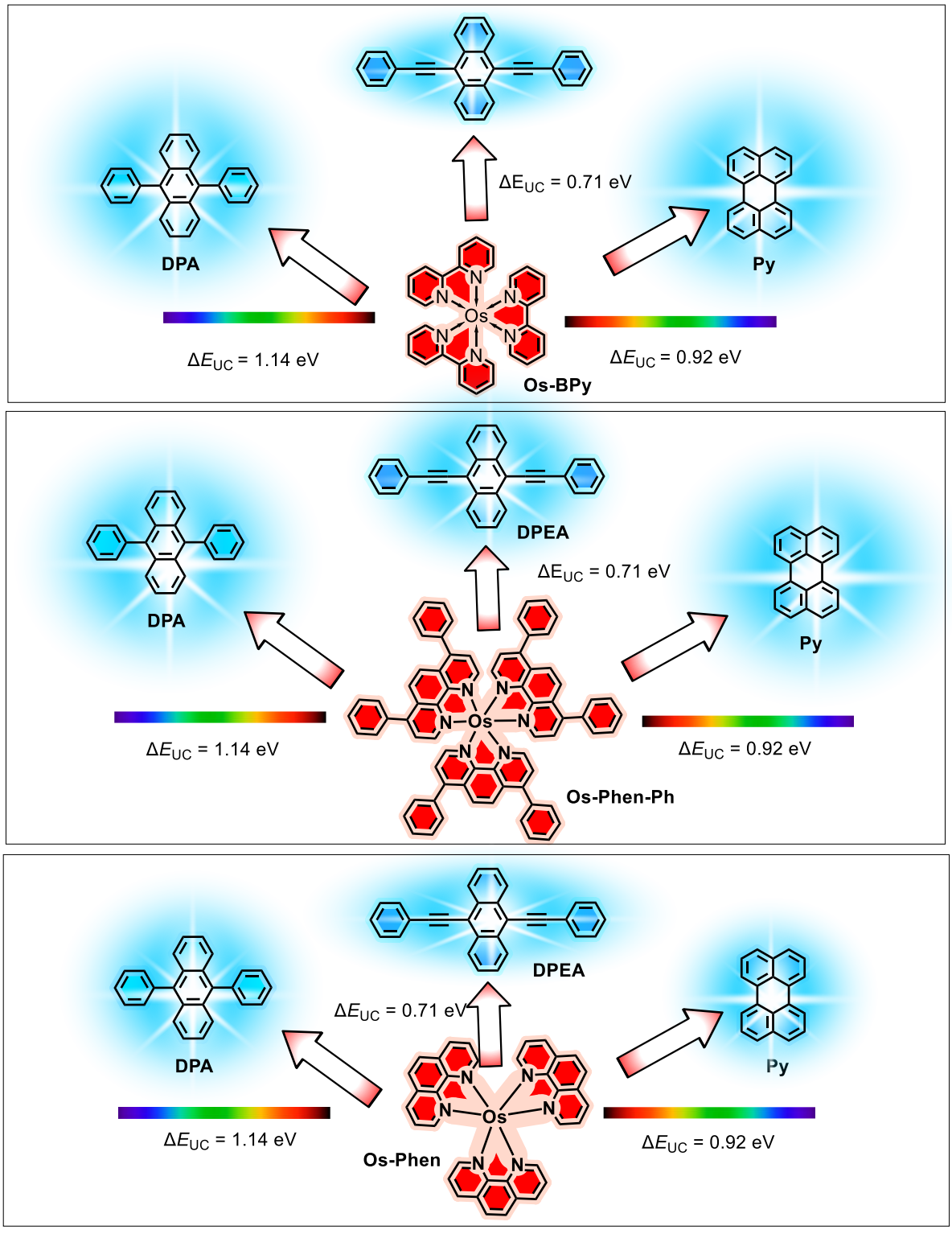

Figure 21. TTA-PUC systems consisting of Os-based sensitizers (a) **Os-Bpy**, (b) **Os-Phen**, and (c) **Os-Phen-Ph** that are directly excited into a low-lying ^{3}MLCT state; **DPA**, **Py** and **DPEA** are

paired as triplet acceptors. Values of corresponding anti-Stokes shifts determined for these systems are also reported.

5.1 TEnM from metal center to organic chromophore for prolonged lifetime

The triplet excited state lifetime of a compound is of great importance because of its pivotal role in various photophysical phenomena such as electron and energy transfer. It is especially crucial for intermolecular processes that are diffusion-controlled. Their efficiency is directly related to the length of triplet excited state lifetimes of the molecules being involved, as proven by many applications such as PDT,[233] photocatalysis,[234–236] and TTA-PUC.[31,36] For transition metal complexes the triplet lifetimes are usually short due to the SOC effect of heavy metals. By shifting the triplet to a ligand center upon ^{3}MLCT excitation, the triplet lifetime can be prolonged due to the reduced SOC effect. Zhao and co-workers synthesized an osmium tris(2,2′-bipyridine) complex with an appended Bodipy unit (**Os-BDP**; Figure 22), aimed at shifting the ^{3}MLCT state of the osmium complex (1.72 eV) via TEnM to the Bodipy unit (1.67 eV) which has a lower-triplet energy state compared with the osmium complex.[230] Their results demonstrated that the triplet lifetime of the Bodipy-appended complex increased significantly to 1.7 μs compared with 23 ns for the reference complex (**Os-Ph**; Figure 22). Excitation of the sensitizer with 635-nm laser light led to up-converted emission of paired perylenebisimide (**PBI**) at 550 nm. Also, the up-conversion quantum yield of 1.2% for **Os-BDP** was higher compared with merely 0.17% for **Os-Ph**. The higher up-conversion quantum yield of **Os-BDP** was attributed to the longer-lived triplet state and the consequently improved TEnM efficiency.

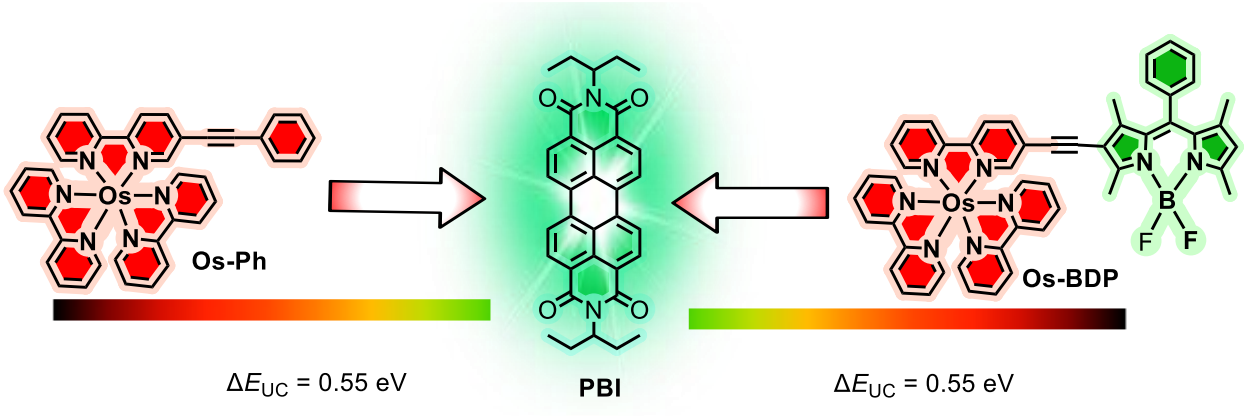

Figure 22. TTA-PUC systems consisting of Os(II)-based sensitizers **Os-Ph** and **Os-BDP** that are directly excited into a low-lying ^{3}MLCT state (ultimately a Bodipy-localized triplet state for **Os-BDP)**, and the **PBI** triplet acceptor. The value of the anti-Stokes shift determined for these systems is also given.

Photoactivation of proteins and light-induced control of protein activity require excitation with visible light that however only barely penetrates living tissues due thier non-homogeneity causing scattering of photons.[237–240] On the other hand far-red, NIR and SWIR photons are capable of deep tissue penetration. Such a PUC system was introduced by Kimizuka and co-workers.[181]. They used **Os(bPey-Tpy)** (Figure 23) with perylene units appended at **Tpy** pincers by phenylene linkers. A very long phosphorescence lifetime (42 µs) was observed for this complex compared to 207 ns determined for the analogous reference osmium(II) complex) with bromophenyl substituents at **Tpy**, **Os-(BrPh-Tpy)**. The extended lifetime was ascribed to a triplet equilibrium between ^{3}MLCT and a perylene-localized triplet state (^{3}IL). The longer span of the lifetime ensured an efficient TEnM in the TTA up-conversion system from sensitizer to acceptor. A higher up-conversion quantum yield (up to 2%) was obtained with this sensitizer paired with the **TTBPy** emitter than measured with **Os-(BrPh-Tpy)**. However, the anti-Stokes shift of 0.86 eV determined for **Os(bPey-Tpy)** is smaller (Table 3) compared to **Os-(BrPh-Tpy)**. Upon excitation, TTA-PUC

(blue emission) was also observed in hydrogel, which was utilized for genome engineering.[229] This application successfully regulated the morphology of hippocampal neurons that play a significant role in long-term memory and cognitive learning.[241]

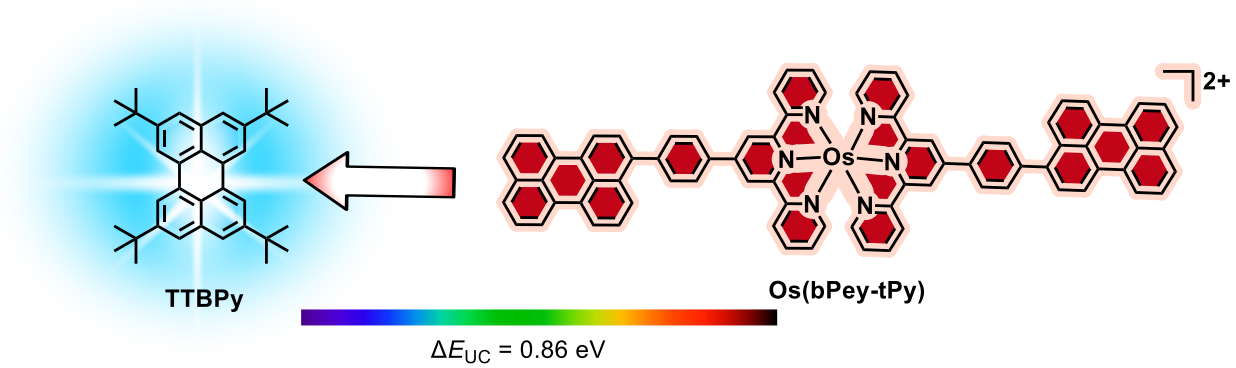

Figure 23. TTA-PUC system consisting of the Os(II)-based sensitizer **Os-(bPey-Tpy)** that is directly excited into a low-lying ^{3}MLCT state (ultimately a pyrene-localized triplet state) and the **TTBPy** triplet acceptor. The corresponding anti-Stokes shift observed for this system also given.

In 2020, **DPA**-appended osmium(II) complexes (**Os-DPA** and **Os-Ph-DPA** in Figure 24) were reported.[232] The molecular structure designing motive for these complexes was the shift of the metal−**Phen** centered ^{3}MLCT state to **DPA** through TEnM and reach a triplet equilibrium. Consequently, the triplet lifetimes of the **DPA**-appended complexes increased significantly to ~ 1 μs compared to the reference complex lacking the **DPA** units (**Os-Phen**; 373 ns). For **Os-DPA** paired with the **DPA** acceptor/emitter molecule, an efficient TTA photon up-conversion was observed (9.7%) The high up-conversion yield can be attributed to efficient TEnM from the sensitizer to the acceptor in TTA-PUC system due to prolonged triplet lifetime of the sensitizer. The anti-Stokes shift for this system reached the value of 1.12 eV.

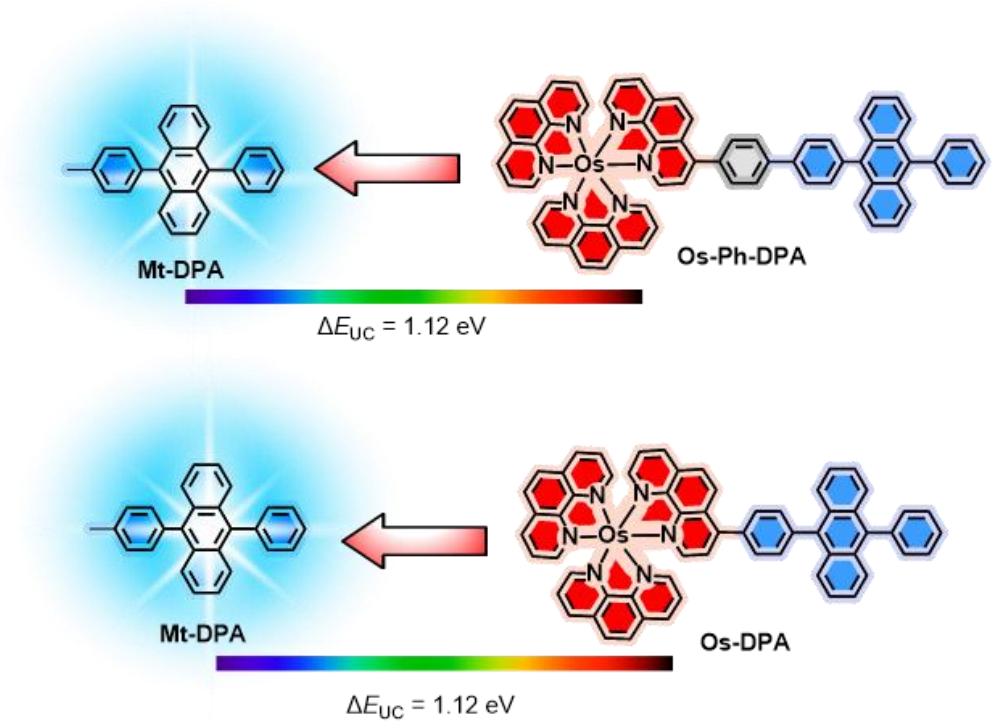

Figure 24. TTA-PUC systems consisting of the Os(II) based sensitizers **Os-Ph-DPA** and **Os-DPA** that are directly excited into a low-lying ^{3}MLCT state (ultimately a **DPA**-localized triplet state) and the **DPA** triplet acceptor. The values of the anti-Stokes shifts measured for these systems are also given.

6. CONCLUSIONS AND OUTLOOK

Enormous progress has been witnessed in the field of TTA-PUC in designing new triplet photosensitizers, and various methodologies have been opted to reduce energy loss during ISC. However, there are still numerous challenges to overcome and augment the efficiency of these sensitizers. From the molecular design point of view, the prediction of charge-transfer absorption bands in the UV-Vis-IR spectral range is still a main hurdle to design such photosensitizers and hence photosensitizers which are capable of being photoexcited at CT are rarely reported.

Moreover, the molar absorption coefficient of a CT absorption band is not large in all the solvents, resulting inefficient light-harvesting capability of these sensitizers which is one of the vital requirements and has a strong impact on the efficiency of TTA-PUC. Although TADF photosensitizers have demonstrated remarkably high up-conversion quantum yields as well as exceptionally large anti-Stokes shifts owing to their high triplet energy levels, designing TADF photosensitizers addressed with near-IR excitation and their use in TTA-PUC remains a less investigated area in this field. Osmium(II) complexes represent a new emerging class of photosensitizers for TTA-PUC field due to their capability of being sensitized directly into their triplet states by virtue of the appearance of $S_0 \rightarrow T_1$ transitions in their electronic absorption spectra, which permits to bypass energy losses during ISC. However, the low intensity of the $S_0 \rightarrow T_1$ transitions in these sensitizers reduces their light-harvesting ability as one of the vital requirements for a photosensitizer with a high TTA-PUC quantum yield. Moreover, the triplet lifetimes of these Os(II) sensitizers are usually very short, which is limiting the TEnM during TTA-PUC. These two drawbacks are reflected in low up-conversion quantum yields obtained with such systems. Although TEnM strategies have been used to shift the triplet state localization from a metal center to a remote ligand to decrease the heavy metal effect and achieve prolonged lifetimes, there is still much space for further update in this field.

In short, in this review various strategies recently exploited to minimize energy-loss during ISC in molecular photosensitizers designed for TTA-PUC, have been critically evaluated. We have summarized these techniques, analyzed in detail the ISC mechanism and highlighted challenges in this field. It is anticipated that this overview will be of considerable interest to the scientific community active in this area of research.

■REFERENCES

(1) Huang, L.; Le, T.; Huang, K.; Han, G. Enzymatic Enhancing of Triplet-Triplet Annihilation Upconversion by Breaking Oxygen Quenching for Background-Free Biological Sensing. *Nat. Commun.* **2021**, *12* (1), 1898. https://doi.org/10.1038/s41467-021-22282-1.

(2) Xu, M.; Zou, X.; Su, Q.; Yuan, W.; Cao, C.; Wang, Q.; Zhu, X.; Feng, W.; Li, F. Ratiometric Nanothermometer in Vivo Based on Triplet Sensitized Upconversion. *Nat. Commun.* **2018**, *9* (1), 2698. https://doi.org/10.1038/s41467-018-05160-1.

(3) Askes, S. H. C.; Mora, N. L.; Harkes, R.; Koning, R. I.; Koster, B.; Schmidt, T.; Kros, A.; Bonnet, S. Imaging the Lipid Bilayer of Giant Unilamellar Vesicles Using Red-to-Blue Light Upconversion. *Chem. Commun.* **2015**, *51* (44), 9137–9140. https://doi.org/10.1039/C5CC02197A.

(4) Liu, Q.; Xu, M.; Yang, T.; Tian, B.; Zhang, X.; Li, F. Highly Photostable Near-IR-Excitation Upconversion Nanocapsules Based on Triplet–Triplet Annihilation for in Vivo Bioimaging Application. *ACS Appl. Mater. Interfaces* **2018**, *10* (12), 9883–9888. https://doi.org/10.1021/acsami.7b17929.

(5) Huang, L.; Kakadiaris, E.; Vaneckova, T.; Huang, K.; Vaculovicova, M.; Han, G. Designing next Generation of Photon Upconversion: Recent Advances in Organic Triplet-Triplet Annihilation Upconversion Nanoparticles. *Biomaterials* **2019**, *201*, 77–86. https://doi.org/https://doi.org/10.1016/j.biomaterials.2019.02.008.

(6) Huang, L.; Zhao, Y.; Zhang, H.; Huang, K.; Yang, J.; Han, G. Expanding Anti-Stokes Shifting in Triplet–Triplet Annihilation Upconversion for in Vivo Anticancer Prodrug Activation. *Angew. Chem. Int. Ed.* **2017**, *56* (46), 14400–14404. https://doi.org/https://doi.org/10.1002/anie.201704430.

(7) Ravetz, B. D.; Pun, A. B.; Churchill, E. M.; Congreve, D. N.; Rovis, T.; Campos, L. M. Photoredox Catalysis Using Infrared Light via Triplet Fusion Upconversion. *Nature* **2019**, *565* (7739), 343–346. https://doi.org/10.1038/s41586-018-0835-2.

(8) Huang, L.; Wu, W.; Li, Y.; Huang, K.; Zeng, L.; Lin, W.; Han, G. Highly Effective Near-Infrared Activating Triplet–Triplet Annihilation Upconversion for Photoredox Catalysis. *J. Am. Chem. Soc.* **2020**, *142* (43), 18460–18470. https://doi.org/10.1021/jacs.0c06976.

(9) F. Schulze, T.; Czolk, J.; Cheng, Y.-Y.; Fückel, B.; W. MacQueen, R.; Khoury, T.; J. Crossley, M.; Stannowski, B.; Lips, K.; Lemmer, U.; Colsmann, A.; W. Schmidt, T. Efficiency Enhancement of Organic and Thin-Film Silicon Solar Cells with Photochemical Upconversion. *J. Phys. Chem. C* **2012**, *116* (43), 22794–22801. https://doi.org/10.1021/jp309636m.

(10) Gao, C.; Wong, W. W. H.; Qin, Z.; Lo, S.-C.; Namdas, E. B.; Dong, H.; Hu, W. Application of Triplet–Triplet Annihilation Upconversion in Organic Optoelectronic Devices: Advances and Perspectives. *Adv. Mater.* **2021**, *33* (45), 2100704. https://doi.org/https://doi.org/10.1002/adma.202100704.

(11) Askes, S. H. C.; Bahreman, A.; Bonnet, S. Activation of a Photodissociative Ruthenium Complex by Triplet–Triplet Annihilation Upconversion in Liposomes. *Angew. Chemie Int. Ed.* **2014**, *53* (4), 1029–1033. https://doi.org/https://doi.org/10.1002/anie.201309389.

(12) Lin, T.-A.; Perkinson, C. F.; Baldo, M. A. Strategies for High-Performance Solid-State Triplet–Triplet-Annihilation-Based Photon Upconversion. *Adv. Mater.* **2020**, *32* (26), 1908175. https://doi.org/https://doi.org/10.1002/adma.201908175.

(13) Schulze, T. F.; Schmidt, T. W. Photochemical Upconversion: Present Status and Prospects for Its Application to Solar Energy Conversion. *Energy Environ. Sci.* **2015**, *8* (1), 103–125.

(14) Zhou, J.; Liu, Q.; Feng, W.; Sun, Y.; Li, F. Upconversion Luminescent Materials: Advances and Applications. *Chem. Rev.* **2015**, *115* (1), 395–465. https://doi.org/10.1021/cr400478f.

(15) Sharma, K. S.; Thoh, M.; Dubey, A. K.; Phadnis, P. P.; Sharma, D.; Sandur, S. K.; Vatsa, R. K. The Synthesis of Rare Earth Metal-Doped Upconversion Nanoparticles Coated with d-Glucose or 2-Deoxy-d-Glucose and Their Evaluation for Diagnosis and Therapy in Cancer. *New J. Chem.* **2020**, *44* (32), 13834–13842. https://doi.org/10.1039/D0NJ00666A.

(16) Zhang, C.; Yang, L.; Zhao, J.; Liu, B.; Han, M.-Y.; Zhang, Z. White-Light Emission from an Integrated Upconversion Nanostructure: Toward Multicolor Displays Modulated by Laser Power. *Angew. Chem. Int. Ed.* **2015**, *54* (39), 11531–11535. https://doi.org/https://doi.org/10.1002/anie.201504518.

(17) Ye, C.; Zhou, L.; Wang, X.; Liang, Z. Photon Upconversion: From Two-Photon Absorption (TPA) to Triplet–Triplet Annihilation (TTA). *Phys. Chem. Chem. Phys.* **2016**, *18* (16), 10818–10835. https://doi.org/10.1039/C5CP07296D.

(18) Albota, M.; Beljonne, D.; Brédas, J.-L.; Ehrlich, J. E.; Fu, J.-Y.; Heikal, A. A.; Hess, S. E.; Kogej, T.; Levin, M. D.; Marder, S. R.; McCord-Maughon, D.; Perry, J. W.; Röckel, H.; Rumi, M.; Subramaniam, G.; Webb, W. W.; Wu, X.-L.; Xu, C. Design of Organic Molecules with Large Two-Photon Absorption Cross Sections. *Science (80-.).* **1998**, *281* (5383), 1653–1656. https://doi.org/10.1126/science.281.5383.1653.

(19) Horiuchi, N. Upconversion Nanocrystals. *Nat. Photonics* **2012**, *6* (11), 716. https://doi.org/10.1038/nphoton.2012.288.

(20) Gai, S.; Li, C.; Yang, P.; Lin, J. Recent Progress in Rare Earth Micro/Nanocrystals: Soft Chemical Synthesis, Luminescent Properties, and Biomedical Applications. *Chem. Rev.* **2014**, *114* (4), 2343–2389. https://doi.org/10.1021/cr4001594.

(21) Bharmoria, P.; Bildirir, H.; Moth-Poulsen, K. Triplet-Triplet Annihilation Based near Infrared to Visible Molecular Photon Upconversion. *Chem. Soc. Rev.* **2020**, *49* (18), 6529–6554. https://doi.org/10.1039/d0cs00257g.

(22) Yanai, N.; Kimizuka, N. New Triplet Sensitization Routes for Photon Upconversion: Thermally Activated Delayed Fluorescence Molecules, Inorganic Nanocrystals, and Singlet-to-Triplet Absorption. *Acc. Chem. Res.* **2017**, *50* (10), 2487–2495. https://doi.org/10.1021/acs.accounts.7b00235.

(23) Lee, S. H.; Thévenaz, D. C.; Weder, C.; Simon, Y. C. Glassy Poly(Methacrylate) Terpolymers with Covalently Attached Emitters and Sensitizers for Low-Power Light Upconversion. *J. Polym. Sci. Part A Polym. Chem.* **2015**, *53* (14), 1629–1639. https://doi.org/https://doi.org/10.1002/pola.27626.

(24) Zhou, J.; Jin, D. Triplet State Brightens Upconversion. *Nat. Photonics* **2018**, *12* (7), 378–379. https://doi.org/10.1038/s41566-018-0188-2.

(25) Garfield, D. J.; Borys, N. J.; Hamed, S. M.; Torquato, N. A.; Tajon, C. A.; Tian, B.; Shevitski, B.; Barnard, E. S.; Suh, Y. D.; Aloni, S.; Neaton, J. B.; Chan, E. M.; Cohen, B. E.; Schuck, P. J. Enrichment of Molecular Antenna Triplets Amplifies Upconverting Nanoparticle Emission. *Nat. Photonics* **2018**, *12* (7), 402–407. https://doi.org/10.1038/s41566-018-0156-x.

(26) Luo, X.; Han, Y.; Chen, Z.; Li, Y.; Liang, G.; Liu, X.; Ding, T.; Nie, C.; Wang, M.; Castellano, F. N.; Wu, K. Mechanisms of Triplet Energy Transfer across the Inorganic Nanocrystal/Organic Molecule Interface. *Nat. Commun.* **2020**, *11* (1), 28. https://doi.org/10.1038/s41467-019-13951-3.

(27) Lai, R.; Liu, Y.; Luo, X.; Chen, L.; Han, Y.; Lv, M.; Liang, G.; Chen, J.; Zhang, C.; Di, D.;

Scholes, G. D.; Castellano, F. N.; Wu, K. Shallow Distance-Dependent Triplet Energy Migration Mediated by Endothermic Charge-Transfer. *Nat. Commun.* **2021**, *12* (1), 1532. https://doi.org/10.1038/s41467-021-21561-1.

(28) Yu, S.; Zeng, Y.; Chen, J.; Yu, T.; Zhang, X.; Yang, G.; Li, Y. Intramolecular Triplet–Triplet Energy Transfer Enhanced Triplet–Triplet Annihilation Upconversion with a Short-Lived Triplet State Platinum(Ii) Terpyridyl Acetylide Photosensitizer. *RSC Adv.* **2015**, *5* (86), 70640–70648. https://doi.org/10.1039/C5RA12579K.

(29) Liu, S.; Wang, X.; Liu, H.; Shen, L.; Zhao, D.; Li, X. Enhancing Triplet Sensitization Ability of Donor–Acceptor Dyads via Intramolecular Triplet Energy Transfer. *J. Mater. Chem. C* **2020**, *8* (10), 3536–3544. https://doi.org/10.1039/C9TC06337D.

(30) Ju, X.; Zhu, L.; Li, L.; Ye, C.; Liang, Z.; Chen, S.; Wang, X. A Novel Low-Powered Upconversion Strategy to Enhance the Anti-Stokes Shift: Cascading One-Photon Hot-Band Absorption and Triplet Sensitization Based on Pd(Ii)Octaethylporphyrin. *J. Mater. Chem. C* **2021**, *9* (21), 6749–6753. https://doi.org/10.1039/D1TC00721A.

(31) Singh-Rachford, T. N.; Castellano, F. N. Photon Upconversion Based on Sensitized Triplet–Triplet Annihilation. *Coord. Chem. Rev.* **2010**, *254* (21), 2560–2573. https://doi.org/https://doi.org/10.1016/j.ccr.2010.01.003.

(32) Lu, Y.; Wang, J.; McGoldrick, N.; Cui, X.; Zhao, J.; Caverly, C.; Twamley, B.; Ó Máille, G. M.; Irwin, B.; Conway-Kenny, R. Iridium (III) Complexes Bearing Pyrene-functionalized 1,10-phenanthroline Ligands as Highly Efficient Sensitizers for Triplet–Triplet Annihilation Upconversion. *Angew. Chem. Int. Ed.* **2016**, *55* (47), 14688–14692.

(33) Kimizuka, N.; Yanai, N.; Morikawa, M. Photon Upconversion and Molecular Solar Energy Storage by Maximizing the Potential of Molecular Self-Assembly. *Langmuir* **2016**, *32* (47),

12304–12322. https://doi.org/10.1021/acs.langmuir.6b03363.

(34) Haefele, A.; Blumhoff, J.; Khnayzer, R. S.; Castellano, F. N. Getting to the (Square) Root of the Problem: How to Make Noncoherent Pumped Upconversion Linear. *J. Phys. Chem. Lett.* **2012**, *3* (3), 299–303. https://doi.org/10.1021/jz300012u.

(35) Cheng, Y. Y.; Fückel, B.; Khoury, T.; Clady, R. G. C. R.; Tayebjee, M. J. Y.; Ekins-Daukes, N. J.; Crossley, M. J.; Schmidt, T. W. Kinetic Analysis of Photochemical Upconversion by Triplet−triplet Annihilation: Beyond Any Spin Statistical Limit. *J. Phys. Chem. Lett.* **2010**, *1* (12), 1795–1799. https://doi.org/10.1021/jz100566u.

(36) Monguzzi, A.; Tubino, R.; Hoseinkhani, S.; Campione, M.; Meinardi, F. Low Power, Non-Coherent Sensitized Photon up-Conversion: Modelling and Perspectives. *Phys. Chem. Chem. Phys.* **2012**, *14* (13), 4322–4332. https://doi.org/10.1039/C2CP23900K.

(37) Valeur, B. *Molecular Fluorescence - Principles and Applications*; John Wiley & Sons, Ltd, 2001; Vol. 8. https://doi.org/10.1002/3527600248.

(38) Turrro, N. J. R., Scaiano, J. C. *Principles of Molecular Photochemistry: An Introduction.*; University Science Books, Sausalito, CA, 2009.

(39) Lakowicz, J. R. *Principles of Fluorescence Spectroscopy*; Springer science & business media, 2013. https://doi.org/10.1007/978-0-387-46312-4.

(40) Perutz, R. N.; Procacci, B. Photochemistry of Transition Metal Hydrides. *Chem. Rev.* **2016**, *116* (15), 8506–8544. https://doi.org/10.1021/acs.chemrev.6b00204.

(41) Matsika, S. Electronic Structure Methods for the Description of Nonadiabatic Effects and Conical Intersections. *Chem. Rev.* **2021**, *121* (15), 9407–9449. https://doi.org/10.1021/acs.chemrev.1c00074.

(42) McGlynn, S. P.; Azumi, T.; Kinoshita, M. Molecular Spectroscopy of the Triplet State;

Prentice-Hall International, Hemel Hemptead (U.K.), 1969.

(43) Liu, Y.; Li, C.; Ren, Z.; Yan, S.; Bryce, M. R. All-Organic Thermally Activated Delayed Fluorescence Materials for Organic Light-Emitting Diodes. *Nat. Rev. Mater.* **2018**, *3*. https://doi.org/10.1038/natrevmats.2018.20.

(44) Schultz, D. M.; Yoon, T. P. Solar Synthesis: Prospects in Visible Light Photocatalysis. *Science (80-.).* **2014**, *343* (6174), 1239176. https://doi.org/10.1126/science.1239176.

(45) Spencer, J. A.; Ferraro, F.; Roussakis, E.; Klein, A.; Wu, J.; Runnels, J. M.; Zaher, W.; Mortensen, L. J.; Alt, C.; Turcotte, R.; Yusuf, R.; Côté, D.; Vinogradov, S. A.; Scadden, D. T.; Lin, C. P. Direct Measurement of Local Oxygen Concentration in the Bone Marrow of Live Animals. *Nature* **2014**, *508* (7495), 269–273. https://doi.org/10.1038/nature13034.

(46) Turro, N. J.; Ramamurthy, V.; Scaiano, J. C. *Modern Molecular Photochemistry of Organic Molecules*; Viva Books University Science Books, Sausalito, 2017.

(47) Manna, M. K.; Shokri, S.; Wiederrecht, G. P.; Gosztola, D. J.; Ayitou, A. J.-L. New Perspectives for Triplet–Triplet Annihilation Based Photon Upconversion Using All-Organic Energy Donor & Acceptor Chromophores. *Chem. Commun.* **2018**, *54* (46), 5809–5818. https://doi.org/10.1039/C8CC01553H.

(48) Zhang, X.; Sukhanov, A. A.; Yildiz, E. A.; Kandrashkin, Y. E.; Zhao, J.; Yaglioglu, H. G.; Voronkova, V. K. Radical-Enhanced Intersystem Crossing in a Bay-Substituted Perylene Bisimide−TEMPO Dyad and the Electron Spin Polarization Dynamics upon Photoexcitation. *ChemPhysChem* **2021**, *22* (1), 55–68. https://doi.org/https://doi.org/10.1002/cphc.202000861.

(49) Wang, Z.; Gao, Y.; Hussain, M.; Kundu, S.; Rane, V.; Hayvali, M.; Yildiz, E. A.; Zhao, J.; Yaglioglu, H. G.; Das, R.; Luo, L.; Li, J. Efficient Radical-Enhanced Intersystem Crossing

in an NDI-TEMPO Dyad: Photophysics, Electron Spin Polarization, and Application in Photodynamic Therapy. *Chem. – A Eur. J.* **2018**, *24* (70), 18663–18675. https://doi.org/10.1002/chem.201804212.

(50) Wang, Z.; Zhao, J.; Barbon, A.; Toffoletti, A.; Liu, Y.; An, Y.; Xu, L.; Karatay, A.; Yaglioglu, H. G.; Yildiz, E. A.; Hayvali, M. Radical-Enhanced Intersystem Crossing in New Bodipy Derivatives and Application for Efficient Triplet–Triplet Annihilation Upconversion. *J. Am. Chem. Soc.* **2017**, *139* (23), 7831–7842. https://doi.org/10.1021/jacs.7b02063.

(51) Nagarajan, K.; Mallia, A. R.; Muraleedharan, K.; Hariharan, M. Enhanced Intersystem Crossing in Core-Twisted Aromatics. *Chem. Sci.* **2017**, *8* (3), 1776–1782. https://doi.org/10.1039/C6SC05126J.

(52) Wang, Z.; Huang, L.; Yan, Y.; El-Zohry, A. M.; Toffoletti, A.; Zhao, J.; Barbon, A.; Dick, B.; Mohammed, O. F.; Han, G. Elucidation of the Intersystem Crossing Mechanism in a Helical BODIPY for Low-Dose Photodynamic Therapy. *Angew. Chem. Int. Ed.* **2020**, *59* (37), 16114–16121. https://doi.org/https://doi.org/10.1002/anie.202005269.

(53) Dong, Y.; Kumar, P.; Maity, P.; Kurganskii, I.; Li, S.; Elmali, A.; Zhao, J.; Escudero, D.; Wu, H.; Karatay, A.; Mohammed, O. F.; Fedin, M. Twisted BODIPY Derivative: Intersystem Crossing, Electron Spin Polarization and Application as a Novel Photodynamic Therapy Reagent. *Phys. Chem. Chem. Phys.* **2021**, *23* (14), 8641–8652. https://doi.org/10.1039/D1CP00948F.

(54) Hussain, M.; Zhao, J.; Yang, W.; Zhong, F.; Karatay, A.; Yaglioglu, H. G.; Yildiz, E. A.; Hayvali, M. Intersystem Crossing and Triplet Excited State Properties of Thionated Naphthalenediimide Derivatives. *J. Lumin.* **2017**, *192*, 211–217.

https://doi.org/https://doi.org/10.1016/j.jlumin.2017.06.050.

(55) Ortiz-Rodríguez, L. A.; Crespo-Hernández, C. E. Thionated Organic Compounds as Emerging Heavy-Atom-Free Photodynamic Therapy Agents. *Chem. Sci.* **2020**, *11* (41), 11113–11123. https://doi.org/10.1039/D0SC04747C.

(56) Xiao, Y.; Huang, X.; Feng, J.; Ni, Z.; Gai, L.; Xiao, X.; Sui, X.; Lu, H. A Simple Route toward Triplet-Forming Thionated BODIPY-Based Photosensitizers. *Dyes Pigm.* **2022**, *200*, 110167. https://doi.org/https://doi.org/10.1016/j.dyepig.2022.110167.

(57) Tilley, A. J.; Pensack, R. D.; Lee, T. S.; Djukic, B.; Scholes, G. D.; Seferos, D. S. Ultrafast Triplet Formation in Thionated Perylene Diimides. *J. Phys. Chem. C* **2014**, *118* (19), 9996–10004. https://doi.org/10.1021/jp503708d.

(58) Huang, Y.-F.; Chen, H.-L.; Ting, J. W.; Liao, C.-S.; Larsen, R. W.; Fann, W. Direct Measurement of the Triplet Quantum Yield of Poly(3-Dodecylthiophene) in Solution. *J. Phys. Chem. B* **2004**, *108* (28), 9619–9622. https://doi.org/10.1021/jp0380273.

(59) Tofighi, S.; Zhao, P.; O'Donnell, R. M.; Shi, J.; Zavalij, P. Y.; Bondar, M. V; Hagan, D. J.; Van Stryland, E. W. Fast Triplet Population in Iridium(III) Complexes with Less than Unity Singlet to Triplet Quantum Yield. *J. Phys. Chem. C* **2019**, *123* (22), 13846–13855. https://doi.org/10.1021/acs.jpcc.9b00539.

(60) Devir-Wolfman, A. H.; Khachatryan, B.; Gautam, B. R.; Tzabary, L.; Keren, A.; Tessler, N.; Vardeny, Z. V.; Ehrenfreund, E. Short-Lived Charge-Transfer Excitons in Organic Photovoltaic Cells Studied by High-Field Magneto-Photocurrent. *Nat. Commun.* **2014**, *5* (1), 4529. https://doi.org/10.1038/ncomms5529.

(61) Clarke, T. M.; Durrant, J. R. Charge Photogeneration in Organic Solar Cells. *Chem. Rev.* **2010**, *110* (11), 6736–6767. https://doi.org/10.1021/cr900271s.

(62) Xu, Y.; Li, A.; Yao, T.; Ma, C.; Zhang, X.; Shah, J. H.; Han, H. Strategies for Efficient Charge Separation and Transfer in Artificial Photosynthesis of Solar Fuels. *ChemSusChem* **2017**, *10* (22), 4277–4305. https://doi.org/https://doi.org/10.1002/cssc.201701598.

(63) Frischmann, P. D.; Mahata, K.; Würthner, F. Powering the Future of Molecular Artificial Photosynthesis with Light-Harvesting Metallosupramolecular Dye Assemblies. *Chem. Soc. Rev.* **2013**, *42* (4), 1847–1870. https://doi.org/10.1039/C2CS35223K.

(64) Wang, Z.; Hu, Y.; Zhang, S.; Sun, Y. Artificial Photosynthesis Systems for Solar Energy Conversion and Storage: Platforms and Their Realities. *Chem. Soc. Rev.* **2022**, *51* (15), 6704–6737. https://doi.org/10.1039/D1CS01008E.

(65) Bryden, M. A.; Zysman-Colman, E. Organic Thermally Activated Delayed Fluorescence (TADF) Compounds Used in Photocatalysis. *Chem. Soc. Rev.* **2021**, *50* (13), 7587–7680. https://doi.org/10.1039/D1CS00198A.

(66) Sartor, S. M.; McCarthy, B. G.; Pearson, R. M.; Miyake, G. M.; Damrauer, N. H. Exploiting Charge-Transfer States for Maximizing Intersystem Crossing Yields in Organic Photoredox Catalysts. *J. Am. Chem. Soc.* **2018**, *140* (14), 4778–4781. https://doi.org/10.1021/jacs.8b01001.

(67) Kang, Y. K.; Iovine, P. M.; Therien, M. J. Electron Transfer Reactions of Rigid, Cofacially Compressed, π-Stacked Porphyrin–Bridge–Quinone Systems. *Coord. Chem. Rev.* **2011**, *255* (7), 804–824. https://doi.org/https://doi.org/10.1016/j.ccr.2010.12.011.

(68) Yoshida, M.; Sakai, H.; Ohkubo, K.; Fukuzumi, S.; Hasobe, T. Inter- and Intramolecular Electron-Transfer Reduction Properties of Coronenediimide Derivatives via Photoinduced Processes. *J. Phys. Chem. C* **2018**, *122* (25), 13333–13346. https://doi.org/10.1021/acs.jpcc.7b09817.

(69) Chen, D.-G.; Ranganathan, R.; Lin, J.-A.; Huang, C.-Y.; Ho, M.-L.; Chi, Y.; Chou, P.-T. Ratiometric Tuning of Luminescence: Interplay between the Locally Excited and Interligand Charge-Transfer States in Pyrazolate-Based Boron Compounds. *J. Phys. Chem. C* **2019**, *123* (7), 4022–4028. https://doi.org/10.1021/acs.jpcc.8b11100.

(70) Grabowski, Z. R.; Rotkiewicz, K.; Rettig, W. Structural Changes Accompanying Intramolecular Electron Transfer: Focus on Twisted Intramolecular Charge-Transfer States and Structures. *Chem. Rev.* **2003**, *103* (10), 3899–4032. https://doi.org/10.1021/cr9407451.

(71) Noda, H.; Nakanotani, H.; Adachi, C. Excited State Engineering for Efficient Reverse Intersystem Crossing. *Sci. Adv.* **2022**, *4* (6), eaao6910. https://doi.org/10.1126/sciadv.aao6910.

(72) Barati-darband, F.; Izadyar, M.; Arkan, F. Solvent Effects on Intra-/Intermolecular Charge Transfer in Indoloquinoxaline-Based Dyes. *J. Phys. Chem. A* **2019**, *123* (13), 2831–2842. https://doi.org/10.1021/acs.jpca.9b00812.

(73) Ma, W.; Jiao, Y.; Li, H.; Guo, H.; Kaxiras, E.; Meng, S. Role of Explicitly Included Solvents on Ultrafast Electron Injection and Recombination Dynamics at TiO2/Dye Interfaces. *ACS Appl. Mater. Interfaces* **2020**, *12* (43), 49174–49181. https://doi.org/10.1021/acsami.0c12972.

(74) Cotter, L. F.; Rimgard, B. P.; Parada, G. A.; Mayer, J. M.; Hammarström, L. Solvent and Temperature Effects on Photoinduced Proton-Coupled Electron Transfer in the Marcus Inverted Region. *J. Phys. Chem. A* **2021**, *125* (35), 7670–7684. https://doi.org/10.1021/acs.jpca.1c05764.

(75) El-Sayed, M. A. Effect of Spin Orbit Interactions on the Dipolar Nature of the Radiative Microwave Zero-field Transitions in Aromatic Molecules. *J. Chem. Phys.* **1974**, *60* (11),

4502–4507. https://doi.org/10.1063/1.1680930.

(76) Okada, T.; Karaki, I.; Matsuzawa, E.; Mataga, N.; Sakata, Y.; Misumi, S. Ultrafast Intersystem Crossing in Some Intramolecular Heteroexcimers. *J. Phys. Chem.* **1981**, *85* (26), 3957–3960. https://doi.org/10.1021/j150626a002.

(77) Van Willigen, H.; Jones, G.; Farahat, M. S. Time-Resolved EPR Study of Photoexcited Triplet-State Formation in Electron-Donor-Substituted Acridinium Ions. *J. Phys. Chem.* **1996**, *100* (9), 3312–3316. https://doi.org/10.1021/jp953176+.

(78) Dance, Z. E. X.; Mi, Q.; McCamant, D. W.; Ahrens, M. J.; Ratner, M. A.; Wasielewski, M. R. Time-Resolved EPR Studies of Photogenerated Radical Ion Pairs Separated by p-Phenylene Oligomers and of Triplet States Resulting from Charge Recombination. *J. Phys. Chem. B* **2006**, *110* (50), 25163–25173. https://doi.org/10.1021/jp063690n.

(79) Dance, Z. E. X.; Mickley, S. M.; Wilson, T. M.; Ricks, A. B.; Scott, A. M.; Ratner, M. A.; Wasielewski, M. R. Intersystem Crossing Mediated by Photoinduced Intramolecular Charge Transfer: Julolidine−anthracene Molecules with Perpendicular π Systems. *J. Phys. Chem. A* **2008**, *112* (18), 4194–4201. https://doi.org/10.1021/jp800561g.

(80) Colvin, M. T.; Ricks, A. B.; Scott, A. M.; Co, D. T.; Wasielewski, M. R. Intersystem Crossing Involving Strongly Spin Exchange-Coupled Radical Ion Pairs in Donor–Bridge–Acceptor Molecules. *J. Phys. Chem. A* **2012**, *116* (8), 1923–1930. https://doi.org/10.1021/jp212546w.

(81) Filatov, M. A.; Karuthedath, S.; Polestshuk, P. M.; Savoie, H.; Flanagan, K. J.; Sy, C.; Sitte, E.; Telitchko, M.; Laquai, F.; Boyle, R. W.; Senge, M. O. Generation of Triplet Excited States via Photoinduced Electron Transfer in Meso-Anthra-BODIPY: Fluorogenic Response toward Singlet Oxygen in Solution and in Vitro. *J. Am. Chem. Soc.* **2017**, *139*

(18), 6282–6285. https://doi.org/10.1021/jacs.7b00551.

(82) Shao, S.; Gobeze, H. B.; Bandi, V.; Funk, C.; Heine, B.; Duffy, M. J.; Nesterov, V.; Karr, P. A.; D'Souza, F. Triplet BODIPY and AzaBODIPY Derived Donor-acceptor Dyads: Competitive Electron Transfer versus Intersystem Crossing upon Photoexcitation. *ChemPhotoChem* **2020**, *4* (1), 68–81. https://doi.org/10.1002/cptc.201900189.

(83) Montero, R.; Martínez-Martínez, V.; Longarte, A.; Epelde-Elezcano, N.; Palao, E.; Lamas, I.; Manzano, H.; Agarrabeitia, A. R.; López Arbeloa, I.; Ortiz, M. J.; Garcia-Moreno, I. Singlet Fission Mediated Photophysics of BODIPY Dimers. *J. Phys. Chem. Lett.* **2018**, *9* (3), 641–646. https://doi.org/10.1021/acs.jpclett.7b03074.

(84) Wiebeler, C.; Plasser, F.; Hedley, G. J.; Ruseckas, A.; Samuel, I. D. W.; Schumacher, S. Ultrafast Electronic Energy Transfer in an Orthogonal Molecular Dyad. *J. Phys. Chem. Lett.* **2017**, *8* (5), 1086–1092. https://doi.org/10.1021/acs.jpclett.7b00089.

(85) Hedley, G. J.; Ruseckas, A.; Benniston, A. C.; Harriman, A.; Samuel, I. D. W. Ultrafast Electronic Energy Transfer beyond the Weak Coupling Limit in a Proximal but Orthogonal Molecular Dyad. *J. Phys. Chem. A* **2015**, *119* (51), 12665–12671. https://doi.org/10.1021/acs.jpca.5b08640.

(86) Martinez, J. F.; La Porte, N. T.; Mauck, C. M.; Wasielewski, M. R. Photo-Driven Electron Transfer from the Highly Reducing Excited State of Naphthalene Diimide Radical Anion to a CO2 Reduction Catalyst within a Molecular Triad. *Faraday Discuss.* **2017**, *198* (0), 235–249. https://doi.org/10.1039/C6FD00219F.

(87) Kozycz, L. M.; Gao, D.; Tilley, A. J.; Seferos, D. S. One Donor–Two Acceptor (D–A1)-(D–A2) Random Terpolymers Containing Perylene Diimide, Naphthalene Diimide, and Carbazole Units. *J. Polym. Sci. Part A Polym. Chem.* **2014**, *52* (23), 3337–3345.

https://doi.org/10.1002/pola.27395.

(88) Hussain, M.; El-Zohry, A. M.; Hou, Y.; Toffoletti, A.; Zhao, J.; Barbon, A.; Mohammed, O. F. Spin–Orbit Charge-Transfer Intersystem Crossing of Compact Naphthalenediimide-Carbazole Electron-Donor–Acceptor Triads. *J. Phys. Chem. B* **2021**, *125* (38), 10813–10831. https://doi.org/10.1021/acs.jpcb.1c06498.

(89) Villabona-Monsalve, J. P.; Tcyrulnikov, N. A.; Lorenzo, E. R.; LaBine, N.; Burdick, R.; Krzyaniak, M. D.; Young, R. M.; Wasielewski, M. R.; Goodson, T. Two-Photon Absorption in Electron Donor–Acceptor Dyads and Triads Using Classical and Entangled Photons: Potential Systems for Photon-to-Spin Quantum Transduction. *J. Phys. Chem. C* **2022**, *126* (14), 6334–6343. https://doi.org/10.1021/acs.jpcc.2c00830.

(90) Yun, Y. J.; Manna, M. K.; Kamatham, N.; Li, J.; Liu, S.; Peccati, F.; Pemberton, B. C.; Wiederrecht, G. P.; Gosztola, D. J.; Jiménez-Osés, G.; Rogachev, A. Y.; Ayitou, A. J.-L. Synthesis and Photophysics of Phenylene Based Triplet Donor–Acceptor Dyads: Ortho vs. Para Positional Effect on Intramolecular Triplet Energy Transfer. *J. Photochem. Photobiol.* **2022**, *10*, 100112. https://doi.org/https://doi.org/10.1016/j.jpap.2022.100112.

(91) Filatov, M. A.; Karuthedath, S.; Polestshuk, P. M.; Callaghan, S.; Flanagan, K. J.; Wiesner, T.; Laquai, F.; Senge, M. O. BODIPY-Pyrene and Perylene Dyads as Heavy-Atom-Free Singlet Oxygen Sensitizers. *ChemPhotoChem* **2018**, *2* (7), 606–615. https://doi.org/10.1002/cptc.201800020.

(92) Huang, G.-J.; Harris, M. A.; Krzyaniak, M. D.; Margulies, E. A.; Dyar, S. M.; Lindquist, R. J.; Wu, Y.; Roznyatovskiy, V. V; Wu, Y.-L.; Young, R. M.; Wasielewski, M. R. Photoinduced Charge and Energy Transfer within Meta- and Para-Linked Chlorophyll a-Perylene-3,4:9,10-Bis(Dicarboximide) Donor–Acceptor Dyads. *J. Phys. Chem. B* **2016**, *120*

(4), 756–765. https://doi.org/10.1021/acs.jpcb.5b10806.

(93) Guo, Y.; Ma, Z.; Niu, X.; Zhang, W.; Tao, M.; Guo, Q.; Wang, Z.; Xia, A. Bridge-Mediated Charge Separation in Isomeric N-Annulated Perylene Diimide Dimers. *J. Am. Chem. Soc.* **2019**, *141* (32), 12789–12796. https://doi.org/10.1021/jacs.9b05723.

(94) Hong, Y.; Schlosser, F.; Kim, W.; Würthner, F.; Kim, D. Ultrafast Symmetry-Breaking Charge Separation in a Perylene Bisimide Dimer Enabled by Vibronic Coupling and Breakdown of Adiabaticity. *J. Am. Chem. Soc.* **2022**, *144* (34), 15539–15548. https://doi.org/10.1021/jacs.2c03916.

(95) Loong, H.; Zhou, J.; Jiang, N.; Feng, Y.; Xie, G.; Liu, L.; Xie, Z. Photoinduced Cascading Charge Transfer in Perylene Bisimide-Based Triads. *J. Phys. Chem. B* **2022**, *126* (12), 2441–2448. https://doi.org/10.1021/acs.jpcb.2c00965.

(96) Levy, D.; Arnold, B. R. Analysis of Charge-Transfer Absorption and Emission Spectra on an Absolute Scale: Evaluation of Free Energies, Matrix Elements, and Reorganization Energies. *J. Phys. Chem. A* **2005**, *109* (38), 8572–8578. https://doi.org/10.1021/jp052532d.

(97) Verhoeven, J. W.; Scherer, T.; Wegewijs, B.; Hermant, R. M.; Jortner, J.; Bixon, M.; Depaemelaere, S.; de Schryver, F. C. Electronic Coupling in Inter- and Intramolecular Donor-Acceptor Systems as Revealed by Their Solvent-Dependent Charge-Transfer Fluorescence. *Recl. Trav. Chim. Pays-Bas* **1995**, *114* (11–12), 443–448. https://doi.org/https://doi.org/10.1002/recl.19951141104.

(98) Verhoeven, J. W.; van Ramesdonk, H. J.; Groeneveld, M. M.; Benniston, A. C.; Harriman, A. Long-Lived Charge-Transfer States in Compact Donor–Acceptor Dyads. *ChemPhysChem* **2005**, *6* (11), 2251–2260. https://doi.org/10.1002/cphc.200500029.

(99) Hu, J.; Li, Y.; Zhu, H.; Qiu, S.; He, G.; Zhu, X.; Xia, A. Photophysical Properties of

Intramolecular Charge Transfer in a Tribranched Donor–π–Acceptor Chromophore. *ChemPhysChem* **2015**, *16* (11), 2357–2365. https://doi.org/https://doi.org/10.1002/cphc.201500290.

(100) Pal, S. K.; Sahu, T.; Misra, T.; Ganguly, T.; Pradhan, T. K.; De, A. Synthesis, Characterization and Laser Flash Photolysis Studies of Some Naphthothiophenes Bearing Electron Donor and Acceptor Functional Groups. *J. Photochem. Photobiol. A Chem.* **2005**, *174* (2), 138–148. https://doi.org/https://doi.org/10.1016/j.jphotochem.2005.03.005.

(101) Zhao, Y.; Li, X.; Wang, Z.; Yang, W.; Chen, K.; Zhao, J.; Gurzadyan, G. G. Precise Control of the Electronic Coupling Magnitude between the Electron Donor and Acceptor in Perylenebisimide Derivatives via Conformation Restriction and Its Effect on Photophysical Properties. *J. Phys. Chem. C* **2018**, *122* (7), 3756–3772. https://doi.org/10.1021/acs.jpcc.7b11872.

(102) Higginbotham, H. F.; Pander, P.; Rybakiewicz, R.; Etherington, M. K.; Maniam, S.; Zagorska, M.; Pron, A.; Monkman, A. P.; Data, P. Triphenylamine Disubstituted Naphthalene Diimide: Elucidation of Excited States Involved in TADF and Application in near-Infrared Organic Light Emitting Diodes. *J. Mater. Chem. C* **2018**, *6* (30), 8219–8225. https://doi.org/10.1039/C8TC02936A.

(103) Sasaki, S.; Hattori, K.; Igawa, K.; Konishi, G. Directional Control of π-Conjugation Enabled by Distortion of the Donor Plane in Diarylaminoanthracenes: A Photophysical Study. *J. Phys. Chem. A* **2015**, *119* (20), 4898–4906. https://doi.org/10.1021/acs.jpca.5b03238.

(104) Dey, J.; Warner, I. M. Dual Fluorescence of 9-(N,N-Dimethylamino)Anthracene: Effect of Solvent Polarity and Viscosity. *J. Phys. Chem. A* **1997**, *101* (27), 4872–4878. https://doi.org/10.1021/jp9638696.

(105) Wang, Z.; Zhao, J.; Di Donato, M.; Mazzone, G. Increasing the Anti-Stokes Shift in TTA Upconversion with Photosensitizers Showing Red-Shifted Spin-Allowed Charge Transfer Absorption but a Non-Compromised Triplet State Energy Level. *Chem. Commun.* **2019**, *55* (10), 1510–1513. https://doi.org/10.1039/c8cc08159j.

(106) Wu, T. C.; Congreve, D. N.; Baldo, M. A. Solid State Photon Upconversion Utilizing Thermally Activated Delayed Fluorescence Molecules as Triplet Sensitizer. *Appl. Phys. Lett.* **2015**, *107* (3), 31103. https://doi.org/10.1063/1.4926914.

(107) Yanai, N.; Kozue, M.; Amemori, S.; Kabe, R.; Adachi, C.; Kimizuka, N. Increased Vis-to-UV Upconversion Performance by Energy Level Matching between a TADF Donor and High Triplet Energy Acceptors. *J. Mater. Chem. C* **2016**, *4* (27), 6447–6451. https://doi.org/10.1039/C6TC01816E.

(108) Lee, H.-L.; Lee, M.-S.; Park, H.; Han, W.-S.; Kim, J.-H. Visible-to-UV Triplet-Triplet Annihilation Upconversion from a Thermally Activated Delayed Fluorescence/Pyrene Pair in an Air-Saturated Solution. *Korean J. Chem. Eng.* **2019**, *36* (11), 1791–1798. https://doi.org/10.1007/s11814-019-0355-2.

(109) Zähringer, T. J. B.; Bertrams, M.-S.; Kerzig, C. Purely Organic Vis-to-UV Upconversion with an Excited Annihilator Singlet beyond 4 EV. *J. Mater. Chem. C* **2022**, *10* (12), 4568–4573. https://doi.org/10.1039/D1TC04782E.

(110) Han, D.; Yang, X.; Han, J.; Zhou, J.; Jiao, T.; Duan, P. Sequentially Amplified Circularly Polarized Ultraviolet Luminescence for Enantioselective Photopolymerization. *Nat. Commun.* **2020**, *11* (1), 5659. https://doi.org/10.1038/s41467-020-19479-1.

(111) Wei, D.; Ni, F.; Zhu, Z.; Zou, Y.; Yang, C. A Red Thermally Activated Delayed Fluorescence Material as a Triplet Sensitizer for Triplet–Triplet Annihilation up-

Conversion with High Efficiency and Low Energy Loss. *J. Mater. Chem. C* **2017**, *5* (48), 12674–12677. https://doi.org/10.1039/C7TC04096B.

(112) Chen, W.; Song, F.; Tang, S.; Hong, G.; Wu, Y.; Peng, X. Red-to-Blue Photon up-Conversion with High Efficiency Based on a TADF Fluorescein Derivative. *Chem. Commun.* **2019**, *55* (30), 4375–4378. https://doi.org/10.1039/C9CC01868A.

(113) Zhao, Y.; Wu, Y.; Chen, W.; Zhang, R.; Hong, G.; Tian, J.; Wang, H.; Zheng, D.; Wu, C.; Jiang, X.; Huo, X.; Sun, L.; Deng, W.; Han, K.; Song, F. The Second Excited Triplet-State Facilitates TADF and Triplet–Triplet Annihilation Photon Upconversion via a Thermally Activated Reverse Internal Conversion. *Adv. Opt. Mater.* **2022**, *10* (6), 2102275. https://doi.org/https://doi.org/10.1002/adom.202102275.

(114) Yang, Z.; Mao, Z.; Xie, Z.; Zhang, Y.; Liu, S.; Zhao, J.; Xu, J.; Chi, Z.; Aldred, M. P. Recent Advances in Organic Thermally Activated Delayed Fluorescence Materials. *Chem. Soc. Rev.* **2017**, *46* (3), 915–1016. https://doi.org/10.1039/C6CS00368K.

(115) Huang, T.; Jiang, W.; Duan, L. Recent Progress in Solution Processable TADF Materials for Organic Light-Emitting Diodes. *J. Mater. Chem. C* **2018**, *6* (21), 5577–5596. https://doi.org/10.1039/C8TC01139G.

(116) Chen, X.-K.; Kim, D.; Brédas, J.-L. Thermally Activated Delayed Fluorescence (TADF) Path toward Efficient Electroluminescence in Purely Organic Materials: Molecular Level Insight. *Acc. Chem. Res.* **2018**, *51* (9), 2215–2224. https://doi.org/10.1021/acs.accounts.8b00174.

(117) Lee, J.-H.; Chen, C.-H.; Lee, P.-H.; Lin, H.-Y.; Leung, M.; Chiu, T.-L.; Lin, C.-F. Blue Organic Light-Emitting Diodes: Current Status, Challenges, and Future Outlook. *J. Mater. Chem. C* **2019**, *7* (20), 5874–5888. https://doi.org/10.1039/C9TC00204A.

(118) Zou, S.-J.; Shen, Y.; Xie, F.-M.; Chen, J.-D.; Li, Y.-Q.; Tang, J.-X. Recent Advances in Organic Light-Emitting Diodes: Toward Smart Lighting and Displays. *Mater. Chem. Front.* **2020**, *4* (3), 788–820. https://doi.org/10.1039/C9QM00716D.

(119) Czerwieniec, R.; Leitl, M. J.; Homeier, H. H. H.; Yersin, H. Cu(I) Complexes – Thermally Activated Delayed Fluorescence. Photophysical Approach and Material Design. *Coord. Chem. Rev.* **2016**, *325*, 2–28. https://doi.org/https://doi.org/10.1016/j.ccr.2016.06.016.

(120) Shu, Y.; Levine, B. G. Simulated Evolution of Fluorophores for Light Emitting Diodes. *J. Chem. Phys.* **2015**, *142* (10), 104104. https://doi.org/10.1063/1.4914294.

(121) Masui, K.; Nakanotani, H.; Adachi, C. Analysis of Exciton Annihilation in High-Efficiency Sky-Blue Organic Light-Emitting Diodes with Thermally Activated Delayed Fluorescence. *Org. Electron.* **2013**, *14* (11), 2721–2726. https://doi.org/https://doi.org/10.1016/j.orgel.2013.07.010.

(122) Uoyama, H.; Goushi, K.; Shizu, K.; Nomura, H.; Adachi, C. Highly Efficient Organic Light-Emitting Diodes from Delayed Fluorescence. *Nature* **2012**, *492* (7428), 234–238. https://doi.org/10.1038/nature11687.

(123) Lee, S. Y.; Yasuda, T.; Yang, Y. S.; Zhang, Q.; Adachi, C. Luminous Butterflies: Efficient Exciton Harvesting by Benzophenone Derivatives for Full-Color Delayed Fluorescence OLEDs. *Angew. Chem. Int. Ed.* **2014**, *53* (25), 6402–6406. https://doi.org/https://doi.org/10.1002/anie.201402992.

(124) Penfold, T. J.; Gindensperger, E.; Daniel, C.; Marian, C. M. Spin-Vibronic Mechanism for Intersystem Crossing. *Chem. Rev.* **2018**, *118* (15), 6975–7025. https://doi.org/10.1021/acs.chemrev.7b00617.

(125) Ruhstaller, B.; Carter, S. A.; Barth, S.; Riel, H.; Riess, W.; Scott, J. C. Transient and Steady-

State Behavior of Space Charges in Multilayer Organic Light-Emitting Diodes. *J. Appl. Phys.* **2001**, *89* (8), 4575–4586. https://doi.org/10.1063/1.1352027.

(126) Chen, J.; Xiao, X.; Li, S.; Duan, Y.; Wang, G.; Liao, Y.; Peng, Q.; Fu, H.; Geng, H.; Shuai, Z. A Novel Strategy toward Thermally Activated Delayed Fluorescence from a Locally Excited State. *J. Phys. Chem. Lett.* **2022**, *13* (11), 2653–2660. https://doi.org/10.1021/acs.jpclett.2c00224.

(127) Marian, C. M. Mechanism of the Triplet-to-Singlet Upconversion in the Assistant Dopant ACRXTN. *J. Phys. Chem. C* **2016**, *120* (7), 3715–3721. https://doi.org/10.1021/acs.jpcc.6b00060.

(128) El-Sayed, M. A. Triplet State. Its Radiative and Nonradiative Properties. *Acc. Chem. Res.* **1968**, *1* (1), 8–16. https://doi.org/10.1021/ar50001a002.

(129) Lim, B. T.; Okajima, S.; Chandra, A. K.; Lim, E. C. Radiationless Transitions in Electron Donor-Acceptor Complexes: Selection Rules for S1 → T Intersystem Crossing and Efficiency of S1 → S0 Internal Conversion. *Chem. Phys. Lett.* **1981**, *79* (1), 22–27. https://doi.org/https://doi.org/10.1016/0009-2614(81)85280-3.

(130) Baba, M. Intersystem Crossing in the 1nπ* and 1ππ* States. *J. Phys. Chem. A* **2011**, *115* (34), 9514–9519. https://doi.org/10.1021/jp111892y.

(131) Etherington, M. K.; Gibson, J.; Higginbotham, H. F.; Penfold, T. J.; Monkman, A. P. Revealing the Spin-Vibronic Coupling Mechanism of Thermally Activated Delayed Fluorescence. *Nat. Commun.* **2016**, *7*, 13680. https://doi.org/10.1038/ncomms13680.

(132) Noda, H.; Chen, X.-K.; Nakanotani, H.; Hosokai, T.; Miyajima, M.; Notsuka, N.; Kashima, Y.; Brédas, J.-L.; Adachi, C. Critical Role of Intermediate Electronic States for Spin-Flip Processes in Charge-Transfer-Type Organic Molecules with Multiple Donors and

Acceptors. *Nat. Mater.* **2019**, *18* (10), 1084–1090. https://doi.org/10.1038/s41563-019-0465-6.

(133) Hosokai, T.; Noda, H.; Nakanotani, H.; Nawata, T.; Nakayama, Y.; Matsuzaki, H.; Adachi, C. Solvent-Dependent Investigation of Carbazole Benzonitrile Derivatives: Does the ^{3}LE–^{1}CT Energy Gap Facilitate Thermally Activated Delayed Fluorescence? *J. Photonics Energy* **2018**, *8* (3), 32102. https://doi.org/10.1117/1.JPE.8.032102.

(134) Gibson, J.; Monkman, A. P.; Penfold, T. J. The Importance of Vibronic Coupling for Efficient Reverse Intersystem Crossing in Thermally Activated Delayed Fluorescence Molecules. *ChemPhysChem* **2016**, *17* (19), 2956–2961. https://doi.org/https://doi.org/10.1002/cphc.201600662.

(135) Dias, F. B.; Santos, J.; Graves, D. R.; Data, P.; Nobuyasu, R. S.; Fox, M. A.; Batsanov, A. S.; Palmeira, T.; Berberan-Santos, M. N.; Bryce, M. R.; Monkman, A. P. The Role of Local Triplet Excited States and D-A Relative Orientation in Thermally Activated Delayed Fluorescence: Photophysics and Devices. *Adv. Sci.* **2016**, *3* (12), 1600080. https://doi.org/10.1002/advs.201600080.

(136) Santos, P. L.; Ward, J. S.; Data, P.; Batsanov, A. S.; Bryce, M. R.; Dias, F. B.; Monkman, A. P. Engineering the Singlet–Triplet Energy Splitting in a TADF Molecule. *J. Mater. Chem. C* **2016**, *4* (17), 3815–3824. https://doi.org/10.1039/C5TC03849A.

(137) Samanta, P. K.; Kim, D.; Coropceanu, V.; Brédas, J.-L. Up-Conversion Intersystem Crossing Rates in Organic Emitters for Thermally Activated Delayed Fluorescence: Impact of the Nature of Singlet vs Triplet Excited States. *J. Am. Chem. Soc.* **2017**, *139* (11), 4042–4051. https://doi.org/10.1021/jacs.6b12124.

(138) Wang, L.; Yin, H.; Jabed, M.; Hetu, M.; Wang, C.; Monro, S.; Zhu, X.; Kilina, S.;

Mcfarland, S.; Sun, W. Π-Expansive Heteroleptic Ruthenium(II) Complexes as Reverse Saturable Absorbers and Photosensitizers for Photodynamic Therapy. *Inorg. Chem.* **2017**, *56*. https://doi.org/10.1021/acs.inorgchem.6b02624.

(139) Lu, T.; Wang, C.; Lystrom, L.; Pei, C.; Kilina, S.; Sun, W. Effects of Extending the π-Conjugation of the Acetylide Ligand on the Photophysics and Reverse Saturable Absorption of Pt(II) Bipyridine Bisacetylide Complexes. *Phys. Chem. Chem. Phys.* **2016**, *18*. https://doi.org/10.1039/c6cp02628a.

(140) Liu, R.; Dandu, N.; McCleese, C.; Li, Y.; Lu, T.; Li, H.; Yost, D.; Wang, C.; Kilina, S.; Burda, C.; Sun, W. Influence of a Naphthaldiimide Substituent at the Diimine Ligand on the Photophysics and Reverse Saturable Absorption of PtII Diimine Complexes and Cationic IrIII Complexes. *Eur. J. Inorg. Chem.* **2015**, *2015* (31), 5241–5253. https://doi.org/https://doi.org/10.1002/ejic.201500882.

(141) Liu, R.; Li, Y.; Chang, J.; Waclawik, E.; Sun, W. Pt(II) Bipyridyl Complexes Bearing Substituted Fluorenyl Motif on the Bipyridyl and Acetylide Ligands: Synthesis, Photophysics, and Reverse Saturable Absorption. *Inorg. Chem.* **2014**, *53*. https://doi.org/10.1021/ic500646r.

(142) Sun, W.; Zhang, B.; Li, Y.; Liu, R.; Pritchett, T.; Haley, J. Extending the Bandwidth of Reverse Saturable Absorption in Platinum Complexes Using Two-Photon-Initiated Excited-State Absorption. *ACS Appl. Mater. Interfaces* **2012**, *5*. https://doi.org/10.1021/am3018724.

(143) Gut, A.; Łapok, Ł.; Drelinkiewicz, D.; Pędziński, T.; Marciniak, B.; Nowakowska, M. Visible-Light Photoactive, Highly Efficient Triplet Sensitizers Based on Iodinated Aza-BODIPYs: Synthesis, Photophysics and Redox Properties. *Chem. – An Asian J.* **2018**, *13* (1), 55–65. https://doi.org/https://doi.org/10.1002/asia.201701485.

(144) Bassan, E.; Gualandi, A.; Cozzi, P. G.; Ceroni, P. Design of BODIPY Dyes as Triplet Photosensitizers: Electronic Properties Tailored for Solar Energy Conversion, Photoredox Catalysis and Photodynamic Therapy. *Chem. Sci.* **2021**, *12* (19), 6607–6628. https://doi.org/10.1039/D1SC00732G.

(145) Zhang, X.-F.; Zhang, I.; Liu, L. Photophysics of Halogenated Fluoresceins: Involvement of Both Intramolecular Electron Transfer and Heavy Atom Effect in the Deactivation of Excited States. *Photochem. Photobiol.* **2010**, *86* (3), 492–498. https://doi.org/10.1111/j.1751-1097.2010.00706.x.

(146) Richert, S.; Tait, C. E.; Timmel, C. R. Delocalisation of Photoexcited Triplet States Probed by Transient EPR and Hyperfine Spectroscopy. *J. Magn. Reson.* **2017**, *280*, 103–116. https://doi.org/https://doi.org/10.1016/j.jmr.2017.01.005.

(147) Ogiwara, T.; Wakikawa, Y.; Ikoma, T. Mechanism of Intersystem Crossing of Thermally Activated Delayed Fluorescence Molecules. *J. Phys. Chem. A* **2015**, *119* (14), 3415–3418. https://doi.org/10.1021/acs.jpca.5b02253.

(148) Green, M. A.; Ho-Baillie, A.; Snaith, H. J. The Emergence of Perovskite Solar Cells. *Nat. Photonics* **2014**, *8* (7), 506–514. https://doi.org/10.1038/nphoton.2014.134.

(149) S. Richards, B.; Hudry, D.; Busko, D.; Turshatov, A.; A. Howard, I. Photon Upconversion for Photovoltaics and Photocatalysis: A Critical Review. *Chem. Rev.* **2021**, *121* (15), 9165–9195. https://doi.org/10.1021/acs.chemrev.1c00034.

(150) Prier, C. K.; Rankic, D. A.; MacMillan, D. W. C. Visible Light Photoredox Catalysis with Transition Metal Complexes: Applications in Organic Synthesis. *Chem. Rev.* **2013**, *113* (7), 5322–5363. https://doi.org/10.1021/cr300503r.

(151) Narayanam, J. M. R.; Stephenson, C. R. J. Visible Light Photoredox Catalysis: Applications

in Organic Synthesis. *Chem. Soc. Rev.* **2011**, *40* (1), 102–113.

(152) Bertrams, M.-S.; Kerzig, C. Converting P-Terphenyl into a Novel Organo-Catalyst for LED-Driven Energy and Electron Transfer Photoreactions in Water. *Chem. Commun.* **2021**, *57* (55), 6752–6755. https://doi.org/10.1039/D1CC01947C.

(153) David, A. H. G.; Casares, R.; Cuerva, J. M.; Campaña, A. G.; Blanco, V. A [2]Rotaxane-Based Circularly Polarized Luminescence Switch. *J. Am. Chem. Soc.* **2019**, *141* (45), 18064–18074. https://doi.org/10.1021/jacs.9b07143.

(154) Song, F.; Wei, G.; Jiang, X.; Li, F.; Zhu, C.; Cheng, Y. Chiral Sensing for Induced Circularly Polarized Luminescence Using an Eu(III)-Containing Polymer and d- or l-Proline. *Chem. Commun.* **2013**, *49* (51), 5772–5774. https://doi.org/10.1039/C3CC42323A.

(155) Carr, R.; Evans, N. H.; Parker, D. Lanthanide Complexes as Chiral Probes Exploiting Circularly Polarized Luminescence. *Chem. Soc. Rev.* **2012**, *41* (23), 7673–7686. https://doi.org/10.1039/C2CS35242G.

(156) Wang, Y.-F.; Liu, X.; Zhu, Y.; Li, M.; Chen, C.-F. Aromatic-Imide-Based TADF Enantiomers for Efficient Circularly Polarized Electroluminescence. *J. Mater. Chem. C* **2022**, *10* (12), 4805–4812. https://doi.org/10.1039/D1TC04893G.

(157) Muller, G. Luminescent Chiral Lanthanide(III) Complexes as Potential Molecular Probes. *Dalton Trans.* **2009**, No. 44, 9692–9707. https://doi.org/10.1039/b909430j.

(158) Kawasaki, T.; Sato, M.; Ishiguro, S.; Saito, T.; Morishita, Y.; Sato, I.; Nishino, H.; Inoue, Y.; Soai, K. Enantioselective Synthesis of near Enantiopure Compound by Asymmetric Autocatalysis Triggered by Asymmetric Photolysis with Circularly Polarized Light. *J. Am. Chem. Soc.* **2005**, *127* (10), 3274–3275. https://doi.org/10.1021/ja0422108.

(159) Yeom, J.; Yeom, B.; Chan, H.; Smith, K. W.; Dominguez-Medina, S.; Bahng, J. H.; Zhao,

G.; Chang, W.-S.; Chang, S.-J.; Chuvilin, A.; Melnikau, D.; Rogach, A. L.; Zhang, P.; Link, S.; Král, P.; Kotov, N. A. Chiral Templating of Self-Assembling Nanostructures by Circularly Polarized Light. *Nat. Mater.* **2015**, *14* (1), 66–72. https://doi.org/10.1038/nmat4125.

(160) Yan, Z.-P.; Luo, X.-F.; Liu, W.-Q.; Wu, Z.-G.; Liang, X.; Liao, K.; Wang, Y.; Zheng, Y.-X.; Zhou, L.; Zuo, J.-L.; Pan, Y.; Zhang, H. Configurationally Stable Platinahelicene Enantiomers for Efficient Circularly Polarized Phosphorescent Organic Light-Emitting Diodes. *Chemistry* **2019**, *25* (22), 5672–5676. https://doi.org/10.1002/chem.201900955.

(161) Zhang, D.-W.; Li, M.; Chen, C.-F. Recent Advances in Circularly Polarized Electroluminescence Based on Organic Light-Emitting Diodes. *Chem. Soc. Rev.* **2020**, *49* (5), 1331–1343. https://doi.org/10.1039/C9CS00680J.

(162) Li, M.; Li, S.-H.; Zhang, D.; Cai, M.; Duan, L.; Fung, M.-K.; Chen, C.-F. Stable Enantiomers Displaying Thermally Activated Delayed Fluorescence: Efficient OLEDs with Circularly Polarized Electroluminescence. *Angew. Chem. Int. Ed.* **2018**, *57* (11), 2889–2893. https://doi.org/https://doi.org/10.1002/anie.201800198.

(163) Han, J.; Guo, S.; Lu, H.; Liu, S.; Zhao, Q.; Huang, W. Recent Progress on Circularly Polarized Luminescent Materials for Organic Optoelectronic Devices. *Adv. Opt. Mater.* **2018**, *6* (17), 1800538. https://doi.org/https://doi.org/10.1002/adom.201800538.

(164) Peng, J.; Guo, X.; Jiang, X.; Zhao, D.; Ma, Y. Developing Efficient Heavy-Atom-Free Photosensitizers Applicable to TTA Upconversion in Polymer Films. *Chem. Sci.* **2016**, *7* (2), 1233–1237. https://doi.org/10.1039/C5SC03245H.

(165) Chen, Q.; Liu, Y.; Guo, X.; Peng, J.; Garakyaraghi, S.; Papa, C. M.; Castellano, F. N.; Zhao, D.; Ma, Y. Energy Transfer Dynamics in Triplet–Triplet Annihilation Upconversion Using

a Bichromophoric Heavy-Atom-Free Sensitizer. *J. Phys. Chem. A* **2018**, *122* (33), 6673–6682. https://doi.org/10.1021/acs.jpca.8b05901.

(166) Omer, K. M.; Ku, S.-Y.; Wong, K.-T.; Bard, A. J. Green Electrogenerated Chemiluminescence of Highly Fluorescent Benzothiadiazole and Fluorene Derivatives. *J. Am. Chem. Soc.* **2009**, *131* (30), 10733–10741. https://doi.org/10.1021/ja904135y.

(167) Wang, S.; Yan, X.; Cheng, Z.; Zhang, H.; Liu, Y.; Wang, Y. Highly Efficient Near-Infrared Delayed Fluorescence Organic Light Eeitting Diodes Using a Phenanthrene-Based Charge-Transfer Compound. *Angew. Chem. Int. Ed.* **2015**, *54* (44), 13068–13072. https://doi.org/https://doi.org/10.1002/anie.201506687.

(168) Ni, F.; Wu, Z.; Zhu, Z.; Chen, T.; Wu, K.; Zhong, C.; An, K.; Wei, D.; Ma, D.; Yang, C. Teaching an Old Acceptor New Tricks: Rationally Employing 2,1,3-Benzothiadiazole as Input to Design a Highly Efficient Red Thermally Activated Delayed Fluorescence Emitter. *J. Mater. Chem. C* **2017**, *5* (6), 1363–1368. https://doi.org/10.1039/C7TC00025A.

(169) Bhosale, S. V; Jani, C. H.; Langford, S. J. Chemistry of Naphthalene Diimides. *Chem. Soc. Rev.* **2008**, *37* (2), 331–342. https://doi.org/10.1039/B615857A.

(170) Pan, M.; Lin, X.-M.; Li, G.-B.; Su, C.-Y. Progress in the Study of Metal–Organic Materials Applying Naphthalene Diimide (NDI) Ligands. *Coord. Chem. Rev.* **2011**, *255* (15–16), 1921–1936.

(171) Al Kobaisi, M.; Bhosale, S. V; Latham, K.; Raynor, A. M.; Bhosale, S. V. Functional Naphthalene Diimides: Synthesis, Properties, and Applications. *Chem. Rev.* **2016**, *116* (19), 11685–11796. https://doi.org/10.1021/acs.chemrev.6b00160.

(172) Bhat, S. A.; Das, C.; Maji, T. K. Metallated Azo-Naphthalene Diimide Based Redox-Active Porous Organic Polymer as an Efficient Water Oxidation Electrocatalyst. *J. Mater. Chem.*

A **2018**, *6* (40), 19834–19842. https://doi.org/10.1039/C8TA06588H.

(173) Hirota, N.; Yamauchi, S. Short-Lived Excited Triplet States Studied by Time-Resolved EPR Spectroscopy. *J. Photochem. Photobiol. C Photochem. Rev.* **2003**, *4* (2), 109–124. https://doi.org/https://doi.org/10.1016/S1389-5567(03)00024-8.

(174) Gillett, A. J.; Privitera, A.; Dilmurat, R.; Karki, A.; Qian, D.; Pershin, A.; Londi, G.; Myers, W. K.; Lee, J.; Yuan, J.; Ko, S.-J.; Riede, M. K.; Gao, F.; Bazan, G. C.; Rao, A.; Nguyen, T.-Q.; Beljonne, D.; Friend, R. H. The Role of Charge Recombination to Triplet Excitons in Organic Solar Cells. *Nature* **2021**, *597* (7878), 666–671. https://doi.org/10.1038/s41586-021-03840-5.

(175) Xiong, X.; Song, F.; Sun, S.; Fan, J.; Peng, X. Red-Emissive Fluorescein Derivatives and Detection of Bovine Serum Albumin. *Asian J. Org. Chem.* **2013**, *2* (2), 145–149. https://doi.org/https://doi.org/10.1002/ajoc.201200109.

(176) Xiong, X.; Song, F.; Wang, J.; Zhang, Y.; Xue, Y.; Sun, L.; Jiang, N.; Gao, P.; Tian, L.; Peng, X. Thermally Activated Delayed Fluorescence of Fluorescein Derivative for Time-Resolved and Confocal Fluorescence Imaging. *J. Am. Chem. Soc.* **2014**, *136* (27), 9590–9597. https://doi.org/10.1021/ja502292p.

(177) Yurash, B.; Dixon, A.; Espinoza, C.; Mikhailovsky, A.; Chae, S.; Nakanotani, H.; Adachi, C.; Nguyen, T.-Q. Efficiency of Thermally Activated Delayed Fluorescence Sensitized Triplet Upconversion Doubled in Three-Component System. *Adv. Mater.* **2022**, *34* (5), 2103976. https://doi.org/https://doi.org/10.1002/adma.202103976.

(178) Yaxiong, W.; Ke, P.; Xiaosong, C.; Yuanming, L.; Xiaoguo, Z.; Chuluo, Y. Multiple Resonance Thermally Activated Delayed Fluorescence Sensitizers Enable Green-to-Ultraviolet Photon Upconversion: Application in Photochemical Transformations. *CCS*

Chem. **2022**, *4* (12), 1–12. https://doi.org/10.31635/ccschem.022.202101507.

(179) Yang, M.; Sheykhi, S.; Zhang, Y.; Milsmann, C.; Castellano, F. N. Chem. Soc. Rev. *Chem. Sci.* **2021**, *12* (26), 9069–9077. https://doi.org/10.1039/D1SC01662H.

(180) Huang, Z.; Li, X.; Mahboub, M.; Hanson, K. M.; Nichols, V. M.; Le, H.; Tang, M. L.; Bardeen, C. J. Hybrid Molecule-Nanocrystal Photon Upconversion across the Visible and near-Infrared. *Nano Lett.* **2015**, *15* (8), 5552–5557. https://doi.org/10.1021/acs.nanolett.5b02130.

(181) Sasaki, Y.; Amemori, S.; Kouno, H.; Yanai, N.; Kimizuka, N. Near Infrared-to-Blue Photon Upconversion by Exploiting Direct S–T Absorption of a Molecular Sensitizer. *J. Mater. Chem. C* **2017**, *5* (21), 5063–5067. https://doi.org/10.1039/C7TC00827A.

(182) Ogawa, T.; Hosoyamada, M.; Yurash, B.; Nguyen, T.-Q.; Yanai, N.; Kimizuka, N. Donor–Acceptor–Collector Ternary Crystalline Films for Efficient Solid-State Photon Upconversion. *J. Am. Chem. Soc.* **2018**, *140* (28), 8788–8796. https://doi.org/10.1021/jacs.8b04542.

(183) Kondo, Y.; Yoshiura, K.; Kitera, S.; Nishi, H.; Oda, S.; Gotoh, H.; Sasada, Y.; Yanai, M.; Hatakeyama, T. Narrowband Deep-Blue Organic Light-Emitting Diode Featuring an Organoboron-Based Emitter. *Nat. Photonics* **2019**, *13* (10), 678–682. https://doi.org/10.1038/s41566-019-0476-5.

(184) Santoro, F.; Lami, A.; Improta, R.; Bloino, J.; Barone, V. Effective Method for the Computation of Optical Spectra of Large Molecules at Finite Temperature Including the Duschinsky and Herzberg-Teller Effect: The Qx Band of Porphyrin as a Case Study. *J. Chem. Phys.* **2008**, *128* (22), 224311. https://doi.org/10.1063/1.2929846.

(185) Hatakeyama, T.; Shiren, K.; Nakajima, K.; Nomura, S.; Nakatsuka, S.; Kinoshita, K.; Ni,

J.; Ono, Y.; Ikuta, T. Ultrapure Blue Thermally Activated Delayed Fluorescence Molecules: Efficient HOMO–LUMO Separation by the Multiple Resonance Effect. *Adv. Mater.* **2016**, *28* (14), 2777–2781. https://doi.org/https://doi.org/10.1002/adma.201505491.

(186) Sun, D.; Suresh, S. M.; Hall, D.; Zhang, M.; Si, C.; Cordes, D. B.; Slawin, A. M. Z.; Olivier, Y.; Zhang, X.; Zysman-Colman, E. The Design of an Extended Multiple Resonance TADF Emitter Based on a Polycyclic Amine/Carbonyl System. *Mater. Chem. Front.* **2020**, *4* (7), 2018–2022. https://doi.org/10.1039/D0QM00190B.

(187) Osawa, M.; Kawata, I.; Ishii, R.; Igawa, S.; Hashimoto, M.; Hoshino, M. Application of Neutral D10 Coinage Metal Complexes with an Anionic Bidentate Ligand in Delayed Fluorescence-Type Organic Light-Emitting Diodes. *J. Mater. Chem. C* **2013**, *1* (28), 4375–4383. https://doi.org/10.1039/C3TC30524D.

(188) Leitl, M. J.; Krylova, V. A.; Djurovich, P. I.; Thompson, M. E.; Yersin, H. Phosphorescence versus Thermally Activated Delayed Fluorescence. Controlling Singlet–Triplet Splitting in Brightly Emitting and Sublimable Cu(I) Compounds. *J. Am. Chem. Soc.* **2014**, *136* (45), 16032–16038. https://doi.org/10.1021/ja508155x.

(189) Hasegawa, T.; Kobayashi, A.; Ohara, H.; Yoshida, M.; Kato, M. Emission Tuning of Luminescent Copper(I) Complexes by Vapor-Induced Ligand Exchange Reactions. *Inorg. Chem.* **2017**, *56* (9), 4928–4936. https://doi.org/10.1021/acs.inorgchem.6b03122.

(190) Sakai, Y.; Sagara, Y.; Nomura, H.; Nakamura, N.; Suzuki, Y.; Miyazaki, H.; Adachi, C. Zinc Complexes Exhibiting Highly Efficient Thermally Activated Delayed Fluorescence and Their Application to Organic Light-Emitting Diodes. *Chem. Commun.* **2015**, *51* (15), 3181–3184. https://doi.org/10.1039/C4CC09403D.

(191) To, W.-P.; Zhou, D.; Tong, G. S. M.; Cheng, G.; Yang, C.; Che, C.-M. Highly Luminescent

Pincer Gold(III) Aryl Emitters: Thermally Activated Delayed Fluorescence and Solution-Processed OLEDs. *Angew. Chemie Int. Ed.* **2017**, *56* (45), 14036–14041. https://doi.org/https://doi.org/10.1002/anie.201707193.

(192) Chen, J.; Teng, T.; Kang, L.; Chen, X.-L.; Wu, X.-Y.; Yu, R.; Lu, C.-Z. Highly Efficient Thermally Activated Delayed Fluorescence in Dinuclear Ag(I) Complexes with a Bis-Bidentate Tetraphosphane Bridging Ligand. *Inorg. Chem.* **2016**, *55* (19), 9528–9536. https://doi.org/10.1021/acs.inorgchem.6b00068.

(193) Shafikov, M. Z.; Suleymanova, A. F.; Czerwieniec, R.; Yersin, H. Thermally Activated Delayed Fluorescence from Ag(I) Complexes: A Route to 100% Quantum Yield at Unprecedentedly Short Decay Time. *Inorg. Chem.* **2017**, *56* (21), 13274–13285. https://doi.org/10.1021/acs.inorgchem.7b02002.

(194) Li, T.; Schaab, J.; Djurovich, P. I.; Thompson, M. E. Toward Rational Design of TADF Two-Coordinate Coinage Metal Complexes: Understanding the Relationship between Natural Transition Orbital Overlap and Photophysical Properties. *J. Mater. Chem. C* **2022**, *10* (12), 4674–4683. https://doi.org/10.1039/D2TC00163B.

(195) Arias-Rotondo, D. M.; McCusker, J. K. The Photophysics of Photoredox Catalysis: A Roadmap for Catalyst Design. *Chem. Soc. Rev.* **2016**, *45* (21), 5803–5820. https://doi.org/10.1039/C6CS00526H.

(196) Zhang, Y.; Petersen, J. L.; Milsmann, C. A Luminescent Zirconium(IV) Complex as a Molecular Photosensitizer for Visible Light Photoredox Catalysis. *J. Am. Chem. Soc.* **2016**, *138* (40), 13115–13118. https://doi.org/10.1021/jacs.6b05934.

(197) Zhang, Y.; Petersen, J. L.; Milsmann, C. Photochemical C–C Bond Formation in Luminescent Zirconium Complexes with CNN Pincer Ligands. *Organometallics* **2018**, *37*

(23), 4488–4499. https://doi.org/10.1021/acs.organomet.8b00388.

(198) Fan, C.; Wei, L.; Niu, T.; Rao, M.; Cheng, G.; Chruma, J. J.; Wu, W.; Yang, C. Efficient Triplet–Triplet Annihilation Upconversion with an Anti-Stokes Shift of 1.08 EV Achieved by Chemically Tuning Sensitizers. *J. Am. Chem. Soc.* **2019**, *141* (38), 15070–15077. https://doi.org/10.1021/jacs.9b05824.

(199) Chábera, P.; Liu, Y.; Prakash, O.; Thyrhaug, E.; Nahhas, A. El; Honarfar, A.; Essén, S.; Fredin, L. A.; Harlang, T. C. B.; Kjær, K. S.; Handrup, K.; Ericson, F.; Tatsuno, H.; Morgan, K.; Schnadt, J.; Häggström, L.; Ericsson, T.; Sobkowiak, A.; Lidin, S.; Huang, P.; Styring, S.; Uhlig, J.; Bendix, J.; Lomoth, R.; Sundström, V.; Persson, P.; Wärnmark, K. A Low-Spin Fe(Iii) Complex with 100-Ps Ligand-to-Metal Charge Transfer Photoluminescence. *Nature* **2017**, *543* (7647), 695–699. https://doi.org/10.1038/nature21430.

(200) Kjær, K. S.; Kaul, N.; Prakash, O.; Chábera, P.; Rosemann, N. W.; Honarfar, A.; Gordivska, O.; Fredin, L. A.; Bergquist, K.-E.; Häggström, L.; Ericsson, T.; Lindh, L.; Yartsev, A.; Styring, S.; Huang, P.; Uhlig, J.; Bendix, J.; Strand, D.; Sundström, V.; Persson, P.; Lomoth, R.; Wärnmark, K. Luminescence and Reactivity of a Charge-Transfer Excited Iron Complex with Nanosecond Lifetime. *Science (80-.).* **2019**, *363* (6424), 249–253. https://doi.org/10.1126/science.aau7160.

(201) Zhang, Y.; Lee, T. S.; Petersen, J. L.; Milsmann, C. A Zirconium Photosensitizer with a Long-Lived Excited State: Mechanistic Insight into Photoinduced Single-Electron Transfer. *J. Am. Chem. Soc.* **2018**, *140* (18), 5934–5947. https://doi.org/10.1021/jacs.8b00742.

(202) Zhang, Y.; Lee, T. S.; Favale, J. M.; Leary, D. C.; Petersen, J. L.; Scholes, G. D.; Castellano, F. N.; Milsmann, C. Delayed Fluorescence from a Zirconium(Iv) Photosensitizer with Ligand-to-Metal Charge-Transfer Excited States. *Nat. Chem.* **2020**, *12* (4), 345–352.

https://doi.org/10.1038/s41557-020-0430-7.

(203) Amemori, S.; Sasaki, Y.; Yanai, N.; Kimizuka, N. Near-Infrared-to-Visible Photon Upconversion Sensitized by a Metal Complex with Spin-Forbidden yet Strong S0-T1 Absorption. *J. Am. Chem. Soc.* **2016**, *138* (28), 8702–8705. https://doi.org/10.1021/jacs.6b04692.

(204) Mahboub, M.; Huang, Z.; Tang, M. L. Efficient Infrared-to-Visible Upconversion with Subsolar Irradiance. *Nano Lett.* **2016**, *16* (11), 7169–7175. https://doi.org/10.1021/acs.nanolett.6b03503.

(205) Mahboub, M.; Huang, Z.; Tang, M. L. Correction to Efficient Infrared-to-Visible Upconversion with Subsolar Irradiance. *Nano Lett.* **2016**, *16* (12), 8037. https://doi.org/10.1021/acs.nanolett.6b04941.

(206) Sun, M.-J.; Shao, J.-Y.; Yao, C.-J.; Zhong, Y.-W.; Yao, J. Osmium Bisterpyridine Complexes with Redox-Active Amine Substituents: A Comparison Study with Ruthenium Analogues. *Inorg. Chem.* **2015**, *54* (16), 8136–8147. https://doi.org/10.1021/acs.inorgchem.5b01420.

(207) Moore, S. A.; Nagle, J. K.; Wolf, M. O.; Patrick, B. O. Coordination Mode Dependent Excited State Behavior in Group 8 Phosphino(Terthiophene) Complexes. *Inorg. Chem.* **2011**, *50* (11), 5113–5122. https://doi.org/10.1021/ic200392n.

(208) Cerón-Camacho, R.; Hernández, S.; Le Lagadec, R.; Ryabov, A. D. Cyclometalated [Os(C–N)x(N–N)3−x]M+ Mimetics of Tris(2,2′-Bipyridine)Osmium(Ii): Covering a 2 V Potential Range by Known (x = 0, 1) and New (x = 2, 3) Species (C–N = o-2-Phenylpyridinato). *Chem. Commun.* **2011**, *47* (10), 2823–2825. https://doi.org/10.1039/C0CC04582A.

(209) Das, S.; Saha, D.; Mardanya, S.; Baitalik, S. A Combined Experimental and DFT/TDDFT

Investigation of Structural, Electronic, and PH-Induced Tuning of Photophysical and Redox Properties of Osmium(Ii) Mixed-Chelates Derived from Imidazole-4,5-Dicarboxylic Acid and 2,2′-Bipyridine. *Dalton Trans.* **2012**, *41* (39), 12296–12310. https://doi.org/10.1039/C2DT31321A.

(210) Shao, J.-Y.; Zhong, Y.-W. Monometallic Osmium(II) Complexes with Bis(N-Methylbenzimidazolyl)Benzene or -Pyridine: A Comparison Study with Ruthenium(II) Analogues. *Inorg. Chem.* **2013**, *52* (11), 6464–6472. https://doi.org/10.1021/ic400385b.

(211) Sommer, M. G.; Schweinfurth, D.; Weisser, F.; Hohloch, S.; Sarkar, B. Substituent-Induced Reactivity in Quinonoid-Bridged Dinuclear Complexes: Comparison between the Ruthenium and Osmium Systems. *Organometallics* **2013**, *32* (7), 2069–2078. https://doi.org/10.1021/om300939x.

(212) Das, A.; Agarwala, H.; Kundu, T.; Ghosh, P.; Mondal, S.; Mobin, S. M.; Lahiri, G. K. Electronic Structures and Selective Fluoride Sensing Features of $Os(Bpy)_2(HL^{2-})$ and $[\{Os(Bpy)_2\}_2(\mu\text{-}HL^{2-})]^{2+}$ (H_3L: 5-(1H-Benzo[d]Imidazol-2-Yl)-1H-Imidazole-4-Carboxylic Acid). *Dalton Trans.* **2014**, *43* (37), 13932–13947. https://doi.org/10.1039/C4DT01821D.

(213) Chang, S.-H.; Chang, C.-F.; Liao, J.-L.; Chi, Y.; Zhou, D.-Y.; Liao, L.-S.; Jiang, T.-Y.; Chou, T.-P.; Li, E. Y.; Lee, G.-H.; Kuo, T.-Y.; Chou, P.-T. Emissive Osmium(II) Complexes with Tetradentate Bis(Pyridylpyrazolate) Chelates. *Inorg. Chem.* **2013**, *52* (10), 5867–5875. https://doi.org/10.1021/ic302829e.

(214) Chung, L.-H.; Chan, S.-C.; Lee, W.-C.; Wong, C.-Y. Emissive Osmium(II) Complexes Supported by N-Heterocyclic Carbene-Based C∧C∧C-Pincer Ligands and Aromatic Diimines. *Inorg. Chem.* **2012**, *51* (16), 8693–8703. https://doi.org/10.1021/ic202726g.

(215) Nie, H.-J.; Shao, J.-Y.; Yao, C.-J.; Zhong, Y.-W. Organic–Inorganic Mixed-Valence Systems with Strongly-Coupled Triarylamine and Cyclometalated Osmium. *Chem. Commun.* **2014**, *50* (70), 10082–10085. https://doi.org/10.1039/C4CC04268A.

(216) Lamansky, S.; Djurovich, P.; Murphy, D.; Abdel-Razzaq, F.; Lee, H.-E.; Adachi, C.; Burrows, P. E.; Forrest, S. R.; Thompson, M. E. Highly Phosphorescent Bis-Cyclometalated Iridium Complexes: Synthesis, Photophysical Characterization, and Use in Organic Light Emitting Diodes. *J. Am. Chem. Soc.* **2001**, *123* (18), 4304–4312. https://doi.org/10.1021/ja003693s.

(217) Altobello, S.; Argazzi, R.; Caramori, S.; Contado, C.; Da Fré, S.; Rubino, P.; Choné, C.; Larramona, G.; Bignozzi, C. A. Sensitization of Nanocrystalline TiO2 with Black Absorbers Based on Os and Ru Polypyridine Complexes. *J. Am. Chem. Soc.* **2005**, *127* (44), 15342–15343. https://doi.org/10.1021/ja053438d.

(218) Kinoshita, T.; Fujisawa, J.; Nakazaki, J.; Uchida, S.; Kubo, T.; Segawa, H. Enhancement of Near-IR Photoelectric Conversion in Dye-Sensitized Solar Cells Using an Osmium Sensitizer with Strong Spin-Forbidden Transition. *J. Phys. Chem. Lett.* **2012**, *3* (3), 394–398. https://doi.org/10.1021/jz2016445.

(219) Chen, K.; Hussain, M.; Razi, S.; Hou, Y.; Yildiz, E.; Zhao, J.; Yaglioglu, H. G.; Di Donato, M. Anthryl-Appended Platinum(II) Schiff Base Complexes: Exceptionally Small Stokes Shift, Triplet Excited States Equilibrium, and Application in Triplet–Triplet-Annihilation Upconversion. *Inorg. Chem.* **2019**, *59* (20), 14731–14745. https://doi.org/10.1021/acs.inorgchem.0c01932.

(220) Liu, B.; Jiao, J.; Xu, W.; Zhang, M.; Cui, P.; Guo, Z.; Deng, Y.; Chen, H.; Sun, W. Highly Efficient Far-Red/NIR-Absorbing Neutral Ir(III) Complex Micelles for Potent

Photodynamic/Photothermal Therapy. *Adv. Mater.* **2021**, *33* (32), 2100795. https://doi.org/https://doi.org/10.1002/adma.202100795.

(221) Lu, T.; Lu, C.; Cui, P.; Kilina, S.; Sun, W. Impacts of Extending the π-Conjugation of the 2,2′-Biquinoline Ligand on the Photophysics and Reverse Saturable Absorption of Heteroleptic Cationic Iridium(Iii) Complexes. *J. Mater. Chem. C* **2021**, *9* (44), 15932–15941. https://doi.org/10.1039/D1TC03601G.

(222) Huang, Y.; Liu, D.-E.; An, J.; Liu, B.; Sun, L.; Fu, H.; Yan, S.; Sun, W.; Gao, H. Reactive Oxygen Species Self-Sufficient Multifunctional Nanoplatform for Synergistic Chemo-Photodynamic Therapy with Red/near-Infrared Dual-Imaging. *ACS Appl. Bio Mater.* **2020**, *3* (12), 9135–9144. https://doi.org/10.1021/acsabm.0c01419.

(223) Schmid, L.; Glaser, F.; Schaer, R.; Wenger, O. S. High Triplet Energy Iridium(III) Isocyanoborato Complex for Photochemical Upconversion, Photoredox and Energy Transfer Catalysis. *J. Am. Chem. Soc.* **2022**, *144* (2), 963–976. https://doi.org/10.1021/jacs.1c11667.

(224) Schmid, L.; Kerzig, C.; Prescimone, A.; Wenger, O. S. Photostable Ruthenium(II) Isocyanoborato Luminophores and Their Use in Energy Transfer and Photoredox Catalysis. *J. Am. Chem. Soc.* **2021**, *1* (6), 819–832. https://doi.org/10.1021/jacsau.1c00137.

(225) Koseki, S.; Matsunaga, N.; Asada, T.; Schmidt, M. W.; Gordon, M. S. Spin–Orbit Coupling Constants in Atoms and Ions of Transition Elements: Comparison of Effective Core Potentials, Model Core Potentials, and All-Electron Methods. *J. Phys. Chem. A* **2019**, *123* (12), 2325–2339. https://doi.org/10.1021/acs.jpca.8b09218.

(226) Amemori, S.; Sasaki, Y.; Yanai, N.; Kimizuka, N. Correction to "Near-Infrared-to-Visible Photon Upconversion Sensitized by a Metal Complex with Spin-Forbidden yet Strong S0–

T1 Absorption." *J. Am. Chem. Soc.* **2020**, *142* (17), 8057–8058. https://doi.org/10.1021/jacs.0c03910.

(227) He, S.; Krippes, K.; Ritz, S.; Chen, Z.; Best, A.; Butt, H.-J.; Mailänder, V.; Wu, S. Ultralow-Intensity near-Infrared Light Induces Drug Delivery by Upconverting Nanoparticles. *Chem. Commun.* **2015**, *51* (2), 431–434. https://doi.org/10.1039/C4CC07489K.

(228) Askes, S. H. C.; Leeuwenburgh, V. C.; Pomp, W.; Arjmandi-Tash, H.; Tanase, S.; Schmidt, T.; Bonnet, S. Water-Dispersible Silica-Coated Upconverting Liposomes: Can a Thin Silica Layer Protect TTA-UC against Oxygen Quenching? *ACS Biomater. Sci. Eng.* **2017**, *3* (3), 322–334. https://doi.org/10.1021/acsbiomaterials.6b00678.

(229) Sasaki, Y.; Oshikawa, M.; Bharmoria, P.; Kouno, H.; Hayashi-Takagi, A.; Sato, M.; Ajioka, I.; Yanai, N.; Kimizuka, N. Near-Infrared Optogenetic Genome Engineering Based on Photon-Upconversion Hydrogels. *Angew. Chem. Int. Ed.* **2019**, *58* (49), 17827–17833. https://doi.org/https://doi.org/10.1002/anie.201911025.

(230) Liu, D.; Zhao, Y.; Wang, Z.; Xu, K.; Zhao, J. Exploiting the Benefit of $S_0 \rightarrow T_1$ Excitation in Triplet–Triplet Annihilation Upconversion to Attain Large Anti-Stokes Shifts: Tuning the Triplet State Lifetime of a Tris(2,2′-Bipyridine) Osmium(II) Complex. *Dalton Trans.* **2018**, *47* (26), 8619–8628. https://doi.org/10.1039/C7DT04803C.

(231) Wei, Y.; Zheng, M.; Chen, L.; Zhou, X.; Liu, S. Near-Infrared to Violet Triplet-Triplet Annihilation Fluorescence Upconversion of Os(Ii) Complexes by Strong Spin-Forbidden Transition. *Dalton Trans.* **2019**, *48* (31), 11763–11771. https://doi.org/10.1039/c9dt02276g.

(232) Wei, Y.; Li, Y.; Zheng, M.; Zhou, X.; Zou, Y.; Yang, C. Simultaneously High Upconversion Efficiency and Large Anti-Stokes Shift by Using Os(II) Complex Dyad as Triplet

Photosensitizer. *Adv. Opt. Mater.* **2020**, *8* (9), 1902157. https://doi.org/https://doi.org/10.1002/adom.201902157.

(233) Lincoln, R.; Kohler, L.; Monro, S.; Yin, H.; Stephenson, M.; Zong, R.; Chouai, A.; Dorsey, C.; Hennigar, R.; Thummel, R. P.; McFarland, S. A. Exploitation of Long-Lived 3IL Excited States for Metal–Organic Photodynamic Therapy: Verification in a Metastatic Melanoma Model. *J. Am. Chem. Soc.* **2013**, *135* (45), 17161–17175. https://doi.org/10.1021/ja408426z.

(234) Fukuzumi, S.; Ohkubo, K. Selective Photocatalytic Reactions with Organic Photocatalysts. *Chem. Sci.* **2013**, *4* (2), 561–574. https://doi.org/10.1039/C2SC21449K.

(235) Ravelli, D.; Fagnoni, M.; Albini, A. Photoorganocatalysis. What For? *Chem. Soc. Rev.* **2013**, *42* (1), 97–113. https://doi.org/10.1039/C2CS35250H.

(236) Hari, D. P.; König, B. The Photocatalyzed Meerwein Arylation: Classic Reaction of Aryl Diazonium Salts in a New Light. *Angew. Chem. Int. Ed.* **2013**, *52* (18), 4734–4743.

(237) Peters-Clarke, T. M.; Schauer, K. L.; Riley, N. M.; Lodge, J. M.; Westphall, M. S.; Coon, J. J. Optical Fiber-Enabled Photoactivation of Peptides and Proteins. *Anal. Chem.* **2020**, *92* (18), 12363–12370. https://doi.org/10.1021/acs.analchem.0c02087.

(238) Wang, J.; Xie, H.; Li, H.; Wang, R.; Zhang, B.; Ren, T.; Hua, J.; Chen, N. NIR Fluorescent Probe for In Situ Bioimaging of Endogenous H2S in Rice Roots under Al3+ and Flooding Stresses. *J. Agric. Food Chem.* **2021**, *69* (47), 14330–14339. https://doi.org/10.1021/acs.jafc.1c05247.

(239) Li, C.; Chen, G.; Zhang, Y.; Wu, F.; Wang, Q. Advanced Fluorescence Imaging Technology in the Near-Infrared-II Window for Biomedical Applications. *J. Am. Chem. Soc.* **2020**, *142* (35), 14789–14804. https://doi.org/10.1021/jacs.0c07022.

(240) Hong, G.; Antaris, A. L.; Dai, H. Near-Infrared Fluorophores for Biomedical Imaging. *Nat. Biomed. Eng.* **2017**, *1* (1), 10. https://doi.org/10.1038/s41551-016-0010.

(241) Kawano, F.; Okazaki, R.; Yazawa, M.; Sato, M. A Photoactivatable Cre–LoxP Recombination System for Optogenetic Genome Engineering. *Nat. Chem. Biol.* **2016**, *12* (12), 1059–1064. https://doi.org/10.1038/nchembio.2205.

Abbreviation

TTA-PUC = Triplet-triplet annihilation photon up-conversion

ISC = Intersystem crossing

TADF = Thermally activated delayed-fluorescence

MLCT = Metal-to-ligand charge-transfer

PDT = Photodynamic therapy

TEnM = Triplet−triplet energy migration

CR = Charge recombination

CS = Charge separation

CT = Charge-transfer

RP-ISC = Radical-pair intersystem crossing

SOCT-ISC = Spin-orbital charge-transfer intersystem crossing

OLED = Organic light emitting diode

reISC = Reverse intersystem crossing

DF = Delayed fluorescence

ESP = Electron-spin polarization

EPR = Electron paramagnetic resonance

HFC = Hyperfine coupling

CPL = Circularly polarized luminescence

UC-CPUVL = Upconverted circularly polarized ultraviolet luminescence

MR-TADF = Multiple-resonance thermally activated delayed-fluorescence

LMCT = Ligand to metal charge transfer

IL = Intraligand

NP = nanoparticles

VR = Vibrational relaxation

FRET = Förester resonance energy transfer

TD-DFT = Time dependent density functional theory

TOC

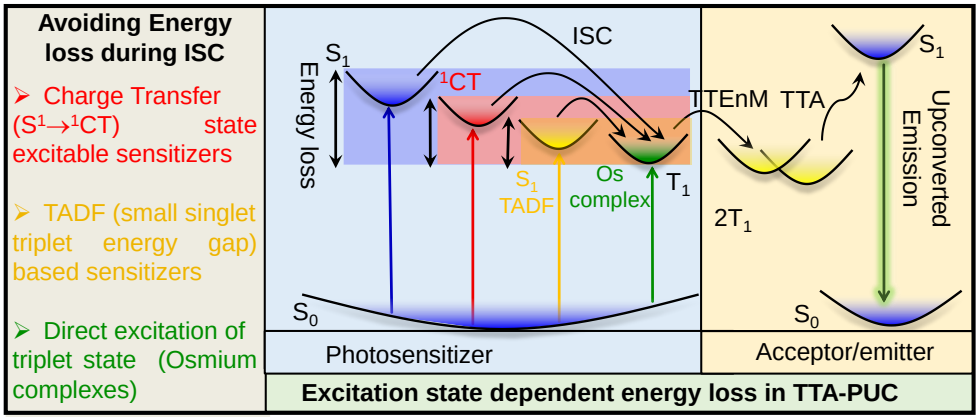
Avoiding Energy loss during ISC
➢ Charge Transfer (S¹→¹CT) state excitable sensitizers
➢ TADF (small singlet triplet energy gap) based sensitizers
➢ Direct excitation of triplet state (Osmium complexes)
ISC
S1
Energy loss
1CT
S1
TADF
Os complex
T1
S0
TTEnM
TTA
2T1
S1
Upconverted Emission
S0
Photosensitizer
Acceptor/emitter
Excitation state dependent energy loss in TTA-PUC